Distribution Agreement

In presenting this thesis or dissertation as a partial fulfillment of the requirements for an advanced degree from Emory University, I thereby grant to Emory University and its agents the non-exclusive license to archive, make accessible, and display my thesis or dissertation in whole or in part in all forms of media, now or hereafter known, including display on the world wide web. I understand that I may select some access restrictions as part of the online submission of this thesis or dissertation. I retain all ownership rights to the copyright of the thesis or dissertation. I also retain the right to use in future works (such as articles or books) all or part of this thesis or dissertation.

Signature:

_____ _____

Erica Tracey Akhter Date

The regulation of the potassium chloride co-transporter KCC2 in spinal motoneurons following peripheral nerve injury

By

Erica Tracey Akhter
Doctor of Philosophy

Graduate Division of Biological and Biomedical Science
Neuroscience

_____
Francisco J. Alvarez, PhD
Advisor

_____
Arthur W. English, PhD
Advisor

_____
Marie-Claude Perreault, PhD
Committee Member

_____
Malu Tansey, PhD
Committee Member

_____
Peter Wenner, PhD
Committee Member

Accepted:

_____
Lisa A. Tedesco, Ph.D.
Dean of the James T. Laney School of Graduate Studies

_____
Date

The regulation of the potassium chloride co-transporter KCC2 in spinal motoneurons following peripheral nerve injury

By

Erica Tracey Akhter
B.S., College of Charleston, 2014

Advisors: Francisco J. Alvarez, PhD
Arthur W. English, PhD

An abstract of
A dissertation submitted to the Faculty of the
James T. Laney School of Graduate Studies of Emory University
in partial fulfillment of the requirements for the degree of
Doctor of Philosophy
in Neuroscience
2019

Abstract

The regulation of the potassium chloride co-transporter KCC2 in spinal motoneurons following peripheral nerve injury

By Erica Tracey Akhter

Following many types of injury, the potassium chloride co-transporter KCC2 is dysregulated on injured neurons or those associated with neurons that have been injured. This changes driving forces for GABAergic and glycinergic inhibitory synapses and in general increases excitability in the affected neurons and networks. This phenomenon has been described in dorsal horn sensory-associated interneurons following peripheral nerve injury (PNI), as well as on motoneurons after spinal cord injury. In these cases, decreased expression of KCC2 is associated with neuropathic pain and spasticity, respectively. However, increasing activity with exercise or electrical stimulation has previously been shown to aid in motor axon regeneration, and KCC2 has not yet been investigated on spinal motoneurons following PNI. Previous studies in the brainstem have indicated that KCC2 is also downregulated in motoneurons axotomized in peripheral nerve injuries, but the significance of this downregulation and the mechanisms regulating it have received less attention. In this dissertation, we investigate the extent and regulation of KCC2 depletion on spinal motoneurons following PNI using a variety of mutant mice, pharmacological interventions, and injury paradigms. Following sciatic nerve injury, *kcc2* mRNA was downregulated in motoneurons within three days of their axotomy. In all cases, two weeks following injury, KCC2 protein was also consistently and drastically depleted on axotomized motoneuron somata and proximal dendrites. This depletion occurs independently from the mechanisms previously established in other regions of the spinal cord after PNI; it is not dependent on microgliosis, motoneuron BDNF release, or TrkB signaling. However, KCC2 is restored if the sciatic nerve is repaired and regeneration is allowed. This restoration is dependent on the presence of an intact neuromuscular junction, but not the functional connection with the muscle. We illustrated that blocking neuromuscular signaling or exercising mice to drive more neural activity had no impact on KCC2 expression. Our results illustrate that KCC2 regulation on axotomized motoneurons occurs via a different mechanism than previously established in other cell types or injury paradigms. This work lays the groundwork for pursuing further questions about the role of downregulation in KCC2, likely accompanied by increases in activity, in aiding motor axon regeneration.

The regulation of the potassium chloride co-transporter KCC2 in spinal motoneurons following peripheral nerve injury

By

Erica Tracey Akhter
B.S., College of Charleston, 2014

Advisors: Francisco J. Alvarez, PhD
Arthur W. English, PhD

An abstract of
A dissertation submitted to the Faculty of the
James T. Laney School of Graduate Studies of Emory University
in partial fulfillment of the requirements for the degree of
Doctor of Philosophy
in Neuroscience
2019

Acknowledgments

"We know what we want to measure, but we frequently find out what we want to measure is not quite what we wanted in order to understand or predict the phenomena that we're interested in… [W]hat we get is maybe sometimes a lot better than what we set out to do, and sometimes its worse."

~My Papaw, Shelby Tilford, PhD
An Oral History

To my committee:

Dr. Perreault, Dr. Tansey, Dr. Wenner, I could not have asked for a more wonderful and supportive group of scientists to guide my path and ask me to explain myself. You have all been more than generous with your time, your resources, and your advice in science and life. Thank you.

To my lab-mates:

There are so many who have helped me: Alicia, Claire, Jill, Laura, Olivia, Ron, Shlok, and Travis specifically deserve an extra special mention.

You have all been scientific assets, freely sharing your knowledge and helping with the intellectual and physical work on experiments. Even more than the science, you have all seen me at my best and worst and kept working with me and making me laugh anyway. You've helped keep me sane and centered and *almost always* made coming to lab a joy.

To my PIs:

Drs Alvarez & English.

You have both shown me the joys and trials of science and living a life around what you are passionate about. I am incredibly lucky to have had you take me into your labs and under your wings. I am incredibly grateful you allowed me to explore for my own passions and make my own path in graduate school. I am incredibly impressed at how you manage the pressures of science and the responsibilities that come with it. I am just a little resentful that I'm just now figuring out most (all?) of the good ideas I had, you actually led me to, but let me keep thinking I came up with on my own. You have shown me what it means to be an excellent mentor and I hope I can guide my future students as well as you have guided me.

To my family:

There are no words. Your support before graduate school empowered me to be confident, to try scary things, to embrace a challenge. Your support during this process has continually reminded me that I am surrounded by goodness, positivity, and people who believe in me even when my own confidence flags. Without you, I would never have looked towards this goal and without you I would never have achieved it.

Table of Contents

Chapter 1: General Introduction

Chapter 2: General Methods

Chapter 3: Characteristics of KCC2 loss on motoneuron somata and proximal dendrites following axotomy.

Chapter 4: Investigation of the role of established regulators of KCC2 following nervous system injury, namely microglia, BDNF and TrkB.

Chapter 5: KCC2 regulation by a muscle-derived signal

Figure Index

Chapter 2: General Methods

Chapter 3: Characteristics of KCC2 loss on motoneuron somata and proximal dendrites following axotomy.

Chapter 4: Investigation of the role of established regulators of KCC2 following nervous system injury, namely microglia, BDNF and TrkB.

Chapter 5: KCC2 regulation by a muscle-derived signal

Appendix 1: Regulation of KCC2 by miRNA's

Chapter 1: Introduction

Modified from the following reference:

Akhter, E.T., English, A.W., Alvarez, F.J. 2019. Invited Book Chapter. Neuronal Chloride Homeostasis and Nerve Injury. Elsevier. (Accepted).

1.1 General Introduction

The neuronal potassium chloride co-transporter KCC2 is dysregulated after numerous types of neuronal injuries and has been related to neuronal dysfunction, hyperalgesia and spasticity (Blaesse et al., 2009; Ben-Ari et al., 2012; Kaila et al., 2014). Typically, KCC2 is responsible for maintaining the low intracellular chloride concentration found in most adult neurons and it is necessary for inhibitory synapse function (Payne et al., 2003; Kaila et al., 2014; Kahle and Delpire, 2016). KCC2 inactivation or removal from the neuronal membrane can result in neuronal hyperexcitability as defined by reduced inhibition (and even excitation) in response to the "inhibitory" neurotransmitters GABA and glycine. As such, alterations in KCC2 after injury are typically considered maladaptive and targeted treatments to prevent KCC2 loss are being developed in a variety of contexts (Wen et al., 2011; Kahle et al., 2014; Doyon et al., 2016b). However, these previous investigations fail to consider the potential positive outcomes of KCC2 inactivity and consequent increased neural activity. Following axotomy in the periphery, treatments that accelerate axon growth include exercise and electrical stimulation, treatments that presumably increase neural activity (Al-Majed et al., 2000a; Al-Majed et al., 2000b; English et al., 2007; English et al., 2009; Udina et al., 2011; Ward et al., 2016; Jaiswal et al., 2017; Jaiswal et al., 2018; Ward et al., 2018). Therefore, it is possible that decreases in KCC2 serve to enhance regeneration by dampening the inhibitory effects of GABA or glycine, potentially even changing them into depolarizing forces that help potentiate axon regeneration. In this document, we describe our work investigating KCC2 regulation on spinal motoneurons with axons injured during peripheral nerve transections as a first step towards manipulating KCC2 activity and understanding it's potential role in regeneration. Concurrently, we introduce some perspective on the variety of actions that potential therapeutic interventions on chloride homeostasis and inhibitory function might have throughout all spinal cord systems.

1.2 Peripheral nerve injury as a model and clinical conundrum

Unlike other models of neural stress, peripheral nerve injury (PNI) allows study of the neural reactions to axon damage independent of the excitotoxic milieu that surrounds cells after more direct and global injuries to the central nervous system. In contrast to axons of central neurons, axons in peripheral nerves regenerate after injury, and the behavioral and physiological outcomes of recovery from PNI are readily measured. This opportunity to examine basic properties of neural injury has drawn many labs to use PNI as a model for the study of cellular responses to damage.

In addition to its utility as a model to address questions from the basic science perspective, improper or failed axon regeneration after nerve injury is also a significant biomedical problem. The first published studies of regeneration after peripheral nerve injury took place in the early twentieth century by Drs. W.H.R. Rivers and H. Head, who intentionally transected Dr. Head's own radial nerve and tracked the restoration of different sensory modalities (Mundie, 1920; Compston, 2009). Studies throughout the early 1900s followed, primarily from observations made during surgeries on soldiers returning wounded from war (Burrow Jle, 1918; Aird, 1946). Today the treatment of peripheral nerve injuries has not much changed (Kouyoumdjian, 2006; Taylor et al., 2008; Brushart, 2011).

Depending on the level of injury, it can take months or years for restoration of sensory and motor function (Burrow Jle, 1918; Mundie, 1920; Aird, 1946; Grinsell and Keating, 2014). In the case of Dr. Head's radial nerve, it took two years to recover "epicritic" localized sensation for "light touch" elicited with a cotton swab (Compston, 2009). Moreover, functional recovery is not fully normal. Development of persistent neuropathic pain is common (Jensen et al., 2001) and is often coupled with a loss of motor control; nearly half of patients fail to recover even gross motor activity after injury and only one out of ten patients eventually regain normal motor coordination (Höke and Brushart, 2010). Clinical studies in humans and experimental studies in lab animals all conclude that regeneration speed is crucial to rehabilitation, as regeneration

capacity and functional recovery progressively decline with time after injury (Sunderland, 1952; Fu and Gordon, 1995a, b; Krarup et al., 2002). This occurs because the regenerative program inside injured neurons and the trophic properties of peripheral Schwann cells in the pathway surrounding the regenerating axons weaken with time after injury and because chronic denervation produces changes in peripheral target tissues, such as muscle, that are frequently irreversible (Gordon, 2009). Moreover, disconnection with the periphery also induces plastic changes in brain and spinal cord circuits, preventing normal sensory and motor function (Cope et al., 1994; Lundborg, 2003; Navarro et al., 2007; Alvarez et al., 2010).

Little progress has been made toward improving regeneration following PNI, with the majority of cases being treated by direct end-to-end nerve repair just as they have been for decades. This consists of epineurial and/or intrafascicular suturing of the proximal and distal stumps of severed nerves, sometimes using interposed autologous nerve grafts or de-cellularized allografts (Aird, 1946; Scholz et al., 2009; Grinsell and Keating, 2014). Microsurgical techniques have not changed significantly since the 1960s (Grinsell and Keating, 2014). Professor Göran Lundborg summarized the current state of affairs in 2002 and 2003, stating, “we have reached a plateau where surgical repair techniques cannot be refined any more” (Lundborg, 2002, 2003).

Direct end-to-end nerve repair (with or without addition of autologous nerves, allografts, or bioengineered conduits to bridge larger gaps) is limited by the biological nature of axon regeneration, consisting of a delayed start after injury followed by slow axon growth (Holmes and Young, 1942; Bora, 1978; Fu and Gordon, 1995a; Elzinga et al., 2015). Additionally, misdirection of axons leads them to functionally inappropriate targets, which can cause a loss of sensorimotor specificity in the periphery and a variety of deficits in motor control (Brushart and Mesulam, 1980; Gordon et al., 1986; Brushart, 1993; Hamilton et al., 2011; Sabatier et al., 2011; de Ruiter et al., 2014). Loss of topographic specificity of reinnervated motoneurons, specifically when flexor motoneurons reinnervate extensor muscles or vice versa, can cause significant co-

contraction of typically antagonistic muscles and induce a variety of functional and kinematic anomalies (English, 2005; English et al., 2009; Hamilton et al., 2011; Sabatier et al., 2011).

It is clear that new approaches are necessary to improve the efficiency of axon regeneration in peripheral nerves. Among the most successful treatments developed to date that facilitate axon growth are exercise and electrical stimulation (Al-Majed et al., 2000b; Gordon et al., 2007; Asensio-Pinilla et al., 2009; Gordon, 2009; Udina et al., 2011; Gordon and English, 2016). Both have been shown to increase speed of regeneration in experimental animals and in one pilot case in patients (electrical stimulation of the median nerve after carpal tunnel decompression) (Gordon et al., 2010). The effectiveness of activity-dependent treatments suggests that a higher level of activity in regenerating neurons facilitates their axon elongation. This invites the following question, which motivates the work described below: If activity is important for promoting regeneration, could hyperexcitability of motoneurons, typically considered a risk to their health, actually promote regeneration following injury?

1.3 Neuronal hyperexcitability: Is it only an unhappy accident?

Neuronal hyperexcitability is a phenomenon associated with many pathological conditions, including seizure disorders, autism, ischemia, spinal cord injury (SCI), amyotrophic lateral sclerosis, and neuropathic pain (Kahle et al., 2008; Tao et al., 2012; Vucic and Rutkove, 2018). One common feature in these disorders is the dysregulation of chloride transporters within neurons and a corresponding alteration in how these neurons respond to “inhibitory” neurotransmitters (Coull et al., 2003; Malek et al., 2003; Prescott et al., 2006; Boulenguez et al., 2010; Fuchs et al., 2010; Stil et al., 2011; Bos et al., 2013; Eftekhari et al., 2013; Amin et al., 2017; Kourdougli et al., 2017). Disinhibition can lead to increased activity throughout the spinal network, and it is these changes that are associated with the most severe functional outcomes. As such, hyperexcitability in general (and chloride dysregulation in particular) are thought of as

maladaptive processes to be treated and prevented. However, there is ample evidence that these changes may also have benefits, including promoting axon growth and regeneration.

During early development, spontaneous activity in hyperexcitable neurons is driven by the action of gamma amino butyric acid (GABA), which is necessary for axon growth and pathfinding (Sernagor et al., 2010). Moreover, after spinal cord injury, spasticity associated with hyperactivity of motoneurons can assist patients with everyday tasks (Skold, 2000). Motoneurons undergo extensive changes in ion channel expression after PNI that modify their electrophysiological properties and make them more likely to reach firing threshold (Eccles et al., 1954; Kuno et al., 1974; Gustafsson, 1979; Gustafsson and Pinter, 1984). The significance of developing a hyperexcitable state is not fully understood, but it has been shown that treatments associated with increasing activity in injured motoneurons enhance functional recovery as described above (English et al., 2007; Sabatier et al., 2008; Gordon and English, 2016).

Changes in motoneuron firing properties do not exist in isolation and must be viewed in the context of their impact on the integration of motoneurons' synaptic inputs. Axotomized motoneurons transiently shed synapses, mostly glutamatergic synapses, from their cell bodies. These are only recovered after the injured motoneurons reinnervate peripheral targets (reviewed in (Alvarez et al., 2010; Gonzalez-Forero and Moreno-Lopez, 2014)). This change in excitatory/inhibitory balance while the motoneuron is regenerating is usually interpreted as a mechanism to counter hyperexcitability such that motoneurons enter a "quiet" phase, focusing resources in gene and protein expression to promote regeneration (Choi, 1992; Oliveira et al., 2004). Indeed, enhanced preservation of inhibitory synapses in axotomized motoneurons increases the speed of muscle reinnervation and recovery of motor function (Berg et al., 2012).

Despite its prevalence, the view that "inhibitory" synapses are serving a protective role does not take into account the alterations in internal chloride (reviewed below), which can cause GABAergic and glycinergic synapses to transform from an inhibitory force to providing excitatory drive to regenerating motoneurons. Viewed in this manner the obvious question is:

why lose glutamatergic synapses only to provide excitation through GABA and glycine? Activity is necessary for axon elongation and path finding in embryonic motoneurons, and this activity is driven by spontaneous bursting generated in the neural tube by activation of $GABA_A$ receptors, which induce large depolarizations in the highly hyperexcitable immature motoneurons (Hanson et al., 2008; Czarnecki et al., 2014; Landmesser, 2018). Adult axotomized motoneurons clearly differ in many properties from these very early motoneurons, but it is possible that GABA/glycine synaptic depolarizations, combined with hyperexcitability as defined by decreasing rheobase or action potential threshold, drive activity in regenerating adult motoneurons and aid in motor axon growth as they do during early development at the onset of synaptogenesis.

Sensory neurons also regenerate after PNI, but in contrast to motoneurons, they lack dendrites and do not receive synapses on their cell bodies that could assist in driving activity. Sensory neurons receive GABAergic synapses only on their central synaptic terminals (Alvarez et al., 1996) and these induce primary afferent depolarization (PAD) in normal adult sensory neurons (Rudomin and Schmidt, 1999), due to their high intracellular chloride concentration (Alvarez-Leefmans et al., 1988; Mao et al., 2012). Like motoneurons, sensory neurons increase their excitability after axotomy by increasing their membrane input resistance, decreasing rheobase and changing ion channel expression (Zhang et al., 1997; Kim et al., 1998; Abdulla et al., 2001). Sensory neurons also increase their already high intracellular chloride concentration after PNI, causing them to fire more in response to centrally elicited primary afferent depolarization. Although it is not fully established that increased PAD aids regenerating sensory afferents, it has been shown that higher internal chloride assists in their regeneration (Pieraut et al., 2007; Modol et al., 2015). The parallel changes in firing properties and the action of inhibitory neurotransmitters in regenerating sensory neurons and motoneurons suggest that both are part of the response associated with a regenerative phenotype. Unfortunately, chloride dysregulation in sensory neurons also induces persistent neuropathic pain (Seltzer et al., 1990;

Jensen et al., 2001; Lu et al., 2008; Huang et al., 2016). Additionally, chloride is dysregulated in spinal interneurons and brain projecting nociceptive neurons (Price et al., 2005; Price et al., 2009). Although these neurons are themselves uninjured, they are affected by the unbalanced sensory afferent inputs and local neuroinflammation that occurs in the spinal cord superficial lamina following PNI. KCC2 also becomes downregulated in these neurons, decreasing inhibitory synaptic strength (Ferrini and De Koninck, 2013; Doyon et al., 2016a). The combined effect of increased chloride in both primary afferent sensory neurons and sensory processing interneurons in the dorsal horn of the spinal cord creates a hyperexcitable network that promotes hyperalgesia (Price et al., 2005; Price et al., 2009). Studies examining these conditions as they relate to pain rarely consider the recovery of normal sensory and motor function, making it difficult to parse positive and negative outcomes of chloride regulation after nerve injury.

1.4 The mysterious shift in motoneuron excitability

Since the 1970s, it has been known that motoneurons become more excitable after their axons have been transected. Axotomized motoneurons in both the spinal cord and brainstem rapidly increase input resistance and decrease rheobase, while action potential amplitude increases and the after-hyperpolarization phase shortens: all are changes leading to increases in firing (Eccles et al., 1954; Kuno et al., 1974; Huizar et al., 1977; Gustafsson, 1979; Takata and Nagahama, 1983; Gustafsson and Pinter, 1984; Nishimura et al., 1992; Gonzalez-Forero et al., 2007). These alterations in excitability are attributed to a host of changes in ion channel expression, including downregulation of leak K^+ channels, reorganization of Na^+ channel composition, and de-clustering of calcium-dependent K^+ channels (Eccles et al., 1958; Iwahashi et al., 1994; Gonzalez-Forero et al., 2007; Kasumacic et al., 2012; Romer et al., 2014; Valdez et al., 2014).

Evidence of the beneficial effects of hyperexcitability for regeneration was first uncovered in *Aplysia* in the early 1990s. Crushing the axon of *Aplysia* neurons increases neural excitability at the soma, lengthens spike durations, and decreases the after-hyperpolarization phase (Clatworthy and Walters, 1994). These changes are due to alterations in ion channel expression that parallel those observed in motoneurons, including reduced potassium leak channels and calcium-activated SK potassium channels (Ungless et al., 2002). Importantly, changes in excitability were associated with axon sprouting and new synapse formation (Steffensen et al., 1995). Although there are many differences between *Aplysia* neurons and mammalian motoneurons, this remarkable homology suggests that increased excitability following injury may have been conserved during evolution as an important factor for axon regeneration (Woolf and Walters, 1991) and thus that it might contribute to the motoneuron regenerative program. However, changes in excitability also need to be understood in the context of modifications to the synaptic inputs on motoneurons that are also triggered by injury.

1.5 Synaptic changes in regenerating motoneurons

Early studies of axotomized motoneurons in mammals noted alterations in both excitatory and inhibitory postsynaptic potentials (Kuno and Llinas, 1970; Takata and Nagahama, 1983). At the time, these changes were explained by the phenomenon of "synaptic stripping". Synaptic stripping, first revealed with electron microcopy in the 1960s and 1970s, consists of the loss of synapses on the cell bodies and proximal dendrites of axotomized motoneurons (Blinzinger and Kreutzberg, 1968; Sumner and Sutherland, 1973; Sumner, 1976; Chen, 1978; Alvarez et al., 2010; Gonzalez-Forero and Moreno-Lopez, 2014). Interestingly, there is a larger loss of excitatory synapses than inhibitory synapses (Brannstrom and Kellerth, 1998, 1999; Linda et al., 2000). Furthermore, remaining GABAergic synapses contain synaptic vesicles with a larger cross-sectional area and GABA content (Vaughan, 1994), perhaps reversing the shift from GABAergic to glycinergic neurotransmission that normally occurs during

postnatal development (Gao et al., 2001; Gonzalez-Forero and Alvarez, 2005). Retention of inhibitory synapses by motoneurons during axon regeneration is typically interpreted as preventing hyperexcitable motoneurons from excessive firing, but such an interpretation assumes that the remaining actions of inhibitory synapses are similar in axotomized and uninjured motoneurons. This is not the case, however. Studies as early as the 1970s illustrated a loss of inhibition efficiency, as defined by the ability of GABA and glycine to induce hyperpolarization, in injured motoneurons. This was first described in cat spinal motoneurons where a reduction in the inhibitory post-synaptic potential (IPSP) amplitude and rise-time of proximal inhibitory synapses was reported using intracellular recordings with sharp electrodes that preserve the natural intracellular chloride gradient (Kuno and Llinas, 1970). This phenomenon was then thoroughly described in strychnine- and picrotoxin-sensitive inhibitory synaptic currents in axotomized cat hypoglossal and trigeminal motoneurons (Takata, 1981; Takata and Nagahama, 1983; Takata and Tomomune, 1986). Interpretation of these results as a consequence of "synaptic stripping" is problematic since immunocytochemistry and electron microscopy studies showed that inhibitory synapses are preserved after axotomy in hypoglossal motoneurons (Sumner, 1975; Sunico et al., 2010; Tatetsu et al., 2012). Alternatively, changes in the driving force of inhibitory synapses by altered chloride homeostasis could play a role in the decrease of IPSP amplitudes. It should be noted that chloride transporters in neurons were identified and cloned in the 1990s (Lytle and Forbush, 1992; Payne et al., 1996) so knowledge of their function and plasticity after PNI was not available for interpretation of these earlier electrophysiological studies.

1.6 KCC2 depletion is a mechanism for altered inhibitory signaling in motoneurons

Since $GABA_A$ and glycine receptors are ligand-gated chloride channels, the internal chloride concentration in neurons sets the polarity and efficacy of their synapses. This

concentration is maintained by the balance of activity between chloride extrusion and accumulating mechanisms which, in CNS neurons, depend on isoform 2 of the potassium chloride co-transporter (KCC2) and isoform 1 of the sodium-potassium-chloride co-transporter (NKCC1), respectively (Payne et al., 2003; Kaila et al., 2014; Kahle and Delpire, 2016). KCC2 is an electrically neutral chloride co-transporter that utilizes the potassium gradient to extrude chloride (Kaila et al., 2014). KCC2 has been shown to be downregulated in motoneurons below the area of spinal cord injury (Lee-Hotta et al., 2019) and in motoneurons of the brainstem after peripheral axotomy. Axotomy-induced KCC2 downregulation leading to excitatory responses to GABA was first described in the dorsal motor nucleus of the vagus (DMV), which innervates postganglionic parasympathetic neurons rather than skeletal muscles (Nabekura et al., 2002). Within three days after axotomy or crush of the vagus nerve in young (p16-18) rats, injured motoneurons increased calcium levels and fired action potentials when exposed to GABA or $GABA_A$ receptor agonists. Moreover, KCC2 mRNA expression, but not NKCC1 mRNA, was greatly diminished.

The findings from the DMV have since been recapitulated in facial (Toyoda et al., 2003; Kim et al., 2018) and hypoglossal motoneurons (Tatetsu et al., 2012). KCC2 mRNA almost completely disappears in the facial nucleus three days after nerve transection. This is coupled with a more depolarized E_{Cl}, increased internal chloride concentration, influx of calcium in response to exposure to GABA, and spontaneous calcium oscillations dependent on $GABA_A$ and NMDA receptor activation (Toyoda et al., 2003). In hypoglossal motoneurons, KCC2 protein is decreased within 7 days after injury (Tatetsu et al., 2012).

Milder KCC2 decreases in the cell bodies of spinal motoneurons after spinal cord injury (SCI) also result in significant changes in motoneuron excitability and behavioral motor spasticity (Boulenguez et al., 2010), both reversed by enhancers of KCC2 activity (Sanchez-Brualla et al., 2017). The exact amplitude of chloride changes in motoneurons after SCI is currently controversial and might be much lower than after PNI. The reversal potential of

inhibitory post-synaptic potentials (E_{IPSP}) on alpha motoneurons has been estimated to depolarize by as much as 10 mV when a spinal cord injury is performed in neonatal rats (Boulenguez et al., 2010), but only by 3 mV after chronic SCI in adult rats (Murray et al., 2011). In contrast, after axotomy of adult facial motoneurons, E_{GABA} depolarizes from -70.9 ±5.3 mV (SD) to -52.1 ±5.7 mV, an almost 19 mV shift (Toyoda et al., 2003). In DMV motoneurons injured in 16-18 day-old rats, E_{GABA} shifts by +13.4 mV, from -60.1 ±6.2 mV to -46.7 ±9.8 mV (Nabekura et al., 2002). Despite the reported differences, motoneurons clearly increase internal chloride more following peripheral axotomy than after SCI.

There are also significant differences in the dynamics and mechanisms of KCC2 downregulation in spinal motoneurons caudal to SCI and brainstem motoneurons axotomized peripherally. After SCI, KCC2 downregulation in the somatic membrane is rapid (decrease plateaus 3 days after injury), but incomplete (Boulenguez et al., 2010) relative to what has been shown in brainstem motoneurons after PNI. These differences in KCC2 dynamics suggest different underlying mechanisms. Indeed, while KCC2 mRNA expression decreases in brainstem motoneurons, the same has not been reported after SCI. KCC2 downregulation after SCI is related to decreased descending serotoninergic inputs and reduced activation of 5-hydroxytryptamine (5-HT) type 2A receptors (Bos et al., 2013). Normally, chronic activation of 5HT-2A receptors in the uninjured spinal cord results in a hyperpolarizing shift in E_{Cl} that is dependent on KCC2 chloride extrusion and mediated through a PKC-dependent pathway. G-coupled receptors and calcium mechanisms can rapidly modulate KCC2 function by phosphorylation-dephosphorylation of KCC2 controlling trafficking, endocytosis, or even ion-transport rates (Medina et al., 2014; Doyon et al., 2016b; Kahle and Delpire, 2016; Tang, 2016). These mechanisms are altered after SCI, causing shifts in chloride equilibrium that result in disinhibition and contribute to spasticity, that patients with SCI can sometimes leverage to facilitate motor tasks. After PNI of brainstem motoneurons, the rhythmic oscillations and firing driven by GABA depolarization, NMDA receptor activation, and calcium entry in motoneurons

does not have a motor behavioral correlate because it occurs in regenerating motoneurons disconnected from muscle. This raises the question of why it may be occurring in the first place.

1.7 Thesis Overview: Does KCC2 decrease on axotomized motoneurons have implications for regeneration? Completing the peripheral picture.

Previous literature has shown that PNI induces a variety of changes in chloride transport mechanisms in injured motoneurons, DRG sensory neurons, and postsynaptic spinal interneurons. High intracellular chloride may aid in regeneration of damaged axons in the periphery, particularly in medium and large DRG neurons (Pieraut et al., 2007), but this mechanism has not been investigated in motoneurons until now. The first step to understanding the implications of KCC2 decreases (and the resultant increase in intracellular chloride) is to understand what mechanisms regulate KCC2 following injury so that they may be manipulated. Our pursuit of this question resulted in three aims: 1) Characterization of KCC2 loss on motoneuron somata and proximal dendrites following axotomy. 2) Investigation of the role of established regulators of KCC2 following nervous system injury, namely microglia, BDNF and TrkB. 3) Examination of a potential role of a retrograde signal from the muscle as a regulator of KCC2 presence on the somatic membrane.

1.8 References

Abdulla FA, Stebbing MJ, Smith PA (2001) Effects of substance P on excitability and ionic currents of normal and axotomized rat dorsal root ganglion neurons. Eur J Neursoci 13:545-552.

Aird I (1946) The surgery of peripheral nerve injury. Postgraduate medical journal 22:225-254.

Al-Majed AA, Brushart TM, Gordon T (2000a) Electrical stimulation accelerates and increases expression of BDNF and trkB mRNA in regenerating rat femoral motoneurons. Eur J Neursoci 12:4381-4390.

Al-Majed AA, Neumann CM, Brushart TM, Gordon T (2000b) Brief electrical stimulation promotes the speed and accuracy of motor axonal regeneration. J Neurosci 20:2602-2608.

Alvarez FJ, Taylor-Blake B, Fyffe RE, De Blas AL, Light AR (1996) Distribution of immunoreactivity for the beta 2 and beta 3 subunits of the GABAA receptor in the mammalian spinal cord. J Comp Neurol 365:392-412.

Alvarez FJ, Bullinger KL, Titus HE, Nardelli P, Cope TC (2010) Permanent reorganization of Ia afferent synapses on motoneurons after peripheral nerve injuries. Ann N Y Acad Sci 1198:231-241.

Alvarez-Leefmans, F.J., Gamino, S. M., Giraldez, F., Nogueron, I (1988) Intracellular chloride regulation in amphibian dorsal root ganglion neurones studied with ion-selective microelectrodes. J Physiol. 406:225-46

Amin H, Marinaro F, Tonelli DP, Berdondini L (2017) Developmental excitatory-to-inhibitory GABA-polarity switch is disrupted in 22q11.2 deletion syndrome: a potential target for clinical therapeutics. Sci Rep 7:15752.

Asensio-Pinilla E, Udina E, Jaramillo J, Navarro X (2009) Electrical stimulation combined with exercise increase axonal regeneration after peripheral nerve injury. Exp Neurol 219:258-265.

Ben-Ari Y, Khalilov I, Kahle KT, Cherubini E (2012) The GABA excitatory/inhibitory shift in brain maturation and neurological disorders. Neuroscientist 18:467-486.

Berg A, Zelano J, Stephan A, Thams S, Barres BA, Pekny M, Pekna M, Cullheim S (2012) Reduced removal of synaptic terminals from axotomized spinal motoneurons in the absence of complement C3. Exp Neurol 237:8-17.

Blaesse P, Airaksinen MS, Rivera C, Kaila K (2009) Cation-chloride cotransporters and neuronal function. Neuron 61:820-838.

Blinzinger K, Kreutzberg G (1968) Displacement of synaptic terminals from regenerating motoneurons by microglial cells. Cell Tissue Res 85:145-157.

Bora FW, Jr. (1978) A comparison of epineurial, perineurial and epiperineurial methods of nerve suture. Clin Orthop Relat R 91-94.

Bos R, Sadlaoud K, Boulenguez P, Buttigieg D, Liabeuf S, Brocard C, Haase G, Bras H, Vinay L (2013) Activation of 5-HT2A receptors upregulates the function of the neuronal K-Cl cotransporter KCC2. PNAS 110:348-353.

Boulenguez P, Liabeuf S, Bos R, Bras H, Jean-Xavier C, Brocard C, Stil A, Darbon P, Cattaert D, Delpire E, Marsala M, Vinay L (2010) Down-regulation of the potassium chloride cotransporter KCC2 contributes to spasticity after spinal cord injury. Nat Med 16:302-307.

Brannstrom T, Kellerth JO (1998) Changes in synaptology of adult cat spinal alpha-motoneurons after axotomy. Exp Brain Res 118:1-13.

Brannstrom T, Kellerth JO (1999) Recovery of synapses in axotomized adult cat spinal motoneurons after reinnervation into muscle. Exp Brain Res 125:19-27.

Brushart T (2011) Nerve Repair. New York, New York: Oxford University Press.

Brushart TM (1993) Motor axons preferentially reinnervate motor pathways. J Neurosci 13:2730-2738.
Brushart TM, Mesulam MM (1980) Transganglionic demonstration of central sensory projections from skin and muscle with HRP-lectin conjugates. Neurosci Lett 17:1-6.
Burrow Jle F (1918) Preliminary note on investigations upon one thousand consecutive cases of peripheral nerve injury. BMJ 2:535-538.
Chen DH (1978) Qualitative and quantitative study of synaptic displacement in chromatolyzed spinal motoneurons of the cat. J Comp Neurol 177:635-664.
Choi DW (1992) Excitotoxic cell death. J Neurobiol 23:1261-1276.
Clatworthy AL, Walters ET (1994) Comparative analysis of hyperexcitability and synaptic facilitation induced by nerve injury in two populations of mechanosensory neurones of Aplysia californica. J Exp Biol 190:217-238.
Compston A (2009) From the Archives: A human experiment in nerve division by WHR Rivers MD FRS, Fellow of St. John's College, Cambridge and Henry Head MD FRS, Physician to the London Hospital, Brain 1908: 31; 323-450. Brain 132:2903-2905.
Cope TC, Bonasera SJ, Nichols TR (1994) Reinnervated muscles fail to produce stretch reflexes. J Neurophysiol 71:817-820.
Coull JA, Boudreau D, Bachand K, Prescott SA, Nault F, Sik A, De Koninck P, De Koninck Y (2003) Trans-synaptic shift in anion gradient in spinal lamina I neurons as a mechanism of neuropathic pain. Nature 424:938-942.
Czarnecki A, Le Corronc H, Rigato C, Le Bras B, Couraud F, Scain AL, Allain AE, Mouffle C, Bullier E, Mangin JM, Branchereau P, Legendre P (2014) Acetylcholine controls GABA-, glutamate-, and glycine-dependent giant depolarizing potentials that govern spontaneous motoneuron activity at the onset of synaptogenesis in the mouse embryonic spinal cord. J Neurosci 34:6389-6404.
de Ruiter GC, Spinner RJ, Verhaagen J, Malessy MJ (2014) Misdirection and guidance of regenerating axons after experimental nerve injury and repair. J Neurosurg 120:493-501.
Doyon N, Vinay L, Prescott SA, De Koninck Y (2016a) Chloride Regulation: A Dynamic Equilibrium Crucial for Synaptic Inhibition. Neuron 89:1157-1172.
Doyon N, Ferrini F, Gagnon M, De Koninck Y (2016b) Treating pathological pain: is KCC2 the key to the gate? Pain 13:469-471.
Eccles JC, Fatt P, Koketsu K (1954) Cholinergic and inhibitory synapses in a pathway from motor-axon collaterals to motoneurones. J Physiol 126:524-562.
Eccles JC, Libet B, Young RR (1958) The behaviour of chromatolysed motoneurones studied by intracellular recording. J Physiol 143:11-40.
Eftekhari S, Mehvari Habibabadi J, Najafi Ziarani M, Hashemi Fesharaki SS, Gharakhani M, Mostafavi H, Joghataei MT, Beladimoghadam N, Rahimian E, Hadjighassem MR (2013) Bumetanide reduces seizure frequency in patients with temporal lobe epilepsy. Epilepsia 54:e9-12.
Elzinga K, Tyreman N, Ladak A, Savaryn B, Olson J, Gordon T (2015) Brief electrical stimulation improves nerve regeneration after delayed repair in Sprague Dawley rats. Exp Neurol 269:142-153.
English AW (2005) Enhancing axon regeneration in peripheral nerves also increases functionally inappropriate reinnervation of targets. J Comp Neurol 490:427-441.
English AW, Cucoranu D, Mulligan A, Sabatier M (2009) Treadmill training enhances axon regeneration in injured mouse peripheral nerves without increased loss of topographic specificity. J Comp Neurol 517:245-255.
English AW, Schwartz G, Meador W, Sabatier MJ, Mulligan A (2007) Electrical stimulation promotes peripheral axon regeneration by enhanced neuronal neurotrophin signaling. Dev Neurobiol 67:158-172.

Ferrini F, De Koninck Y (2013) Microglia control neuronal network excitability via BDNF signalling. Neural Plast 2013:429815.
Fu SY, Gordon T (1995a) Contributing factors to poor functional recovery after delayed nerve repair: prolonged denervation. J Neurosci 15:3886-3895.
Fu SY, Gordon T (1995b) Contributing factors to poor functional recovery after delayed nerve repair: prolonged axotomy. J Neurosci 15:3876-3885.
Fuchs A, Ringer C, Bilkei-Gorzo A, Weihe E, Roeper J, Schutz B (2010) Downregulation of the potassium chloride cotransporter KCC2 in vulnerable motoneurons in the SOD1-G93A mouse model of amyotrophic lateral sclerosis. J Neuropath Exp Neur 69:1057-1070.
Gao BX, Stricker C, Ziskind-Conhaim L (2001) Transition from GABAergic to glycinergic synaptic transmission in newly formed spinal networks. J Neurophysiol 86:492-502.
Gonzalez-Forero D, Alvarez FJ (2005) Differential postnatal maturation of GABAA, glycine receptor, and mixed synaptic currents in Renshaw cells and ventral spinal interneurons. J Neurosci 25:2010-2023.
Gonzalez-Forero D, Moreno-Lopez B (2014) Retrograde response in axotomized motoneurons: nitric oxide as a key player in triggering reversion toward a dedifferentiated phenotype. Neuroscience 283:138-165.
Gonzalez-Forero D, Portillo F, Gomez L, Montero F, Kasparov S, Moreno-Lopez B (2007) Inhibition of resting potassium conductances by long-term activation of the NO/cGMP/protein kinase G pathway: a new mechanism regulating neuronal excitability. J Neurosci 27:6302-6312.
Gordon T (2009) The role of neurotrophic factors in nerve regeneration. Nurosurg Focus 26:E3.
Gordon T, English AW (2016) Strategies to promote peripheral nerve regeneration: electrical stimulation and/or exercise. Eur J Neursoci 43:336-350.
Gordon T, Stein RB, Thomas CK (1986) Organization of motor units following cross-reinnervation of antagonistic muscles in the cat hind limb. J Physiol 374:443-456.
Gordon T, Brushart TM, Amirjani N, Chan KM (2007) The potential of electrical stimulation to promote functional recovery after peripheral nerve injury--comparisons between rats and humans. Acta Neurochir Suppl 100:3-11.
Gordon T, Amirjani N, Edwards DC, Chan KM (2010) Brief post-surgical electrical stimulation accelerates axon regeneration and muscle reinnervation without affecting the functional measures in carpal tunnel syndrome patients. Exp Neurol 223:192-202.
Grinsell D, Keating CP (2014) Peripheral nerve reconstruction after injury: a review of clinical and experimental therapies. Biomed Res Int 2014:698256.
Gustafsson B (1979) Changes in motoneurone electrical properties following axotomy. J Physiol 293:197-215.
Gustafsson B, Pinter MJ (1984) Effects of axotomy on the distribution of passive electrical properties of cat motoneurones. J Physiol 356:433-442.
Hamilton SK, Hinkle ML, Nicolini J, Rambo LN, Rexwinkle AM, Rose SJ, Sabatier MJ, Backus D, English AW (2011) Misdirection of regenerating axons and functional recovery following sciatic nerve injury in rats. J Comp Neurol 519:21-33.
Hanson MG, Milner LD, Landmesser LT (2008) Spontaneous rhythmic activity in early chick spinal cord influences distinct motor axon pathfinding decisions. Brain Res Rev 57:77-85.
Höke A, Brushart T (2010) Challenges and Opportunities for Regeneration in the Peripheral Nervous System. Exp Neurol 223:1-4.
Holmes W, Young JZ (1942) Nerve regeneration after immediate and delayed suture. J Anat 77:63-96.10.
Huang YJ, Lee KH, Murphy L, Garraway SM, Grau JW (2016) Acute spinal cord injury (SCI) transforms how GABA affects nociceptive sensitization. Exp Neurol 285:82-95.

Huizar P, Kuno M, Kudo N, Miyata Y (1977) Reaction of intact spinal motoneurones to partial denervation of the muscle. J Physiol 265:175-191.
Iwahashi Y, Furuyama T, Inagaki S, Morita Y, Takagi H (1994) Distinct regulation of sodium channel types I, II and III following nerve transection. Brain Res Mol Brain Res 22:341-345.
Jaiswal PB, Tung JK, Gross RE, English AW (2017) Motoneuron activity is required for enhancements in functional recovery after peripheral nerve injury in exercised female mice. J Neurosci Res.
Jaiswal PB, Mistretta OC, Ward PJ, English AW (2018) Chemogenetic Enhancement of Axon Regeneration Following Peripheral Nerve Injury in the SLICK-A Mouse. Brain Sci 8.
Jensen TS, Gottrup H, Sindrup SH, Bach FW (2001) The clinical picture of neuropathic pain. Eur J Pharmacol 429:1-11.
Kahle KT, Delpire E (2016) Kinase-KCC2 coupling: Cl- rheostasis, disease susceptibility, therapeutic target. J Neurophysiol 115:8-18.
Kahle KT, Khanna A, Clapham DE, Woolf CJ (2014) Therapeutic restoration of spinal inhibition via druggable enhancement of potassium chloride cotransporter KCC2-mediated chloride extrusion in peripheral neuropathic pain. JAMA Neurol 71:640-645.
Kahle KT, Staley KJ, Nahed BV, Gamba G, Hebert SC, Lifton RP, Mount DB (2008) Roles of the cation-chloride cotransporters in neurological disease. Nat Clin Pract Neurol 4:490-503.
Kaila K, Price TJ, Payne JA, Puskarjov M, Voipio J (2014) Cation-chloride cotransporters in neuronal development, plasticity and disease. Nat Rev Neurosci 15:637-654.
Kasumacic N, Glover JC, Perreault MC (2012) Vestibular-mediated synaptic inputs and pathways to sympathetic preganglionic neurons in the neonatal mouse. J Physiol 590:5809-5826.
Kim J, Kobayashi S, Shimizu-Okabe C, Okabe A, Moon C, Shin T, Takayama C (2018) Changes in the expression and localization of signaling molecules in mouse facial motor neurons during regeneration of facial nerves. J Chem Neuroanat 88:13-21.
Kim YI, Na HS, Kim SH, Han HC, Yoon YW, Sung B, Nam HJ, Shin SL, Hong SK (1998) Cell type-specific changes of the membrane properties of peripherally-axotomized dorsal root ganglion neurons in a rat model of neuropathic pain. Neuroscience 86:301-309.
Kourdougli N, Pellegrino C, Renko JM, Khirug S, Chazal G, Kukko-Lukjanov TK, Lauri SE, Gaiarsa JL, Zhou L, Peret A, Castren E, Tuominen RK, Crepel V, Rivera C (2017) Depolarizing gamma-aminobutyric acid contributes to glutamatergic network rewiring in epilepsy. Ann Neurol 81:251-265.
Kouyoumdjian JA (2006) Peripheral nerve injuries: a retrospective survey of 456 cases. Muscle Nerve 34:785-788.
Krarup C, Archibald SJ, Madison RD (2002) Factors that influence peripheral nerve regeneration: an electrophysiological study of the monkey median nerve. Ann Neurol 51:69-81.
Kuno M, Llinas R (1970) Alterations of synaptic action in chromatolysed motoneurones of the cat. J Physiol 210:823-838.
Kuno M, Miyata Y, Munoz-Martinez EJ (1974) Differential reaction of fast and slow alpha-motoneurones to axotomy. J Physiol 240:725-739.
Landmesser LT (2018) General principles of spinal motor circuit development: early contributions from research on avian embryos. Int J Dev Biol 62:235-243.
Lee-Hotta S, Uchiyama Y, Kametaka S (2019) Role of the BDNF-TrkB pathway in KCC2 regulation and rehabilitation following neuronal injury: A mini review. Neurochem Int 128:32-38.
Linda H, Shupliakov O, Ornung G, Ottersen OP, Storm-Mathisen J, Risling M, Cullheim S (2000) Ultrastructural evidence for a preferential elimination of glutamate-

immunoreactive synaptic terminals from spinal motoneurons after intramedullary axotomy. J Comp Neurol 425:10-23.
Lu Y, Zheng J, Xiong L, Zimmermann M, Yang J (2008) Spinal cord injury-induced attenuation of GABAergic inhibition in spinal dorsal horn circuits is associated with down-regulation of the chloride transporter KCC2 in rat. J Physiol 586:5701-5715.
Lundborg G (2002) Enhancing posttraumatic nerve regeneration. J Peripher Nerv Syst 7:139-140.
Lundborg G (2003) Richard P. Bunge memorial lecture. Nerve injury and repair--a challenge to the plastic brain. J Peripher Nerv Syst 8:209-226.
Lytle C, Forbush B, 3rd (1992) The Na-K-Cl cotransport protein of shark rectal gland. II. Regulation by direct phosphorylation. J Biol Chem 267:25438-25443.
Malek SA, Coderre E, Stys PK (2003) Aberrant chloride transport contributes to anoxic/ischemic white matter injury. J Neurosci 23:3826-3836.
Mao S, Garzon-Muvdi T, Di Fulvio M, Chen Y, Delpire E, Alvarez FJ, Alvarez-Leefmans FJ (2012) Molecular and functional expression of cation-chloride cotransporters in dorsal root ganglion neurons during postnatal maturation. J Neurophysiol 108:834-852.
Medina I, Friedel P, Rivera C, Kahle KT, Kourdougli N, Uvarov P, Pellegrino C (2014) Current view on the functional regulation of the neuronal K(+)-Cl(-) cotransporter KCC2. Front Cell Neurosci 8:27.
Modol L, Santos D, Cobianchi S, Gonzalez-Perez F, Lopez-Alvarez V, Navarro X (2015) NKCC1 Activation Is Required for Myelinated Sensory Neurons Regeneration through JNK-Dependent Pathway. J Neurosci 35:7414-7427.
Mundie GS (1920) Peripheral Nerve Injuries. CMAJ 10:294-296.
Murray KC, Stephens MJ, Rank M, D'Amico J, Gorassini MA, Bennett DJ (2011) Polysynaptic excitatory postsynaptic potentials that trigger spasms after spinal cord injury in rats are inhibited by 5-HT1B and 5-HT1F receptors. J Neurophysiol 106:925-943.
Nabekura J, Ueno T, Okabe A, Furuta A, Iwaki T, Shimizu-Okabe C, Fukuda A, Akaike N (2002) Reduction of KCC2 Expression and GABAa Receptor-Mediated Excitation after In Vivo Axonal Injury. J Neurosci 22:4412-4417.
Navarro X, Vivo M, Valero-Cabre A (2007) Neural plasticity after peripheral nerve injury and regeneration. Prog Neurobiol 82:163-201.
Nishimura Y, Asahara T, Yamamoto T, Tanaka T (1992) Observations on morphology and electrophysiological properties of the normal and axotomized facial motoneurons in the cat. Brain Res 596:305-310.
Oliveira AL, Thams S, Lidman O, Piehl F, Hokfelt T, Karre K, Linda H, Cullheim S (2004) A role for MHC class I molecules in synaptic plasticity and regeneration of neurons after axotomy. Proc Natl Acad Sci USA 101:17843-17848.
Payne JA, Stevenson TJ, Donaldson LF (1996) Molecular characterization of a putative K-Cl cotransporter in rat brain. A neuronal-specific isoform. J Biol Chem 271:16245-16252.
Payne JA, Rivera C, Voipio J, Kaila K (2003) Cation-chloride co-transporters in neuronal communication, development and trauma. Trends Neurosci 26:199-206.
Pieraut S, Laurent-Matha V, Sar C, Hubert T, Mechaly I, Hilaire C, Mersel M, Delpire E, Valmier J, Scamps F (2007) NKCC1 phosphorylation stimulates neurite growth of injured adult sensory neurons. J Neurosci 27:6751-6759.
Prescott SA, Sejnowski TJ, De Koninck Y (2006) Reduction of anion reversal potential subverts the inhibitory control of firing rate in spinal lamina I neurons: towards a biophysical basis for neuropathic pain. Mol Pain 2:32.
Price TJ, Cervero F, de Koninck Y (2005) Role of Cation-Chloride-Cotransporters (CCC) in Pain and Hyperalgesia. Curr Top Med Chem 5:547-555.
Price TJ, Cervero F, Gold MS, Hammond DL, Prescott SA (2009) Chloride regulation in the pain pathway. Brain Res Rev 60:149-170.

Romer SH, Dominguez KM, Gelpi MW, Deardorff AS, Tracy RC, Fyffe RE (2014) Redistribution of Kv2.1 ion channels on spinal motoneurons following peripheral nerve injury. Brain Res 1547:1-15.
Rudomin P, Schmidt RF (1999) Presynaptic inhibition in the vertebrate spinal cord revisited. Exp Brain Res 129:1-37.
Sabatier MJ, Redmon N, Schwartz G, English AW (2008) Treadmill training promotes axon regeneration in injured peripheral nerves. Exp Neurol 211:489-493.
Sabatier MJ, To BN, Nicolini J, English AW (2011) Effect of axon misdirection on recovery of electromyographic activity and kinematics after peripheral nerve injury. Cells Tissues Organs 193:298-309.
Sanchez-Brualla I, Boulenguez P, Brocard C, Liabeuf S, Viallat-Lieutaud A, Navarro X, Udina E, Brocard F (2018) Activation of 5-HT2A receptors restores KCC2 function and reduces neuropathic pain after spinal cord injury. Neuroscience 387:48-57.
Scholz T, Krichevsky A, Sumarto A, Jaffurs D, Wirth GA, Paydar K, Evans GR (2009) Peripheral nerve injuries: an international survey of current treatments and future perspectives. J Reconstr Microsurg 25:339-344.
Seltzer Z, Dubner R, Shir Y (1990) A novel behavioral model of neuropathic pain disorders produced in rats by partial sciatic nerve injury. Pain 43:205-218.
Sernagor E, Chabrol F, Bony G, Cancedda L (2010) GABAergic control of neurite outgrowth and remodeling during development and adult neurogenesis: general rules and differences in diverse systems. Front Cell Neurosci 4:11.
Skold C (2000) Spasticity in spinal cord injury: self- and clinically rated intrinsic fluctuations and intervention-induced changes. Arch Phys Med Rehabil 81:144-149.
Steffensen I, Dulin MF, Walters ET, Morris CE (1995) Peripheral regeneration and central sprouting of sensory neurone axons in Aplysia californica following nerve injury. J Exp Biol 198:2067-2078.
Stil A, Jean-Xavier C, Liabeuf S, Brocard C, Delpire E, Vinay L, Viemari JC (2011) Contribution of the potassium chloride co-transporter KCC2 to the modulation of lumbar spinal networks in mice. Eur J Neursoci 33:1212-1222.
Sumner BE (1975) A quantitative analysis of boutons with different types of synapse in normal and injured hypoglossal nuclei. Exp Neurol 49:406-417.
Sumner BE (1976) Quantitative ultrastructural observations on the inhibited recovery of the hypoglossal nucleus from the axotomy response when regeneration of the hypoglossal nerve is prevented. Exp Brain Res 26:141-150.
Sumner BE, Sutherland FI (1973) Quantitative electron microscopy on the injured hypoglossal nucleus in the rat. J neurocytol 2:315-328.
Sunderland S (1952) Factors influencing the course of regeneration and the quality of the recovery after nerve suture. Brain 75:19-54.
Sunico CR, Gonzalez-Forero D, Dominguez G, Garcia-Verdugo JM, Moreno-Lopez B (2010) Nitric oxide induces pathological synapse loss by a protein kinase G-, Rho kinase-dependent mechanism preceded by myosin light chain phosphorylation. J Neurosci 30:973-984.
Takata M (1981) Lingually induced inhibitory postsynaptic potentials in hypoglossal motoneurons after axotomy. Brain Res 224:165-169.
Takata M, Nagahama T (1983) Synaptic efficacy of inhibitory synapses in hypoglossal motoneurons after transection of the hypoglossal nerves. Neuroscience 10:23-29.
Takata M, Tomomune N (1986) Properties of postsynaptic potentials evoked in hypoglossal motoneurons by inferior alveolar nerve stimulation. Exp Neurol 93:117-127.
Tang BL (2016) K(+)-Cl(-) co-transporter 2 (KCC2) - a membrane trafficking perspective. Mol Membr Biol 33:100-110.

Tao R, Li C, Newburn E, Tianzhang Y, Lipska BK, Herman MM, Weinburger DR, Kleinman JE, Hyde TM (2012) Transcript-Specific Associations of SLC12A5 (KCC2) in Human Prefrontal Cortex with Development, Schizophrenia and Affective Disorders. J Neurosci 32:5216-5222.
Tatetsu M, Kim J, Kina S, Sunakawa H, Takayama C (2012) GABA/glycine signaling during degeneration and regeneration of mouse hypoglossal nerves. Brain Res 1446:22-33.
Taylor CA, Braza D, Rice JB, Dillingham T (2008) The incidence of peripheral nerve injury in extremity trauma. Am J Phys Med Rehabil 87:381-385.
Toyoda H, Ohno K, Yamada J, Ikeda M, Okabe A, Sato K, Hashimoto K, Fukuda A (2003) Induction of NMDA and GABAA receptor-mediated Ca2+ oscillations with KCC2 mRNA downregulation in injured facial motoneurons. J Neurophysiol 89:1353-1362.
Udina E, Puigdemasa A, Navarro X (2011) Passive and active exercise improve regeneration and muscle reinnervation after peripheral nerve injury in the rat. Muscle Nerve 43:500-509.
Ungless MA, Gasull X, Walters ET (2002) Long-term alteration of S-type potassium current and passive membrane properties in aplysia sensory neurons following axotomy. J Neurophysiol 87:2408-2420.
Valdez G, Heyer MP, Feng G, Sanes JR (2014) The role of muscle microRNAs in repairing the neuromuscular junction. PloS one 9:e93140.
Valverde MA, Bond TD, Hardy SP, Taylor JC, Higgins CF, Altamirano J, Alvarez-Leefmans FJ (1996) The multidrug resistance P-glycoprotein modulates cell regulatory volume decrease. EMBO J 15:4460-4468.
Vaughan DW (1994) Effects of peripheral axotomy on presynaptic axon terminals with GABA-like immunoreactivity. Anat Rec 238:248-262.
Vucic S, Rutkove SB (2018) Neurophysiological biomarkers in amyotrophic lateral sclerosis. Curr Opin Neurol 31:640-647.
Ward PJ, Clanton SL, 2nd, English AW (2018) Optogenetically enhanced axon regeneration: motor versus sensory neuron-specific stimulation. Eur J Neursoci 47:294-304.
Ward PJ, Jones LN, Mulligan A, Goolsby W, Wilhelm JC, English AW (2016) Optically-Induced Neuronal Activity Is Sufficient to Promote Functional Motor Axon Regeneration In Vivo. PloS one 11:e0154243.
Wen Y-R, Tan P-H, Cheng J-K, Liu Y-C, Ji R-R (2011) Microglia: A Promising Target for Treating Neuropathic and Postoperative Pain, and Morphine Tolerance. JFMA 110:487-494.
Woolf CJ, Walters ET (1991) Common patterns of plasticity contributing to nociceptive sensitization in mammals and Aplysia. Trends Neurosci 14:74-78.
Zhang JM, Donnelly DF, Song XJ, Lamotte RH (1997) Axotomy increases the excitability of dorsal root ganglion cells with unmyelinated axons. J Neurophysiol 78:2790-2794.

Chapter 2: General Methods

2.1 General Methods

Animal care, procedures, and euthanasia were performed under prior approval by the Institutional Animal Care and Use Committee of Emory University and in accordance with the NIH Guide for the Care and Use of Laboratory Animals. The majority of experiments described used similar design, experimental practices, and quantitative measures. As such, we describe below the techniques used consistently throughout experiments. More specific details on animal genotypes, unique procedures, and experiment-specific methods are described in text associated with specific aims (Chapter 3-Appendix 1).

2.2 Animals

Several lines of transgenic, in addition to wild type, mice of both sexes were used. Except where noted, mice were obtained from The Jackson Laboratory (Bar Harbor, ME) and maintained on a mixed C57Blk/6J and 6N background.

2.3 Tamoxifen treatment

When using tamoxifen-inducible cre mice, the drug (0.75mg/20g body weight, prepared in 10% ethanol, 90% sunflower oil) was administered via modified gavage once a day for three days. Animals were allowed to recover for two weeks, and dosed again for three days to ensure complete induction of cre expression. The procedure was used in experiments using SLICK and *Cx3CR1*$^{CreER/+}$ animals (described in detail in appropriate sections). This protocol has been well established as sufficient to induce recombinase activity in SLICK animals (Wilhelm et al., 2012; Zhu et al., 2016). There was a minimum of three weeks between treatment and sciatic nerve injuries in SLICK animals. In *Cx3cr1*$^{creER/+}$ animals, this interval was extended to five weeks to ensure specificity of gene deletions within only microglia, as described below.

2.4 Retrograde tracer injections

This study focused on one motor pool axotomized after sciatic nerve injuries, the motoneurons innervating the lateral gastrocnemius (LG) muscle. Unless otherwise described, LG motoneurons were retrogradely labeled by intramuscular injection of the long-lasting, non-toxic tracer Fast Blue (® Polysciences, Inc., Eppelheim, Germany) (Bentivoglio et al., 1980). Fast Blue (FB) was injected unilaterally or bilaterally into the LG muscles of adult animals. The animals were anesthetized with isoflurane (4% induction, 2% maintenance) and given pre-operative buprenorphine (0.05 mg/kg, i.p.) to manage possible post-operative pain. Once the animals reached a surgical plane of anesthesia, a small skin incision was made to expose the LG muscle, and a 10 µl Hamilton syringe was introduced to inject 2-5 µl of a 1.5% FB solution into the belly of the muscle. Skin incisions were sutured and the animals were allowed to recover for at least 7 days prior to nerve surgery to ensure complete retrograde transport.

2.5 Surgeries

All nerve surgeries were performed under isoflurane anesthesia (4% induction, 2% maintenance) and the animals were given pre-operative 0.05 mg/kg buprenorphine (i.p.), as before. The sciatic nerve, which includes the axons of the LG and other hind limb motoneurons, was exposed by a mid-thigh skin incision and blunt dissection of the overlying biceps femoris. In animals in the cut/ligated condition, a silk suture was tied tightly around the sciatic nerve and then cut with sharp microscissors ~2 mm below the ligation. In animals of the transection/repair condition, a small rectangle of SILASTIC® film (Dow Corning No. 501-1) was placed beneath the nerve where it was secured with fibrin glue (~5 µL, 2:1:1 thrombin, fibrinogen, fibronectin; (thrombin, MP BioChemicals, LLC Cat#154163, E.C. 3.4.21.5; fibrinogen, Sigma Cat#F3879, E.C. 2325986; fibronectin, Sigma Ca#F1141, E.C. 2891492)) prior to transecting the nerve. In this manner we assured that the proximal and distal segments were aligned and held in position, as has been described elsewhere (English, 2005; Sabatier et al.,

2008; Akhter et al., 2019). Sham animals had the sciatic nerve exposed but not transected. In all animals, the incision was then closed in layers and animals were removed from anesthesia.

2.6 Tissue collection, processing and immunocytochemistry

Animals were allowed to survive 3, 7, 14, 21, 28 or 60 days after nerve surgeries, depending on the experiment. They were then overdosed with Euthasol (100 mg/kg) and transcardially perfused with saline-heparin followed by paraformaldehyde (PFA) (4% in 0.1M phosphate buffer). The spinal cord and injected muscles were harvested and postfixed overnight in 4% PFA prior to cryoprotection in 30% sucrose for at least 24 hours. The spinal cord dura was then removed and the L3-L5 segments isolated. The spinal cords were sectioned in a transverse plane on a freezing sliding microtome at 50 μm thickness and collected free-floating. In preliminary experiments we found a significant change in KCC2 immunolabeling intensity throughout the 50 μm thickness of the sections. To improve antibody penetration, the sections were heated for 20 minutes in 0.01 M sodium citrate with 0.05% tween (pH = 6, maximum temperature 95˚C), washed in 0.01M phosphate buffered saline with 0.3% Triton (PBST), and blocked in normal donkey serum (NDS, 10% in PBS with 1% Triton) for 1 hour. The tissue was then incubated, while shaking for two nights (also to enhance penetration of KCC2 immunostaining) at room temperature, with a mixture of appropriate primary antibodies diluted in PBST. Sections were reacted with primary antibodies against KCC2 and NeuN, and some sections additionally included antibodies to detect microglia (anti-Iba1 or anti-GFP for CX3CR1-GFP amplification in mice carrying this reporter protein). The list of antibodies used, their sources, dilutions used, and RRID numbers are in Table 2.1.

The primary antibody against KCC2 was raised against a peptide sequence containing aa 932 – 1043, which is shared by both KCC2 isoforms (KCC2a and KCC2b) and has been validated in KCC2 knockout tissue (Spoljaric et al., 2019). Sections were then washed in PBST and incubated with appropriate fluorescent-coupled species-specific secondary antibodies for two

hours (Table 2.2, 1:100 in PBST). Immunoreactivity (IR) to KCC2 was visualized after incubating with an AlexaFluor® 647-coupled secondary antibody, NeuN-IR with Cyanine Cy3-coupled antibody, and Iba1-IR or GFP with Fluorescein (FITC)-coupled secondary antibodies. LG motoneurons retrogradely labeled with FB were visualized by their fluorescence (Excitation 405 nm; Emission 420 nm). After washing, the sections were coverslipped with VectaShield (VectorLabs cat# H-1000) and imaged on an Olympus FLUOVIEW FV1000 Confocal Microscope with 10X or 20X objectives and then at high-magnification using a 60X objective with no digital zoom (NA, 1.35, oil-immersion).

2.7 Quantification of KCC2 immunoreactivity on the cell surface

Motoneurons in which somatic KCC2 levels were measured were always filled with Fast Blue (FB) and imaged at 60x1. Unless indicated otherwise, 10 FB+ motoneurons ipsilateral to the injury were analyzed. In the case of animals with the contralateral side used as intact control, 10 FB+ motoneurons were also analyzed on the contralateral side. For all motoneurons, a single z-plane (focal depth ~ 0.49 μm at 633 nm excitation with refractory index n = 1.518 oil immersion 60X objective of NA 1.35) was selected for each FB labeled motoneuron studied. These planes always included a nucleolus and had minimal dendritic departures from the soma. NeuN immunoreactivity was used to aid in finding mid-plane optical sections within the z-stack. KCC2 immunofluorescence intensity around the soma of each motoneuron was quantified using FIJI (Figure 2.1). The Wand (tracing) Tool (Mode: 8-connected, Tolerance: 1000) was used to automatically select the edge of the labeled soma containing FB. This tracing was converted to a 0.42 μm width line superimposed on the neuronal plasma membrane. The average KCC2 Cy5 fluorescent intensity along the line was calculated (gray level, 12 bits). In each section, background measurements were taken from a 9 μm^2 square region of the neuropil in the same optical plane, adjacent to the motoneurons and lacking labeled dendrites. KCC2 immunofluorescence was corrected against this background level by calculating the percent

higher than background [100*(membrane intensity average - background intensity average) / average background intensity].

Data points are presented as averages for each animal, each obtained from 10 motoneurons per animal and side of the spinal cord. Different conditions (i.e., injury, sham, time after injury, genotype, spinal cord side) were compared by obtaining averages of n = 4 to 7 animals per group.

2.8 Statistical Analysis

Statistical tests were performed as described in the results and (power > 0.8) for alpha < 0.05. Data were evaluated with t-tests or one- or two- way ANOVA as appropriate (see statistical tables in respective chapters). Bonferroni post-hoc multiple comparisons tests were performed against controls (WT or transgene negative control animals) unless otherwise described.

2.9 Tables and Figures

Table 2.1 Primary antibodies utilized for immunohistochemistry (IHC)

Antigen	Immunogen	Host/type	Manufacturer	RRID #	Dilution
KCC2	N-terminal His-tag fusion protein; pan-rat KCC2; aa 932-1043	Rabbit/ polyclonal	EMD Millipore catalog #07-432,	AB_1121 3615	1:500
NeuN	Purified cell nuclei from mouse brain	Mouse/ monoclonal A60 clone	EMD Millipore catalog #MAB377	AB_2298 772	1:500
EGFP	Recombinant GFP 6-his tag	Chicken/ polyclonal	Serotec catalog #obt1644	AB_1000 0240	1:1000
Iba1	C-terminus of Iba1	Goat/ polyclonal	Novus catalog #NB 100-1028,	AB_5215 94	1:500

Table 2.2 Secondary antibodies utilized for immunohistochemistry (IHC)

Antigen	Manufacturer	RRID#
AlexaFluor® 647 α Rabbit IgG	Jackson ImmunoResearch Labs Cat# 711-605-152	AB_2492288
Cyanine Cy™3 (Cy3 α Mouse) IgG	Jackson ImmunoResearch Labs Cat# 715-165-150	AB_2340813
Fluorescein (FITC) α Chicken IgG	Jackson ImmunoResearch Labs Cat# 703-095-155	AB_2340356
Fluorescein (FITC) α Goat IgG	Jackson ImmunoResearch Labs Cat# 705-095-147	AB_2340401

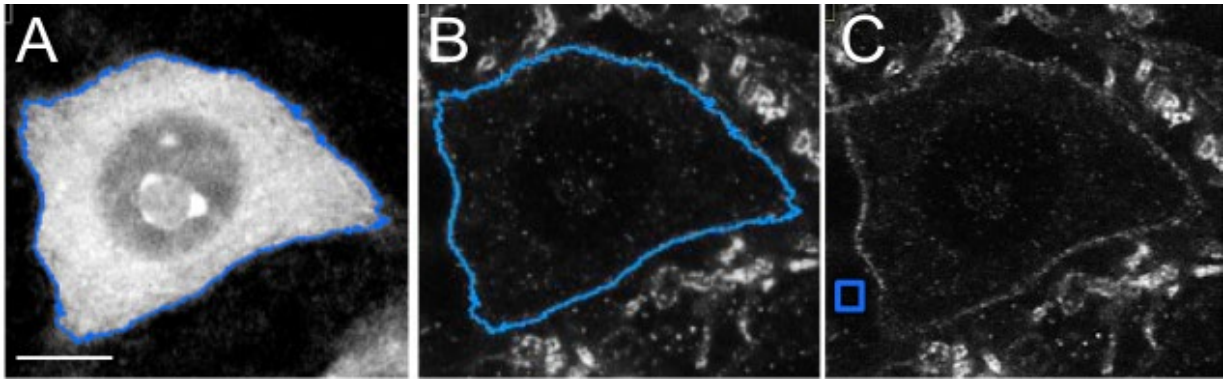

Figure 2.1 Method of KCC2 immunofluorescence quantification on the motoneuron surface. Images of sham-injured LG motoneuron are used to show the method of KCC2 quantification. Scale bar = 10 μm. **A)** Sham-injured LG motoneuron filled with Fast Blue. The blue line marks the automatic tracing of the soma. **B)** Image of the KCC2 channel of same motoneuron with the cell membrane line from which fluorescent intensity is measured. **C)** KCC2 immunofluorescence with example 9 μm^2 of area from which background fluorescence was measured.

2.10 References

Akhter ET*, Rotterman TM*, English AW, Alvarez FJ (2019) Sciatic nerve cut and repair using fibrin glue in mice. Bio Protoc (Resubmitted after revision, July 2019). **these authors contributed equally to the work*

Bentivoglio M, Kuypers HG, Catsman-Berrevoets CE, Loewe H, Dann O (1980) Two new fluorescent retrograde neuronal tracers which are transported over long distances. Neurosci Lett 18:25-30.

Spoljaric I, Spoljaric A, Mavrovic M, Seja P, Puskarjov M, Kaila K (2019) KCC2-Mediated Cl(-) Extrusion Modulates Spontaneous Hippocampal Network Events in Perinatal Rats and Mice. Cell Rep 26:1073-1081.e1073.

Chapter 3: Characteristics of KCC2 loss on motoneuron somata and proximal dendrites following axotomy

---

Modified from the following reference:

Akhter, E.T., Griffith, R., English, A.W., Alvarez, F.J. Removal of the potassium chloride co-transporter KCC2 from the somatodendritic membrane of axotomized motoneurons is independent of BDNF/TrkB signaling but is controlled by neuromuscular innervation. eNeuro. Submitted May 9, 2019. *Currently being revised after reviews.*

3.1 Abstract

We investigated the time course and degree of KCC2 depletion on spinal motoneurons following peripheral axotomy. The loss of KCC2 protein is robust, but slower, than has been reported in the dorsal horn after PNI or in motoneurons caudal to SCI. The loss of protein is preceded by a disappearance of KCC2 mRNA, as has been reported in other motoneuron populations following PNI. Interestingly, we also observed KCC2 mRNA in the dendrites of intact neurons that similarly disappeared after injury. KCC2 was also lost from proximal dendrites, but remained in a gradient along the dendritic length. Almost all dendritic terminations were covered with dense KCC2 protein immunoreactivity that was retained after axotomy. Thus, it is possible that dendritic KCC2 has a different oligomeric composition or is composed of a distinct isoform than the KCC2 found on the soma or proximal dendrite. These possibilities remain for future studies intended to parse the organization and function of KCC2 on different somatodendritic components of motoneurons.

3.2 Introduction

KCC2 loss has previously been described in spinal motoneurons following spinal cord injury (Boulenguez et al., 2010; Bos et al., 2013; Lee-Hotta et al., 2019) and in brainstem motoneurons following axotomy (Nabekura et al., 2002; Toyoda et al., 2003; Tatetsu et al., 2012; Kim et al., 2018), but there have been no previous studies confirming that KCC2 is also lost from motoneurons in the spinal cord following PNI. As such, it was necessary to verify the disappearance of KCC2, determine the degree and time course of the loss, and describe the spatial properties of KCC2 disappearance along the motoneuron somatodendritic membrane in our model. While we expected a robust loss on the soma, at least in the initial times after injury, we were concerned that if KCC2 was preserved on dendrites it may dampen any effects of chloride accumulation within the soma by serving as a functional siphon. Our initial observations showed that KCC2 was not evenly depleted in the neuropil surrounding injured

motoneurons. As such, we performed additional experiments to observe the full dendritic arbor of motoneurons and KCC2 distribution following injury. To label full dendritic arbors we infected motoneurons with isotype 1 adeno-associated viral vectors (AAV1) carrying the gene for the fluorescent reporter protein mCherry. Preliminary results from the Alvarez lab showed that neonatal muscle injections of AAV1 results in robust infection of motoneurons and stable expression of AAV1 delivered genes up to 6 months after infection without affecting motoneuron viability (Gomez-Perez et al., 2016). After PNI, KCC2 is reduced on the membrane of lamina I nociceptive neurons through mechanisms that involve nearby activated microglia (Coull et al., 2005). It is also well known that microglia activate around axotomized motoneurons and fully enwrap their cell bodies (Aldskogius, 2011). To analyze whether there is temporal relationship between KCC2 downregulation and microgliosis around axotomized motoneurons the experiments were performed in an animal model that robustly labels microglia with GFP (CX3CR1-GFP knock-in, Jung et al., 2000).

Finally, we analyzed whether KCC2 loss occurred through post-translational mechanisms affecting the balance between KCC2 insertion and removal from the membrane (as it occurs in spinal motoneurons after spinal cord injury; Boulenguez et al., 2010, or lamina I neurons after PNI; Coull et al., 2005) or by a downregulation of KCC2 gene expression (as occurs in brainstem motoneurons after axotomy; Nabekura et al., 2002; Toyoda et al., 2003; Tatetsu et al., 2012; Kim et al., 2018). To meet this goal we compared the time course of KCC2 protein loss throughout the somatodendritic membrane with loss of *kcc2* mRNA in the cell body. KCC2 mRNA was detected using RNA-Scope®, a new and enhanced in situ hybridization technique (Wang et al., 2012).

Together, these experiments provide a full description of the process of KCC2 removal from the somatodendritic arbor of axotomized motoneurons and its recovery after regeneration. This provides a starting point for investigating the mechanisms that may be inducing the loss after injury in Chapter 4 and mechanisms of recovery in Chapter 5.

3.3 Methods

3.3.1 Time course of KCC2 loss on motoneuron somata following axotomy

Experiments were performed in mice carrying the *Cx3cr1-GFP* knock-in gene (See Table 3.1) in which green fluorescent protein (GFP) replaces one or both copies of the fractalkine receptor gene, thereby enabling visualization of microglia (Jung et al., 2000). CX3CR1 is expressed exclusively in microglia in the CNS and subsets of myeloid cells in the periphery (Mizutani et al., 2012). *Cx3cr1*$^{EGFP/+}$ animals were injected with Fast Blue and underwent unilateral sciatic nerve cut/ligation or sham surgery as described in Chapter 2. The animals were allowed to survive for various times after injury (3, 14, 21, 28 or 60 days) prior to euthanasia as described. Immunohistochemistry and analysis of KCC2-IR on 10 motoneuron somata per animal were performed to establish the temporal course of KCC2 protein loss on the somatic membrane (see Figure 2.1).

3.3.2 Qualitative analyses of KCC2 in motoneuron dendritic arbors

Fast Blue only allows visualization of the soma and most proximal dendrites. To visualize the full dendritic arbor of axotomized motoneurons, a small subset of *Cx3cr1*$^{EGFP/+}$ animals (n = 1 per time point) were injected with AAV1-mCherry (2 µl of ~10^9 IU/m) into the LG muscle at postnatal day 15. The animals were anesthetized with isoflurane (4% induction, 2% maintenance) and given pre-operative buprenorphine (0.05 mg/kg, subcutaneous). Injections were performed with glass microelectrodes inserted into the muscle through the skin. These animals were allowed to survive until adulthood (2-3 months) prior to further manipulation. Neonatal injections greatly increase AAV1 infection rates (Gomez-Perez et al., 2016).

Once animals reached adulthood, unilateral sciatic cut/ligations were performed. Animals were euthanized and tissue was extracted as described above. Sections containing AAV1-mCherry motoneurons were reacted with antibodies against KCC2 and immunoreactivity was detected with Cy5-conjugated secondary antibodies as described in Chapter 2. In these

sections, the mCherry signal was amplified by incubating with an antibody against mCherry raised against purified recombinant mCherry peptide produced in E. coli (1:100; polyclonal goat; MyBioSource Cat# MBS448050) revealed with Cy3-conjugated secondary antibodies (Cyanine Cy™3 (Cy3 α Goat); Jackson ImmunoResearch Labs, Cat# 705-165-147; RRID:AB_2307351). Because these animals were *CX3CR1$^{EGFP/+}$*, EGFP was also amplified with anti-GFP and revealed with FITC-conjugated secondary antibodies described in Chapter 2.

Spinal cord sections containing AAV1-mCherry filled motoneurons and KCC2 immunoreactivity were imaged at high magnification (60x1). At this magnification, the field of view includes only a small region of the whole dendritic arbor in the section. To image the entirety of the dendritic arbor we used image tiling of contiguous z-stacks. The images were imported into Neurolucida (v10.0, MBF Bioscience) to fully reconstruct the cell bodies and dendritic arbors contained within the 50 μm thick section. The dendritic arbors contained within the section were reconstructed in seven motoneurons 14 days after axotomy. Following reconstruction, KCC2-IR labeling in dendritic processes was designated as complete KCC2 depletion (Figure 3.3, green), partial depletion (Figure 3.3, blue), or normal levels of KCC2 (Figure 3.3, pink), by comparing the relative KCC2-IR on the labeled dendrites to the relative levels of KCC2 in dendrites in the surrounding neuropil. The distances of these dendritic segments to the cell body and their total surface areas were tabulated, and a Sholl analysis was performed to calculate the proportion of membrane covered with KCC2 immunoreactivity at different distances from the cell body, using 100 μm bins. Motoneurons from an animal 3 days after injury were also imaged to investigate the possibility that KCC2 is depleted in some regions of the somatodendritic membrane before mRNA downregulation. These motoneurons were not reconstructed as no dendritic regions were observed that lacked KCC2.

3.3.3 *In situ* analysis of KCC2 mRNA using RNA-Scope®

For RNA-Scope labeling, we prepared animals with unilateral sciatic nerve cut/ligations. Animals were euthanized 3, 7 and 14 days after nerve surgeries (n = 3 animals per group). Standard surgical and euthanasia procedures were performed, as described above, with the exception that perfusions were performed with 4% paraformaldehyde in 1X PBS. Following perfusion, spinal cords were harvested and post-fixed overnight at 4°C, followed by stepwise cryoprotection (10% sucrose in 1XPBS overnight, 20% sucrose in 1XPBS overnight, 30% sucrose in 1XPBS overnight) prior to sectioning (16 μm) on a cryostat. Sections were collected on RNAase free slides. Samples were then sent to Advanced Cell Diagnostics (ACD Bio, Newark, CA) on dry ice and processed for RNA-Scope® KCC2 mRNA in-situ hybridization using a probe directed towards the 501-1717 bp region of the KCC2 mRNA (Mm-SLC12A5 ACD cat# 311901). This probe detects mRNA for both KCC2a and KCC2b isoforms and consists of 20 Z probe pairs. We used the ubiquitously expressed peptidylprolyl isomerase B (cyclophilin B) (ACD cat# 313911) as positive control to confirm mRNA preservation, and dihydrodipicolinate reductase (dapB), a gene from Bacillus subtilis (ACD cat# 310043), as negative control to assess background labeling. To improve tissue adherence, sections were baked at 60°C for 45 minutes and then further postfixed on the slide (4% PFA in 1X PBS) for 90 minutes at room temperature before serial dehydration (5 minutes each; 50% EtOH, 70% EtOH, 100% EtOH, 100% EtOH) and air-drying. Standard RNA-Scope procedures (Wang et al., 2012) were used and the KCC2 mRNA binding detected with RNA-Scope® 2.5 HD Reagent Kit-BROWN (cat. no. 322300). The sections were counterstained with standard Nissl stain (Hematoxylin).

Dark- and bright-field images were taken on an Olympus BX60 microscope with Spotcam RX3 camera at 10X and 40X2 magnification, respectively. Images were imported into ImagePro ver 7.0 (Media Cybernetics), and thresholds for KCC2 mRNA signal were determined to segment the KCC2 mRNA labeling from the image. The same thresholds were used for all sections, but different thresholds were used for the cytoplasm and nucleus as the Nissl stain had

a different gray level in nuclei and most KCC2 mRNA signal was usually concentrated on top of the nucleolus. The total area of cytoplasmic or nuclear labeling was calculated (Figure 3.6A-C) and data presented as average percent coverage of KCC2 mRNA labeling in each cell compartment. We noted interanimal variability in the strength of the KCC2 mRNA signals. For this reason we always compared labeling intensities of injured motoneurons to that in motoneurons on the contralateral, uninjured side.

3.4 Results

3.4.1 KCC2 depletion is significant and sustained after 14 days.

In order to determine the optimal time window for quantifying KCC2 loss, we performed a time-series following sciatic nerve cut/ligation in *Cx3cr1*$^{EGFP/+}$ animals. Using antibodies raised against a rat KCC2 sequence (aa 932 – 1043) shared by both KCC2 isoforms (KCC2a and KCC2b), we found a loss of KCC2 immunoreactivity on the sciatic motor pools ipsilateral to the injury after unilateral sciatic nerve transections. *Cx3cr1*$^{EGFP/+}$ animals also allow easy visualization of microglia, and the microglial reaction consistently overlapped with the area of KCC2 depletion that can be seen at low magnification (Figure 3.1A).

For more detailed analysis of KCC2 on individual motoneurons, we used unbiased automatic detection of the cell body plasma membrane based on FB fluorescence (see methods and Figure 2.1). KCC2 immunoreactivity (KCC2-IR) was measured along the membrane of each motoneuron (10 per animal) and adjusted to background fluorescence within the same optical plane. Average KCC2-IR levels are expressed as a percentage of fluorescence intensity above background (0% = background). Thus, “n” always refers to the number of animals analyzed.

Using one-way ANOVA (sham vs injury time points) the loss of KCC2 protein appears to begin at 3 days and reaches a statistically significant loss by two weeks after injury (Figure 3.1B; Statistical Table 3.1A). This loss is sustained for at least 60 days. The onset of KCC2 loss from motoneuron somata is coincident with the onset of microgliosis, beginning in the days after

injury and peaking around two weeks. However, KCC2 loss is sustained after the microglial reaction is resolved (Figure 3.1C,D). This relationship between microglial activation and KCC2 depletion is further explored in Chapter 4.

3.4.2 Reliability of KCC2 quantification

Our time course experiment illustrated by fourteen days after sciatic nerve transection, KCC2 immunoreactivity was strongly reduced or absent from the plasma membranes of cell bodies and proximal dendrites of lateral gastrocnemius (LG) motoneurons labeled with Fast Blue (FB) in *Cx3cr1*$^{EGFP/+}$ animals (Figure 3.1). We confirmed this pattern also occurred in WT mice (Figure 3.2A,B). Thus, this is the time point we chose to utilize in all experiments described below.

Using the same KCC2-IR quantification technique described above, we reliably achieve consistent measurements of KCC2 protein expression along motoneuron somata. In approximately 90% of the motoneurons analyzed in sham or naïve animals, levels of KCC2 fluorescence averaged between 75% and 150% above background (Figure 3.2C). After injury, average KCC2 immunofluorescence estimates dropped to around 50% higher than background, with more than half of the estimates below this level (Figure 3.2C). At this level of measured KCC2 immunofluorescence above background, no KCC2 immunofluorescence was visible along the plasma membrane. This level above background might be due to an offset gray level imposed by the cytoplasm that is always slightly more fluorescent than neuropil background. Similar numbers of male and female mice underwent axotomy, and at 14 days after injury a significant depletion was found in injured animals, but no sex differences were detected in either intact or injured motoneurons (Figure 3.2C). A two-away ANOVA for condition (injured vs. non-injured) and sex showed significant differences according to condition, but not sex, or the interaction of injury and sex (Statistical Table 3.1B). Thus, males and females were pooled in all experiments described below.

3.4.3 KCC2 is preferentially preserved on distal dendrites

Despite the robust loss of KCC2 on the soma, KCC2-IR can be observed on some small dendrite segments within the neuropil around the cell bodies (yellow arrowheads in Figure 3.2A,B), although at a lower density compared to controls. It is possible they are distal segments of axotomized sciatic motoneurons or that they originate from nearby uninjured interneurons or non-sciatic projecting motoneurons. We were concerned that if KCC2 was preserved on dendrites it could act as a siphon to extrude chloride from somatic and proximal dendrite compartments, minimizing potential chloride accumulation and affecting interpretation of the data with respect to responses to GABA/glycine. Thus, we performed experiments to analyze KCC2 coverage throughout the dendrite plasma membrane 14 days after nerve injury. Fast Blue only fills the soma and most proximal dendrites; to visualize the full dendritic arbor, neonatal animals were injected with AAV1-mCherry into the LG. AAV1-mCherry fills the dendritic arbor fully and mCherry expression is preserved until adulthood (Figure 3.3A,B).

These animals underwent sciatic cut/ligation in adulthood, and we analyzed seven motoneurons 14 days after injury that showed optimal dendritic labeling. Three-dimensional reconstructions of motoneuron dendritic arbors were obtained using Neurolucida (Figure 3.3C,D). In the proximal dendrites, KCC2 was depleted to a similar extent as in the soma. However, we observed a gradient in which more KCC2-IR could be observed on the dendrites at progressively greater distances from the soma, and on the most distal dendrites KCC2-IR was fully preserved. The extent of KCC2 depletion varied from neuron to neuron and dendrite to dendrite. Overall, 52.6 ± 13.9% (± SD) of the total dendritic surface area had no KCC2-IR, 33.0 ± 8.3% showed a partial preservation of KCC2-IR, and 14.3 ± 10.8% of dendrites surface showed normal KCC2-IR 14 days after injury (Figure 3.3E). The differences in total surface area with no, partial, or normal KCC2-IR were statistically significant as measured with one-way ANOVA (Statistical Table 3.1C). Using Sholl analysis, we found that the areas with full preservation of KCC2 were always distal and regions with total depletion were always proximal

(Figure 3.3F). In dendritic segments located in the first 100 μm of Sholl distance from the cell body, 87.3 ± 14.9% of their surface was depleted of KCC2, and at 100 to 200 μm distance 47.4 ± 26.8% of the surface was totally depleted. However, in dendritic segments above 200 μm of Sholl distance, partial or total preservation of KCC2-IR was commonly observed (Figure 3.3F-H). In analyses of individual dendrites (Figure 3.3G,H) complete preservation of KCC2 immunoreactivity was found in the terminal dendritic regions (dot marks in dendrograms, Figure 3.3H; dendrite terminations were confirmed by mCherry labeling in varicose terminal dendrites not cut at either surface of the section). KCC2 preservation in the most distal dendrites was independent of whether the dendrites ended in the gray or white matter (Figure 3.3C). The impact of KCC2 retention in these distal regions on overall chloride levels might be minimal since motoneuron dendrites at these distances are of very small caliber and contribute little to the total surface; thus, the overall percentage of dendrite surface with normal KCC2 density is quite small (Figure 3.3E). On the other hand, the impact of partial retention of KCC2 density in mid-distal dendrite regions is yet unknown.

To confirm that the loss of KCC2 in proximal dendrites occurs with a similar temporal pattern as the somatic membrane, we also observed KCC2-IR on AAV1-mCherry filled motoneurons three days after sciatic nerve cut/ligation. As was observed with our full time course describing FB filled soma, three days after injury KCC2-IR was only minimally lost on both the soma and dendrites of AAV1-mCherry filled motoneurons (Figure 3.4). It does not appear that dendritic KCC2 is lost prior to KCC2 on the soma, so we did not perform full reconstructions of these neurons.

3.4.4 KCC2 regulation on axotomized motoneurons occurs at the transcriptional level

Disappearance of KCC2 protein from the membrane of axotomized motoneurons could occur because of membrane protein turnover and degradation, slower KCC2 protein trafficking

to the membrane, and/or reduced gene expression. In dorsal horn interneurons and spinal motoneurons after spinal cord injury, KCC2 downregulation has been reported to occur rapidly and through post-translational KCC2 phosphorylation mechanisms likely affecting trafficking and membrane stabilization of KCC2 (Coull et al., 2005; Boulenguez et al., 2010; Bos et al., 2013; Ferrini and De Koninck, 2013). However, previous studies in axotomized brainstem cranial motoneurons reported a strong downregulation of KCC2 mRNA after PNI. This results in slower removal of KCC2 from the membrane, but the loss is more profound and longer lasting (Toyoda et al., 2003).

To investigate whether the loss of KCC2 in spinal motoneurons after PNI is the result of reduced gene expression, we measured *kcc2* mRNAs using a diaminobenzidine (DAB)-based RNA-Scope® method and a probe that recognizes a 501-1717 bp region shared by both *kcc2* isoforms. In dark-field microscopy we observed complete depletion of *kcc2* mRNA in lamina IX motoneurons in the region corresponding to the sciatic motor pool ipsilateral to the lesion and little changes in other spinal cord laminae or in lamina IX motoneurons on the intact contralateral side (Figure 3.5A). At high magnification there was robust and consistent *kcc2* mRNA signal in the cell bodies and nucleus of all uninjured spinal cord Nissl-stained neurons (Figure 3.5B). Within the nucleus of these cells, there was frequently a large spot of reaction product localized on the nucleolar region. In motoneurons (recognized by their large size in lamina IX), we also observed *kcc2* mRNA reaction product entering proximal dendrites (Figure 3.5B, inset). Both cytoplasmic and nuclear labeling were strongly decreased in axotomized motoneurons (Figure 3.5C). We quantified RNA-Scope® reaction products by measuring the area covered by reaction particles within both the cell body cytoplasm and nucleus of motoneurons in lamina IX sciatic motor pools. Different thresholds were utilized in each cellular compartment (see methods) because of differences in intensity of the reaction product and the different gray levels of the Nissl-stained nucleus vs cytoplasm (Figure 3.6A-C). Since some interanimal variability was observed in the strength of the RNA-Scope® reaction, we compared

motoneurons ipsilateral and contralateral to the injury within animals. By three days after injury, the extent of coverage by *kcc2* mRNA reaction product was reduced by 90.7 ± 1.5% (SE) in the cytoplasm and 89.8 ± 0.6% in the nucleus. These depletions were consistently maintained through 14 days after injury (81.7% ± 2.3 and 80.1 ± 9.4% depletions in cytoplasm and nucleus, respectively). Two-way ANOVA revealed there were no significant differences in the percent depletion of the *kcc2* mRNA signal in cytoplasm or nucleus 3, 7, and 14 days after injury, and no interactions between injury and time in either condition. Only injury status predicted KCC2 levels in both the cytoplasm and nucleus (Statistical Table 3.1D,E), so data from all three time points were pooled. Paired t-tests showed highly significant reductions in *kcc2* mRNA signal in both cytoplasm and nucleus. Thus, KCC2 depletion in spinal motoneurons axotomized after nerve injury occurs through decreases in *kcc2* mRNA levels.

3.5 Discussion

We tested the hypothesis that KCC2 is lost from spinal motoneurons following peripheral axotomy as has been described in other neuronal populations after PNI and spinal motoneurons following spinal cord injury. Using *in situ* RNA-Scope® and an antibody against both KCC2 isoforms, we observed a robust KCC2 loss from the somatic membrane of axotomized motoneurons that extended far into dendritic processes. The loss of *kcc2* mRNA and KCC2 protein occurred with different time courses. Here, we discuss these data in relation to cellular mechanisms that downregulate KCC2 in axotomized motoneurons and the significance of the patterns of KCC2 loss in the cell body versus different dendritic regions.

Loss of KCC2 from axotomized spinal motoneurons is controlled transcriptionally

Three days after injury, loss of KCC2 protein in the cell body was small and non-significant, and there was no appreciable loss on dendrites. However, there was a complete downregulation of *kcc2* mRNA at this time point. The loss in protein is thus preceded by a loss

in *kcc2* mRNA, and a downregulation in *kcc2* gene expression best explains the progressive loss of KCC2 protein from the somatodendritic membrane with time after injury. The loss of KCC2 protein and mRNA more closely resemble the loss of KCC2 in brainstem motoneurons than other spinal neurons after PNI or in motoneurons after spinal cord injury; the process takes days rather than hours, and is regulated at the transcriptional level rather than by phosphorylation or trafficking mechanisms as have been reported in these other systems (Rivera et al., 2002; Bos et al., 2013; Kahle et al., 2013; Medina et al., 2014).

Considerations for the differential regulation of KCC2 in cell bodies and dendritic regions

The specific downregulation of membrane KCC2 from proximal somatodendritic membranes in axotomized spinal motoneurons deserves special mention. Retention of KCC2 in the distal dendrites of spinal motoneurons, despite strong reductions in KCC2 mRNA, suggests differences in KCC2 stability in different dendrite compartments. Interestingly, earlier electrophysiological studies of hypoglossal motoneurons showed that glycinergic (strychnine-sensitive) synapses, found mostly on the somata (Takata and Ogata, 1980) sustained larger decreases in efficacy than more distally located GABAergic (picrotoxin-sensitive) synapses (Takata and Ogata, 1980; Takata and Nagahama, 1983). It is worth noting that in some central neurons, distal dendrites are enriched with the KCC2a isoform (Markkanen et al., 2014) and that KCC2 in dendrites is frequently associated with the maintenance of structural properties at excitatory synapses and less with a chloride transport function (Gulyas et al., 2001; Blaesse and Schmidt, 2015). Recent data from the Alvarez lab using isotype specific antibodies (Paula Calvo, unpublished) shows that KCC2b is uniquely expressed on the somatic membrane of spinal motoneurons. These possible differences in KCC2 isoforms, as well as anchoring, membrane stabilization, and function in distinct dendritic compartments of spinal motoneurons are all

possibilities for explaining the differential loss of KCC2 in motoneuron soma and dendrites that deserve further study.

It should also be noted that, for the first time, we have reported trafficking of *kcc2* mRNA into dendritic compartments of motoneurons. KCC2 transcription of *kcc2* mRNA within the dendrites is one alternative explanation for the differential regulation of dendritic KCC2. Our Nissl stained sections only permitted analyses of proximal dendrites as they emerge from the cell body. Future studies should be performed combining RNA-Scope® *kcc2* mRNA detection and dendritic labeling with AAV1 transfection to localize *kcc2* mRNA throughout the dendritic arbor. The high sensitivity and specificity of the RNA-Scope® technique would allow detection of small quantities of mRNAs in dendritic compartments. Nonetheless, we believe it is unlikely that there is enough preservation of *kcc2* mRNAs in distal dendrites to maintain KCC2 protein; the scattered dots of mRNA signal in the neuropil adjacent to the axotomized motoneurons also disappeared after injury. Therefore, the best explanation at present is that KCC2 in the very distal dendrites has a very low turnover rate, explaining their preservation at the time point of our analyses. In this case we would expect chronic axotomy at longer time points would result in the eventual loss of this KCC2 as well.

It is also possible KCC2 distally is serving a different purpose. Independent of its role in ion transport, KCC2 has been shown to stabilize excitatory synapses and be important in dendritic spine development by regulating actin phosphorylation and stabilization (Li et al., 2007; Llano et al., 2015). KCC2-deficient mice have fewer functional glutamatergic synapses and excessively long dendritic protrusions that cause an increase in the total dendrite length of pyramidal cells (Li et al., 2007). The regions where we see KCC2 preservation on motoneurons (the last 75 to 100 μm of dendrite) typically have very low synaptic densities (Rotterman et al., 2014), making synapse stabilization an unlikely explanation for KCC2 retention there. However, these most distal regions of the dendrites undergo many changes after long-term axotomy without regeneration, including becoming more highly branched, increasing in diameter, and

becoming axon-like in both structure and molecular composition (Rose and Odlozinski, 1998; Rose et al., 2001; MacDermid et al., 2002). At the time points we observed, no drastic changes in distal dendrite morphology were evident, but it is possible that the high density of KCC2, if lost long term, is contributing to the eventual morphological changes observed with longer-term axotomy (Rose and Odlozinski, 1998).

The effect of partial preservation of KCC2 on mid to distal dendrites on the overall regulation of chloride throughout the cell has never been previously considered in the literature. While more studies are beginning to use modeling to illuminate the potential physiological consequences of KCC2 loss (Prescott et al., 2006; Zhang et al., 2014), these have not taken into account the potential for differential KCC2 levels or functions in different somatodendritic membrane compartments. Since even small changes in the chloride reversal potential alter neural responses to GABA/glycine and change neuronal activity, this nuance will be important to incorporate in future models. Regardless, the drastic loss in KCC2 in the cell body and proximal dendrites further supports the possibility of a significant functional consequence of KCC2 loss from the soma following PNI, as has been seen in brainstem motoneurons.

KCC2 and microglia in the dorsal horn

Models of PNI known to induce chronic pain, such as chronic constriction injury (Bennett and Xie, 1988), partial nerve ligation (Seltzer et al., 1990), and spared nerve injury (Decosterd and Woolf, 2000), all result in a development of a hyperexcitable state centrally (Jensen et al., 2001). Downregulation of KCC2 from Lamina I and II neurons receiving inputs from nociceptive afferents and projecting to brain pain centers is a main contributor to this phenomenon (Ferrini and De Koninck, 2013). Unlike DRG neurons and motoneurons, dorsal horn neurons targeted by nociceptive afferents are not directly injured. However, PNI does produce a microglial response around these neurons that involves upregulation and release of BDNF that is sufficient to induce neuropathic pain (Coull et al., 2003; Coull et al., 2005; Zhou et

al., 2011). While the development of neuropathic pain in female mice is independent of microglia, (Sorge et al., 2011; Sorge et al., 2015) in male mice, ATP-activated microglia induce hyperalgesia after PNI (Tsuda et al., 2003), and their release of BDNF—or their stimulation of BDNF release from another cell type—is sufficient to provoke a shift in anion gradient that causes allodynia, both of which can be blocked by blocking TrkB signaling (Coull et al., 2005).

As we (and many others) have shown, there is a robust microglial reaction around motoneurons after PNI as well (Reviewed in (Rotterman et al., Submitted by August 2019)). This reaction begins at 3 days after sciatic nerve axotomy and peaks between seven and fourteen days, concurrent with the onset of KCC2 loss (Rotterman et al., 2019). However, microgliosis is almost completely attenuated by 60 days after injury, whereas KCC2 loss is maintained past this time point. Given the previous findings in the dorsal horn and the notable overlap between the microglial reaction and region of KCC2 depletion in the ventral horn, we hypothesized that induction—if not maintenance—of KCC2 loss on spinal motoneurons after PNI may be due to microglial release of BDNF or microgliosis more generally. We more thoroughly explore this possibility in Chapter 4.

3.6 Tables and Figures

Table 3.1 Mouse strains utilized in Chapter 3

Mouse Strain	Stock No.	References
C57BL/6J (*Wild type*)	RRID:IMSO_JAX: 000664	
CX3CR1^{EGFP}	RRID:IMSR_JAX:005582	Jung et al., 2000

Statistical Table 3.1

Location	Data Reference	Data Structure	Type of Test	Statistical Significance
A	3.1B	Normal Distribution	**One-way ANOVA** $F_{(5, 18)} = 4.72$; $p = 0.0062$	
	Control vs.			
	3 days post ligation		*Post hoc* Bonferroni	$p = 0.94$
	14 days post ligation		*Post hoc* Bonferroni	$p = 0.019$
	21 days post ligation		*Post hoc* Bonferroni	$p = 0.003$
	28 days post ligation		*Post hoc* Bonferroni	$p = 0.023$
	60 days post ligation		*Post hoc* Bonferroni	$p = 0.029$
B	3.2C	Non-normal Distribution Unequal variance	**Two-Way ANOVA** Injury; $F_{(1,103)} = 76.3$; $p<0.001$ Sex; $F_{(1, 103)} = 0.021$; $p = 0.683$ Interaction; $F_{(1, 103)} = 3.16$; $p = 0.086$	
C	3.3E	Normal Distribution Unequal Variance	**One-way ANOVA** $F_{(2,17)} = 17.52$; $p<0.001$	
	None vs Partial		*Post hoc* Bonferroni	$p = 0.0218$
	None vs Normal		*Post hoc* Bonferroni	$p < 0.0001$
	Partial vs Normal		*Post hoc* Bonferroni	$p = 0.0285$
D	3.6D	Normal Distribution Unequal Variance	**Two-Way ANOVA** Side; $F_{(1,17)} = 58.314$; $p<0.001$ Day; $F_{(2,17)} = 1.811$; $p = 0.205$ Interaction; $F_{(2,17)} = 2.308$; $p = 0.142$	
	Intact vs Ligated		**One-tailed paired t test**	$t = 6.07$, $p = 0.0002$
E	3.6E	Normal Distribution Unequal Variance	**Two-Way ANOVA** Side; $F_{(1,17)} = 58.314$; $p <0.001$ Day; $F_{(2,17)} = 0.132$; $p = 0.878$ Interaction; $F_{(2,17)} = 0.463$; $p = 0.640$	
	Intact vs Ligated		**One-tailed paired t test**	$t = 7.591$, $p < 0.0001$

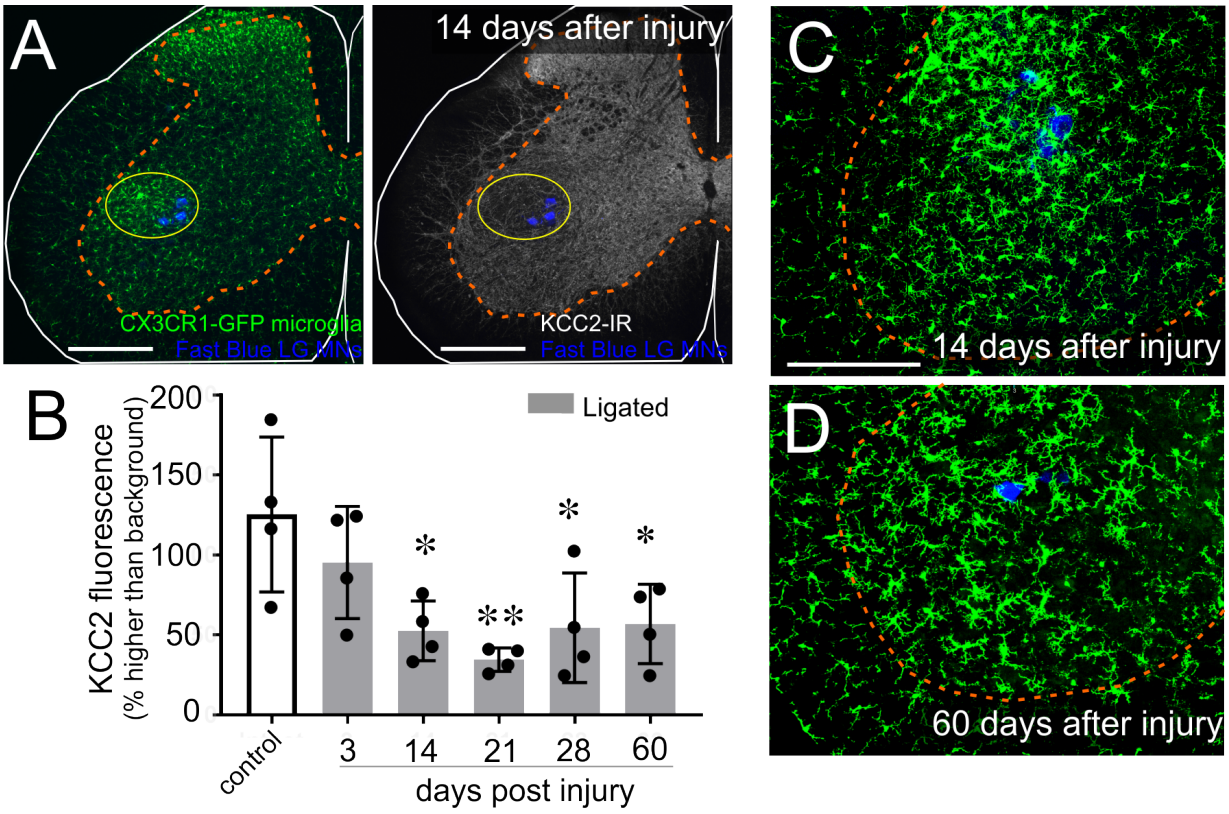

Figure 3.1 The disappearance of KCC2 coincides with microglial onset but persists longer than the microglial reaction. CX3CR1$^{EGFP/+}$ animals underwent unilateral sciatic nerve cut/ligation and were allowed to survive for various time points. **A**) Representative images of microglial (green) and KCC2 (white) immunoreactivity (IR) 14 days after injury, at the peak of the microglial response. Scale bars = 200 μm. Regions of KCC2 depletion overlap with the area of microglial reactivity. **B**) Time course of KCC2 downregulation and recovery in CX3CR1$^{EGFP/+}$ animals with a sciatic nerve cut/ligation. KCC2 protein levels begin decreasing by 3 days and are sustained up to 60 days after axotomy (Statistical Table 3.1A; * $p \leq 0.05$). Error bars = SEM. **C, D**) Microglial reaction (green) around injured LG motoneurons (blue) 14 (**C**) or 60 (**D**) days after sciatic nerve injury. KCC2 IR loss appears to coincide with the onset of microgliosis but persists after the microglia response has attenuated.

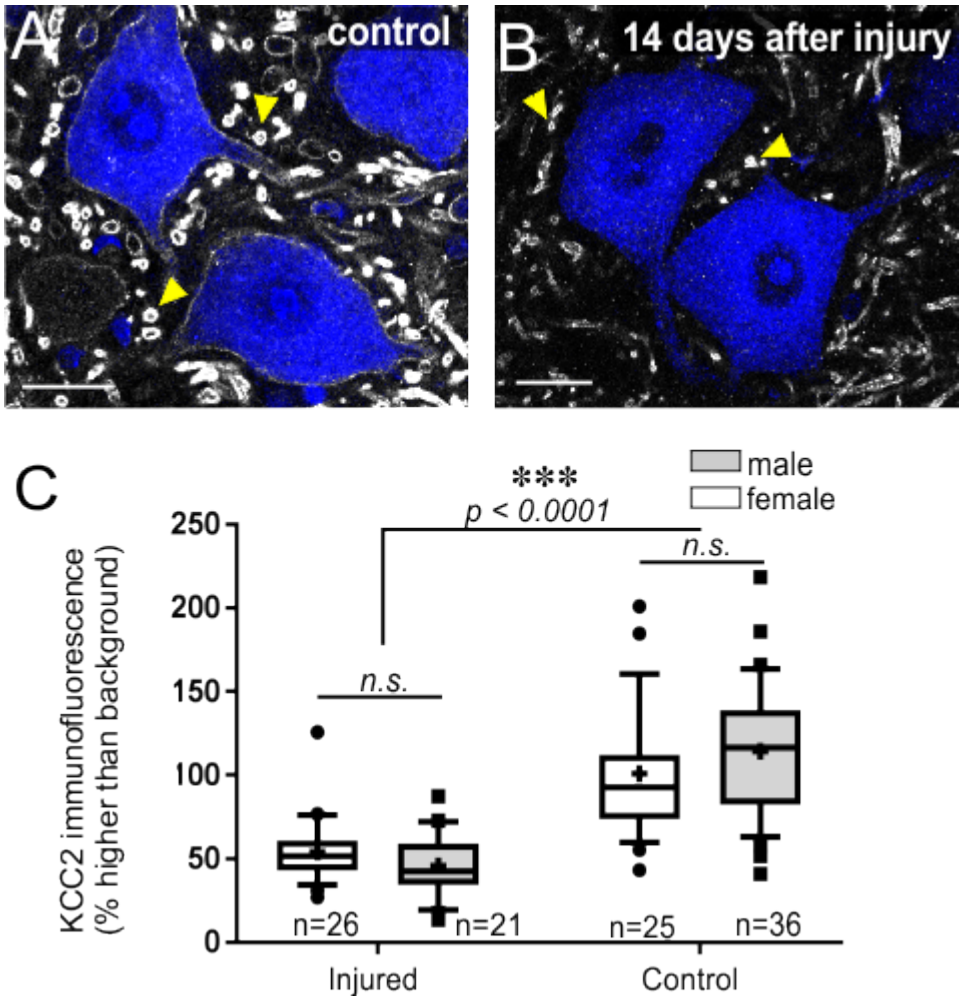
A
control
B
14 days after injury
C
male
female
***
p < 0.0001
n.s.
n.s.
KCC2 immunofluorescence
(% higher than background)
250
200
150
100
50
0
n=26
n=21
n=25
n=36
Injured
Control

Figure 3.2 KCC2 is depleted on motoneuron somata 14 days after injury independent of sex. A, B) Lateral gastrocnemius motoneurons of mice labeled with Fast Blue; KCC2 immunoreactivity (IR) in white: sham (**A**) and cut/ligated (**B**). The axotomized motoneurons lose KCC2 protein on the cell body membrane, but in some dendrites in the neuropil KCC2 is preserved (yellow arrows). Scale bar = 25 μm. **C**) Results of quantitative measures of motoneuron soma surface KCC2-IR in male and female mice 14 days after sciatic cut/ligation. No significant sex differences in KCC2 immunoreactivity were found; only injury state predicted KCC2 levels (Statistical Table 3.1B). Box plots represent 25th, median, and 75th percentile; whiskers = 10th and 90th percentile; outliers = data points outside whiskers. Crosses = mean; n = number of animals. Each animal estimate was obtained from 10 motoneurons.

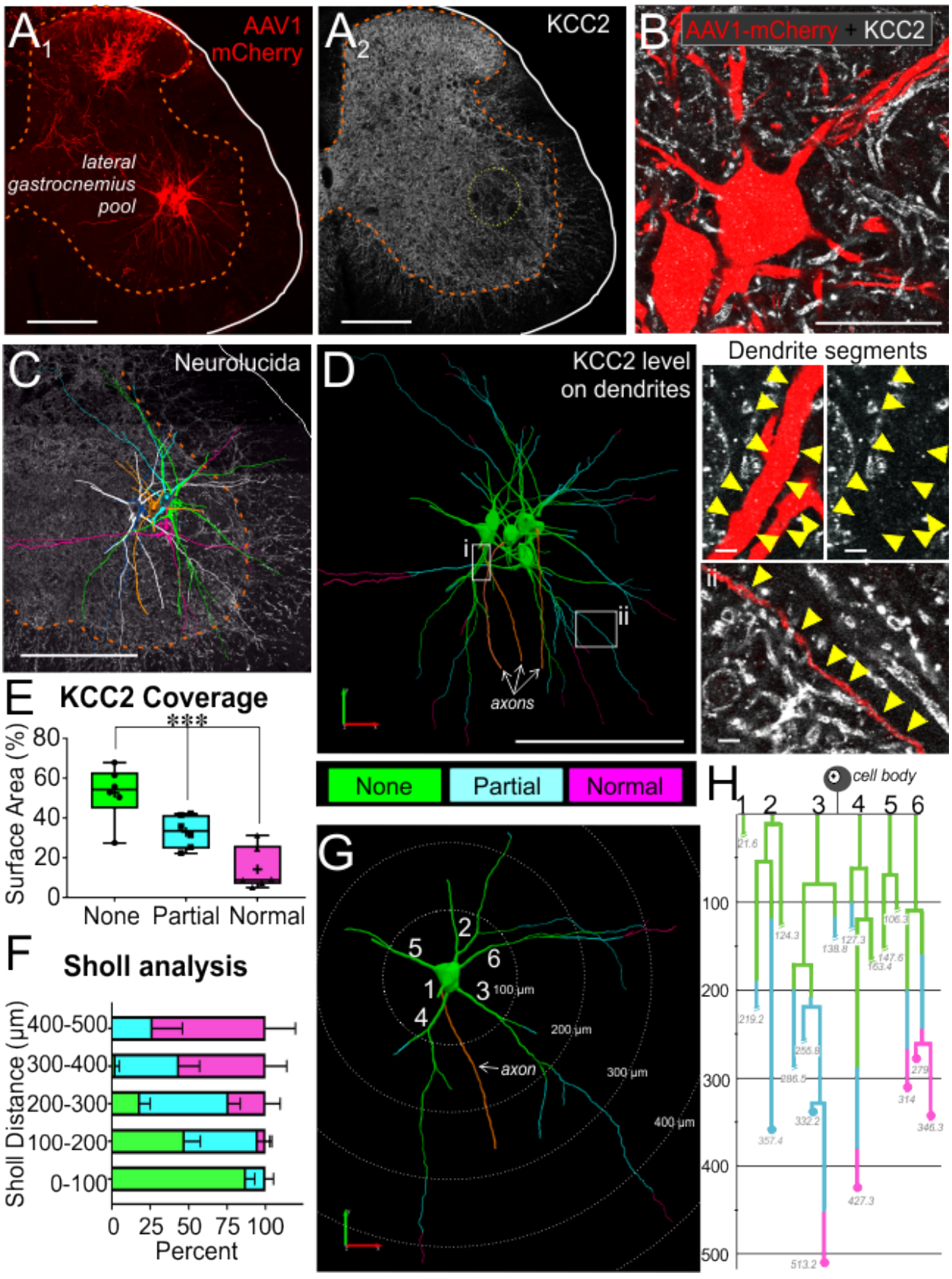
A1
AAV1
mCherry
lateral
gastrocnemius
pool
A2
KCC2
B
AAV1-mCherry + KCC2
C
Neurolucida
D
KCC2 level
on dendrites
i
ii
axons
Dendrite segments
i
ii
None
Partial
Normal
E
KCC2 Coverage
***
Surface Area (%)
80
60
40
20
0
None
Partial
Normal
F
Sholl analysis
Sholl Distance (µm)
400-500
300-400
200-300
100-200
0-100
0
25
50
75
100
Percent
G
2
5
6
1
3
4
100 µm
200 µm
300 µm
400 µm
axon
H
cell body
1
2
3
4
5
6
21.6
124.3
219.2
357.4
138.8
127.3
255.8
296.5
332.2
427.3
513.2
147.6
163.4
106.3
279
314
346.3
100
200
300
400
500

Figure 3.3 KCC2 protein is lost extensively from axotomized motoneuron dendrites 14 days after sciatic cut/ligation. A) AAV1-mCherry filled lateral gastrocnemius motoneurons (**A_1**) and KCC2 immunoreactivity in the same section (**A_2**) 14 days following sciatic cut/ligation. Note some afferents are also labeled in the dorsal horn after AAV1 mCherry muscle injections in neonates. Scale bar = 200 μm. **B**) High magnification confocal image through the soma and proximal dendrites of two motoneurons (mCherry-red). KCC2 immunofluorescence (white) was not observed around the cell body and the proximal dendrite. Scale bar = 50 μm. **C**) Motoneurons were reconstructed in 3D using tiled confocal images. Example of six individual motoneurons (color-coded) reconstructed within one section with KCC2 immunoreactivity in the background. Note the extension of dendrites towards the dorsal horn and also entering the white matter. Scale bar = 200 μm. **D**) Dendrites were color-coded to indicate complete KCC2 loss (green, "none"), partial KCC2 loss (blue), or normal KCC2 levels (pink), relative to surrounding dendrites in the neuropil. Loss of fluorescence in the proximal dendrites was similar to that on the soma membranes (green & region i). Immunoreactivity to KCC2 was partially reduced (blue & region ii) along dendrites for various distances. However, no significant loss of KCC2 was found on distal dendrites. i & ii scale bars = 5 μm. **E**) Box plots of the percentage of surface area in each category (complete depletion, partial depletion, or no depletion) for all dendrites for which the complete length was traceable (not cut short during sectioning)**.** The majority of the available dendritic surface area was completely depleted (Statistical Table 3.1C; *** $p < 0.001$). Box plots represent 25th, median, and 75th percentiles; whiskers = 10th and 90th percentile. Crosses = mean; points represent average for individual neurons (n = 6, 3.12 ± 0.98 dendrites/animal). **F, G**) Sholl analysis (100 μm bins) of dendritic length and KCC2 depletion. **F**) Average (± SD) percent of dendritic lengths within each bin (n = 7 neurons, 5.29 ± 1.1 dendrites per neuron), illustrating that within the first 200 μm the majority of dendrites have no KCC2 visible, whereas normal KCC2 levels can be observed at the most distal ends of dendrites. **G**) Isolated single motoneuron from (C) separated for Sholl

analysis. The majority of KCC2 is completely lost; at 400 μm some dendritic KCC2 is preserved. **H**) Example dendrogram of the motoneuron in (G), color-coded for KCC2 depletion. Dendrite branches ending in circles represent dendrites that were fully contained within the section (quantified in E). Dendrite branches that were cut during sectioning and could not be fully traced are designated with slashes. The majority of dendrites for which the ending could be observed had normal levels of KCC2 present.

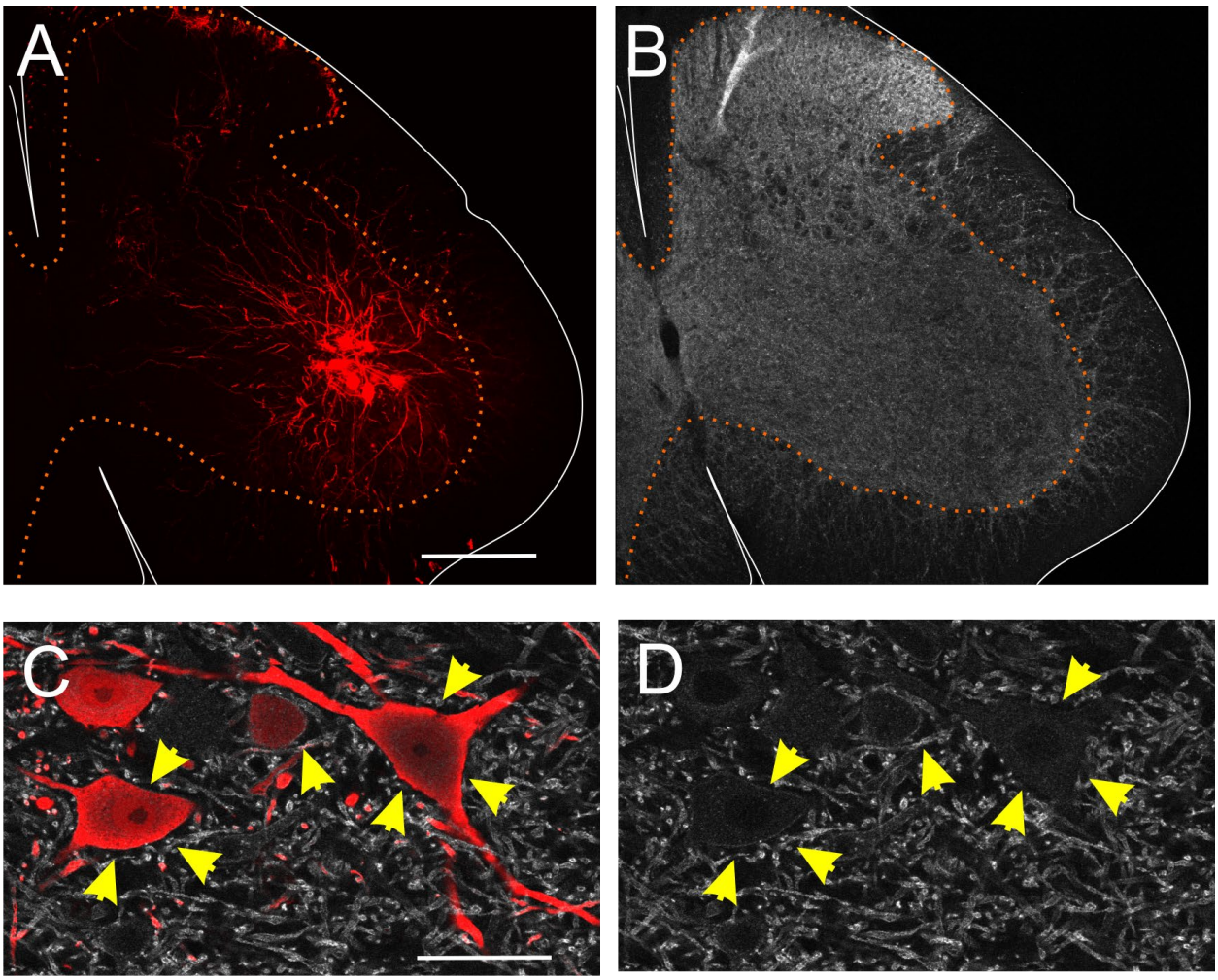

Figure 3.4 KCC2 protein not lost extensively on motoneuron somata or dendrites three days after peripheral axotomy. A, B) AAV1-mCherry filled lateral gastrocnemius motoneurons (**A**) and KCC2 immunoreactivity in the same section (**B**) 3 days following sciatic cut/ligation. **C,D**) High magnification confocal image through the soma and proximal dendrites of three motoneurons (mCherry-red). Variable KCC2 immunofluorescence (white) was observed between motoneurons, but did not differ between somata and proximal dendrites. Scale bar = 50 µm.

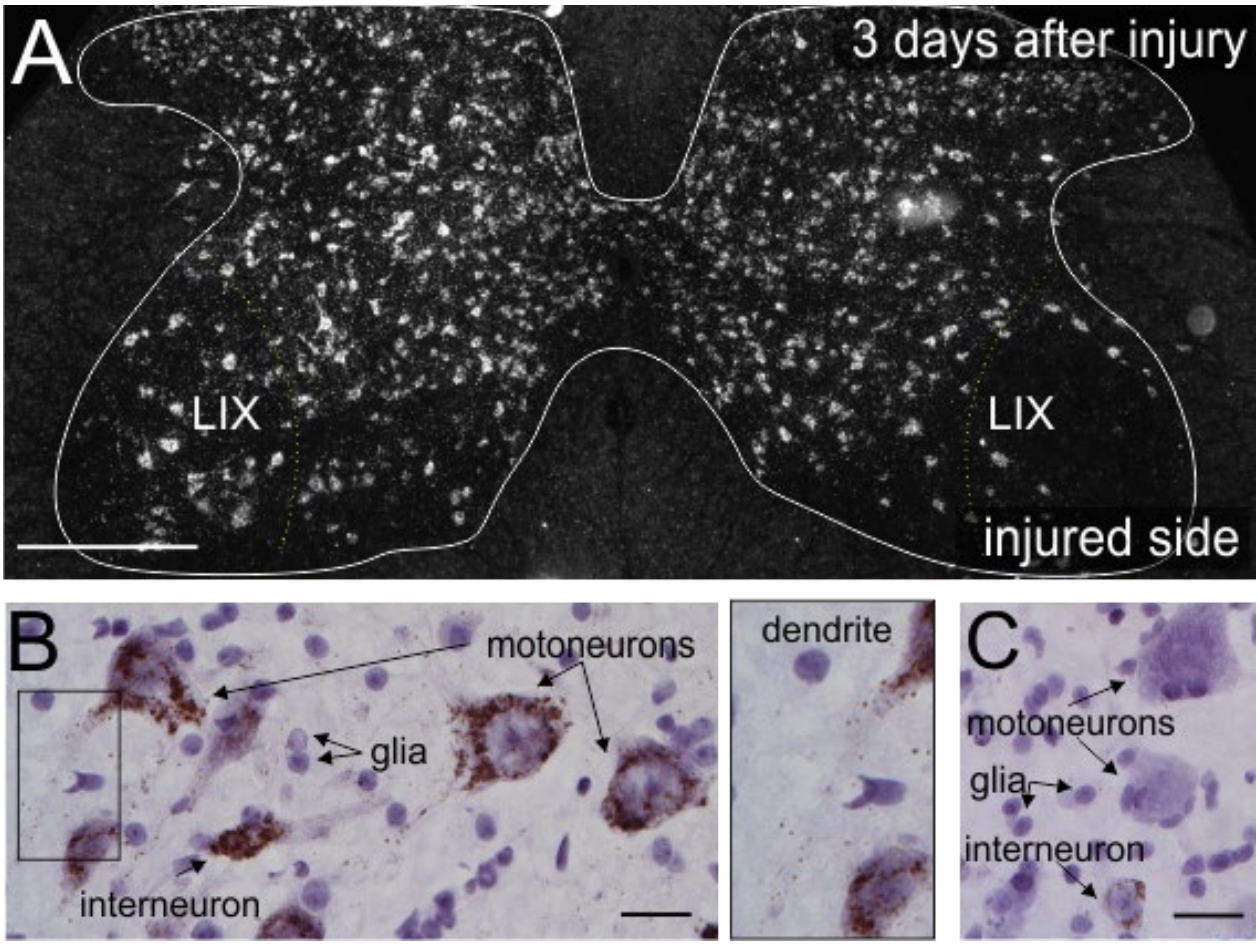

Figure 3.5 KCC2 mRNA is lost by three days after peripheral axotomy. A) Darkfield image of a section three days after unilateral sciatic nerve cut/ligation, processed using RNA-Scope. KCC2 mRNA visualized in white. Scale bar = 200 μm. Very little KCC2 mRNA is found in the area around the injured motor pool (right) in lamina IX (LIX), relative to the contralateral intact motor pools. **B, C**) Brightfield images of motoneurons on the intact (**B**) or cut/ligated (**C**) sides of the spinal cord three days after PNI. Injured motoneurons lose KCC2 mRNA, whereas motoneurons contralateral to injury and interneurons on both sides of the spinal cord maintain KCC2 mRNA. Nuclei from glia are also visible and are more densely concentrated around axotomized neurons. KCC2 mRNA can also be seen extending into dendritic processes of intact motoneurons (rectangle in B, inset). Scale bar = 25 μm.

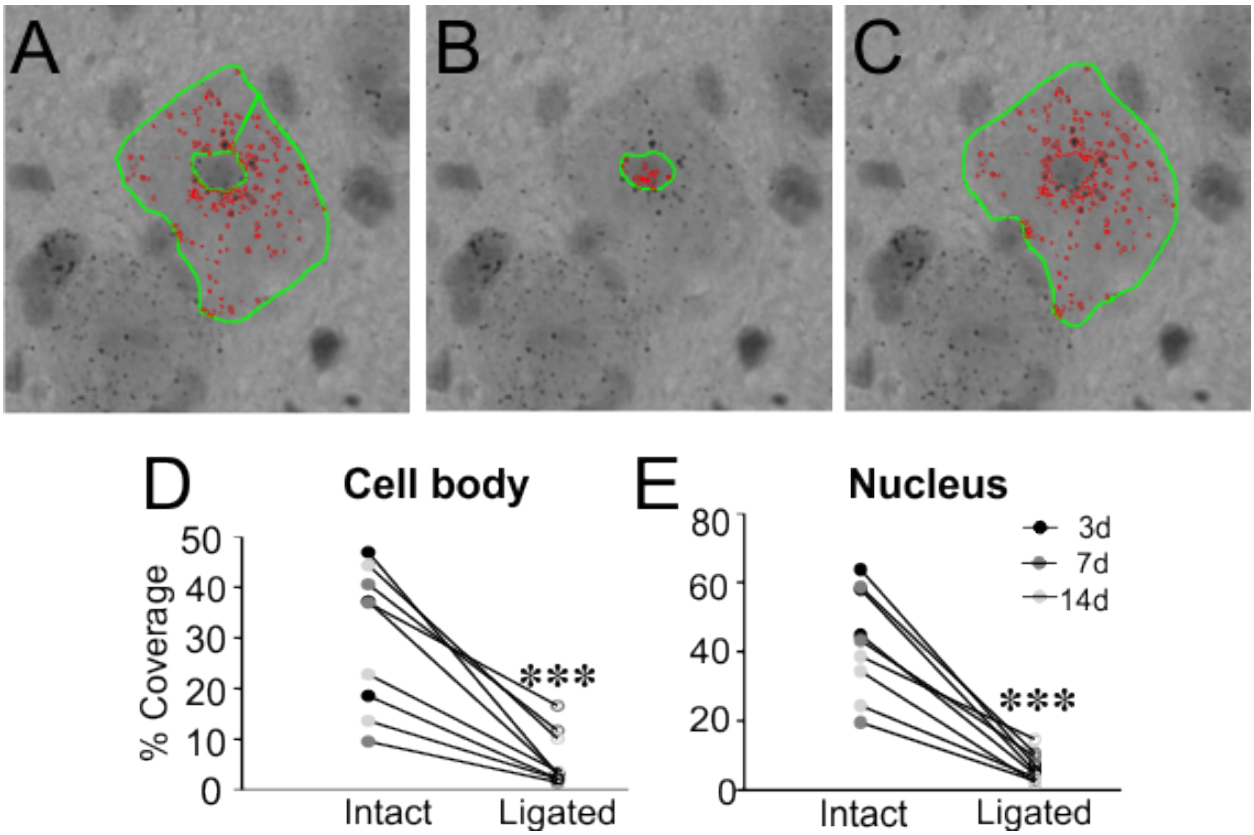

Figure 3.6 Quantification of RNA-Scope®. A,B,C) RNA-Scope® quantification procedure. Thresholding was used to highlight KCC2 mRNA (red). Nissl staining caused differences in background intensity, so difference thresholds were required for cytoplasm and nuclear quantification. Thus, the outlines of the motoneuron somata were traced (green) with the nucleus excluded to get the area of KCC2 mRNA within the cytoplasm (**A**). Nuclei (**B**) were traced and threshold separately. The total area, including cytoplasm and nucleus (**C**), was also traced for comparison of total area to KCC2 mRNA area. **D,E**) Percent KCC2 coverage of soma (**D**) and nucleus (**E**). Animals were euthanized 3, 7, or 14 days (n = 3/group) after unilateral sciatic nerve cut/ligation, and sciatic motoneurons were quantified as described above. There were no differences between levels of KCC2 between time points; only injury state predicted KCC2 levels (Statistical Table 3.1D,E). Thus, data from all time points were pooled and paired t-tests were performed comparing motoneurons ipsilateral and contralateral to injury. (Statistical Table 3.1D,E; *** $p \leq 0.001$).

3.7 References

Aldskogius H (2011) Mechanisms and consequences of microglial responses to peripheral axotomy. Front Biosci (Schol Ed) 3:857-868.

Bennett GJ, Xie YK (1988) A peripheral mononeuropathy in rat that produces disorders of pain sensation like those seen in man. Pain 33:87-107.

Blaesse P, Schmidt T (2015) K-Cl cotransporter KCC2--a moonlighting protein in excitatory and inhibitory synapse development and function. Pflugers Arch Eur J Physiol 467:615-624.

Bos R, Sadlaoud K, Boulenguez P, Buttigieg D, Liabeuf S, Brocard C, Haase G, Bras H, Vinay L (2013) Activation of 5-HT2A receptors upregulates the function of the neuronal K-Cl cotransporter KCC2. PNAS 110:348-353.

Boulenguez P, Liabeuf S, Bos R, Bras H, Jean-Xavier C, Brocard C, Stil A, Darbon P, Cattaert D, Delpire E, Marsala M, Vinay L (2010) Down-regulation of the potassium chloride cotransporter KCC2 contributes to spasticity after spinal cord injury. Nat. Med. 16:302-307.

Coull JA, Boudreau D, Bachand K, Prescott SA, Nault F, Sik A, De Koninck P, De Koninck Y (2003) Trans-synaptic shift in anion gradient in spinal lamina I neurons as a mechanism of neuropathic pain. Nature 424:938-942.

Coull JA, Beggs S, Boudreau D, Boivin D, Tsuda M, Inoue K, Gravel C, Salter MW, De Koninck Y (2005) BDNF from microglia causes the shift in neuronal anion gradient underlying neuropathic pain. Nature 438:1017-1021.

Decosterd I, Woolf CJ (2000) Spared nerve injury: an animal model of persistent peripheral neuropathic pain. Pain 87:149-158.

Ferrini F, De Koninck Y (2013) Microglia control neuronal network excitability via BDNF signalling. Neural Plast 2013:429815.

Gomez-Perez L, Griffith RW, Alvarez FJ (2016) Transgenic expression of rabies glycoprotein in mouse hind limb muscle increases the efficiency of motor pool infection by SADB19dG rabies virus. Annual Meeting of the Society for Neuroscience. San Diego, CA.

Gulyas AI, Sik A, Payne JA, Kaila K, Freund TF (2001) The KCl cotransporter, KCC2, is highly expressed in the vicinity of excitatory synapses in the rat hippocampus. Eur J Neursoci 13:2205-2217.

Jensen TS, Gottrup H, Sindrup SH, Bach FW (2001) The clinical picture of neuropathic pain. Eur J Pharmacol 429:1-11.

Jung S, Aliberti J, Graemmel P, Sunshine MJ, Kreutzberg GW, Sher A, Littman DR (2000) Analysis of fractalkine receptor CX(3)CR1 function by targeted deletion and green fluorescent protein reporter gene insertion. Mol Cell Biol 20:4106-4114.

Kahle KT, Deeb TZ, Puskarjov M, Silayeva L, Liang B, Kaila K, Moss SJ (2013) Modulation of neuronal activity by phosphorylation of the K-Cl cotransporter KCC2. Trends Neurosci 36:726-737.

Kim J, Kobayashi S, Shimizu-Okabe C, Okabe A, Moon C, Shin T, Takayama C (2018) Changes in the expression and localization of signaling molecules in mouse facial motor neurons during regeneration of facial nerves. J Chem Neuroanat 88:13-21.

Lee-Hotta S, Uchiyama Y, Kametaka S (2019) Role of the BDNF-TrkB pathway in KCC2 regulation and rehabilitation following neuronal injury: A mini review. Neurochem Int 128:32-38.

Li H, Khirug S, Cai C, Ludwig A, Blaesse P, Kolikova J, Afzalov R, Coleman SK, Lauri S, Airaksinen MS, Keinanen K, Khiroug L, Saarma M, Kaila K, Rivera C (2007) KCC2 interacts with the dendritic cytoskeleton to promote spine development. Neuron 56:1019-1033.

Llano O, Smirnov S, Soni S, Golubtsov A, Guillemin I, Hotulainen P, Medina I, Nothwang HG, Rivera C, Ludwig A (2015) KCC2 regulates actin dynamics in dendritic spines via interaction with beta-PIX. J Cell Biol 209:671-686.

MacDermid V, Neuber-Hess M, Short C, Rose PK (2002) Alterations to neuronal polarity following permanent axotomy: a quantitative analysis of changes to MAP2a/b and GAP-43 distributions in axotomized motoneurons in the adult cat. J Comp Neurol 450:318-333.

Markkanen M, Karhunen T, Llano O, Ludwig A, Rivera C, Uvarov P, Airaksinen MS (2014) Distribution of neuronal KCC2a and KCC2b isoforms in mouse CNS. J Comp Neurol 522:1897-1914.

Medina I, Friedel P, Rivera C, Kahle KT, Kourdougli N, Uvarov P, Pellegrino C (2014) Current view on the functional regulation of the neuronal K(+)-Cl(-) cotransporter KCC2. Front Cell Neurosci 8:27.

Mizutani M, Pino PA, Saederup N, Charo IF, Ransohoff RM, Cardona AE (2012) The fractalkine receptor but not CCR2 is present on microglia from embryonic development throughout adulthood. J Immuno 188:29-36.

Nabekura J, Ueno T, Okabe A, Furuta A, Iwaki T, Shimizu-Okabe C, Fukuda A, Akaike N (2002) Reduction of KCC2 Expression and GABAa Receptor-Mediated Excitation after In Vivo Axonal Injury. J Neurosci 22:4412-4417.

Prescott SA, Sejnowski TJ, De Koninck Y (2006) Reduction of anion reversal potential subverts the inhibitory control of firing rate in spinal lamina I neurons: towards a biophysical basis for neuropathic pain.Mol Pain 2:32.

Rivera C, Li H, Thomas-Crusells J, Lahtinen H, Viitanen T, Nanobashvili A, Kokaia Z, Airaksinen MS, Voipio J, Kaila K, Saarma M (2002) BDNF-induced TrkB activation down-regulates the K+-Cl- cotransporter KCC2 and impairs neuronal Cl- extrusion. J Cell Biol 159:747-752.

Rose PK, Odlozinski M (1998) Expansion of the dendritic tree of motoneurons innervating neck muscles of the adult cat after permanent axotomy. J Comp Neurol 390:392-411.

Rose PK, MacDermid V, Joshi M, Neuber-Hess M (2001) Emergence of axons from distal dendrites of adult mammalian neurons following a permanent axotomy. Eur J Neursoci 13:1166-1176.

Rotterman TM, Akhter ET, Alvarez FJ (2019) Microgliosis in the ventral horn following peripheral nerve injury. Neural Regen Res (In process)

Rotterman TM, Nardelli P, Cope TC, Alvarez FJ (2014) Normal distribution of VGLUT1 synapses on spinal motoneuron dendrites and their reorganization after nerve injury. J Neurosci 34:3475-3492.

Rotterman TM, Akhter ET, Lane AR, MacPherson KP, Garcia VV, Tansey MG, Alvarez FJ (2019) Spinal motor circuit synaptic plasticity after peripheral nerve injury depends on microglia activation and a CCR2 mechanism. J Neurosci.

Seltzer Z, Dubner R, Shir Y (1990) A novel behavioral model of neuropathic pain disorders produced in rats by partial sciatic nerve injury. Pain 43:205-218.

Sorge RE, LaCroix-Fralish ML, Tuttle AH, Sotocinal SG, Austin JS, Ritchie J, Chanda ML, Graham AC, Topham L, Beggs S, Salter MW, Mogil JS (2011) Spinal cord Toll-like receptor 4 mediates inflammatory and neuropathic hypersensitivity in male but not female mice. J Neurosci 31:15450-15454.

Sorge RE et al. (2015) Different immune cells mediate mechanical pain hypersensitivity in male and female mice. Nat Neurosci 18:1081-1083.

Takata M, Ogata K (1980) Two components of inhibitory postsynaptic potentials evoked in hypoglossal motoneurons by lingual nerve stimulation. Exp Neurol 69:299-310.

Takata M, Nagahama T (1983) Synaptic efficacy of inhibitory synapses in hypoglossal motoneurons after transection of the hypoglossal nerves. Neuroscience 10:23-29.

Tatetsu M, Kim J, Kina S, Sunakawa H, Takayama C (2012) GABA/glycine signaling during degeneration and regeneration of mouse hypoglossal nerves. Brain Res 1446:22-33.
Toyoda H, Ohno K, Yamada J, Ikeda M, Okabe A, Sato K, Hashimoto K, Fukuda A (2003) Induction of NMDA and GABAA receptor-mediated Ca2+ oscillations with KCC2 mRNA downregulation in injured facial motoneurons. The J Neurophysiol 89:1353-1362.
Tsuda M, Shigemoto-Mogami Y, Koizumi S, Mizokoshi A, Kohsaka S, Salter MW, Inoue K (2003) P2X4 receptors induced in spinal microglia gate tactile allodynia after nerve injury. Nature 424:778-783.
Wang F, Flanagan J, Su N, Wang LC, Bui S, Nielson A, Wu X, Vo HT, Ma XJ, Luo Y (2012) RNAscope: a novel in situ RNA analysis platform for formalin-fixed, paraffin-embedded tissues. J Mol Diagn : JMD 14:22-29.
Zhang TC, Janik JJ, Grill WM (2014) Modeling effects of spinal cord stimulation on wide-dynamic range dorsal horn neurons: influence of stimulation frequency and GABAergic inhibition. J Neurophysiol 112:552-567.
Zhou LJ, Yang T, Wei X, Liu Y, Xin WJ, Chen Y, Pang RP, Zang Y, Li YY, Liu XG (2011) Brain-derived neurotrophic factor contributes to spinal long-term potentiation and mechanical hypersensitivity by activation of spinal microglia in rat. Brain Behav Immun 25:322-334.

Chapter 4: Investigation of the role of established regulators of KCC2 following nervous system injury, namely microglia, BDNF, and TrkB

Modified from the following reference:

Akhter, E.T., Griffith, R., English, A.W., Alvarez, F.J. Removal of the potassium chloride co-transporter KCC2 from the somatodendritic membrane of axotomized motoneurons is independent of BDNF/TrkB signaling but is controlled by neuromuscular innervation. eNeuro. Submitted May 9, 2019. *Currently being revised after reviews.*

4.1 Abstract

In this chapter we investigate the role of well-established regulators of KCC2 in the spinal cord following injury. While what regulates KCC2 in brainstem motoneurons following injury to cranial nerves has never been investigated, studies in the dorsal horn after PNI and in spinal motoneurons caudal to SCI have both implicated brain-derived neurotrophic factor (BDNF) as a key regulator. In the dorsal horn specifically, microglia are pointed to as the inducers of KCC2 inactivity through a BDNF-TrkB mechanism. We hypothesized that the mechanism inducing KCC2 downregulation in spinal motoneurons following peripheral axotomy might also be mediated by microglia. However, interfering with microglial BDNF and microglia activation more generally did not impact KCC2 depletion after injury or its presence in intact cells. Motoneurons themselves also release BDNF and TrkB activation as has been reported on spinal cord dorsal horn neurons after nerve injury, motoneurons after spinal cord injury, and in many other central neurons throughout development or a variety of pathologies. To investigate this potential mechanism, we used genetic approaches to interfere with microglia activation or delete *bdnf* from specifically microglia or motoneurons, as well as pharmacology (ANA12) and pharmacogenetically (F616A mice) blocking TrkB activation. In this chapter we show that KCC2 dysregulation in axotomized motoneurons is independent of microglia, BDNF, and TrkB. Thus, KCC2 downregulation in axotomized motoneurons is via a novel mechanism involving KCC2 gene regulation that needs to be further explored.

4.2 Introduction

In Chapter 3 we describe the significant KCC2 loss on spinal motoneurons following peripheral axotomy. The goal of this chapter is to test the possible involvement of brain-derived neurotrophic factor (BDNF) and TrkB activation in this phenomenon. A large body of work has implicated BDNF-TrkB signaling in the regulation of KCC2 levels during development and under a variety of disease conditions by acting on both KCC2 membrane trafficking and gene

expression (reviewed in (Lee-Hotta et al., 2019)). Additionally, a microglia-BDNF-TrkB pathway is often highlighted as responsible for downregulation of KCC2 in dorsal horn neurons following PNI (Rivera et al., 2002; Coull et al., 2005; Miletic and Miletic, 2008; Ferrini and De Koninck, 2013; Medina et al., 2014). After PNI, axotomized motoneurons and peripheral Schwann cells have transient, but robust, increases in BDNF mRNA (Funakoshi et al., 1993; Neeper et al., 1996; Al-Majed et al., 2000) and exercise-dependent facilitation of motor axon growth has been shown to be dependent on BDNF-TrkB signaling (Wilhelm et al., 2012). This body of work led us to hypothesize that a BDNF-TrkB signaling pathway might induce the downregulation of KCC2 in motoneurons after peripheral axotomy as well. To test this hypothesis, we used a combined genetic, pharmacological and pharmacogenetic approach to interfere with microglia activation, BDNF release from microglia and motoneurons and to block TrkB activation after PNI.

In Chapter 3 we showed that at three days after injury, *kcc2* mRNA downregulation coincides temporally with the activation of microglia and their migration towards the cell bodies of axotomized motoneurons. Thus, it is possible that the activation of microglia and/or TrkB activation in axotomized motoneurons could both be involved in the control of *kcc2* expression. There is ample evidence that TrkB activation can downregulate *kcc2* gene expression in many pathologies and neurons (Coull et al., 2005; Boulenguez et al., 2010; Kang et al., 2015; Kourdougli et al., 2017). However, the net effect of BDNF-TrkB on KCC2 plasma membrane levels is complex and context dependent. BDNF-TrkB leads to downregulation of KCC2 in injured neurons, but upregulation of KCC2 in most adult neurons and during development (Rivera et al., 2004). The differences stem from the different balance of intracellular pathways activated downstream of TrkB activation in different situations. In development, BDNF simulates KCC2 expression through early growth response (Egr) 4, and mitogen-activated protein kinase (MAPK) signaling in an activity-independent way (Ludwig et al., 2011a,b). The same activity-independent BDNF pathway in mature neurons, through the PLCγ-calmodulin-dependent protein kinase pathway, inhibits *kcc2* transcription (Rivera et al., 2004). MAPK

signaling induced by BDNF also activates calpain, which can trigger KCC2 degradation within lysosomes (Puskarjov et al., 2012).

In the injury systems that have been well characterized, the PLCγ pathway and increased activity of calpain stimulated by calcium influx are key in BDNF-TrkB dependent loss of KCC2, as is reported in healthy mature neurons (Zhou et al., 2012; Kaila et al., 2014). However, the BDNF-KCC2 relationship after injury is more complicated than studies considered in isolation may suggest. Following spinal cord injury, BDNF initially suppresses KCC2 expression but then increases KCC2 in expression in the days to follow (Shulga et al., 2008; Boulenguez et al., 2010). Injured neurons make many shifts towards an immature state (Shulga et al., 2008), which may explain the switch in BDNF's role after spinal cord injury. These models have also shown that increasing exogenous BDNF levels can both up- or down-regulate KCC2 (Boyce et al., 2012; Ziemlinska et al., 2014)). The complicated effects of BDNF on injured neurons may thus be dependent on the total BDNF concentration surrounding neurons during their specific injury states.

4.3 Methods

4.3.1 Genetic approaches to interfere with microglia and BDNF release

To target microglia for cell-specific deletions of BNDF we used a tamoxifen-inducible cre allele knocked into the *Cx3cr1* locus. Crossing *Cx3cr1*$^{creER/+}$ mice with mice carrying floxed *bdnf* alleles (*bdnf*$^{f/f}$) removed *bdnf* from microglia. *Cx3cr1* is expressed in peripheral myeloid cells as well as in microglia, but peripheral myeloid cells have a higher turnover rate in the bone-marrow (Bennett et al., 2015). Thus, four weeks after tamoxifen treatment only microglia remain *bdnf* genetic KO's, while Cx3cr1-expressing myeloid cells have been newly generated from myeloid precursors that lack Cx3cr1 expression and have therefore not undergone tamoxifen-induced cre recombination. This approach for deleting specific genes from microglia

has been thoroughly characterized in previous publications (Goldmann et al., 2013; Tay et al., 2017).

To prevent the microglia reaction after PNI specifically in the ventral horn of the spinal cord, we studied mice in which the *csf1* gene for Colony Stimulating Factor 1 (CSF1) was knocked out in motoneurons. CSF1 is typically released from injured neurons to activate and recruit microglia (Elmore et al., 2014; Guan et al., 2016). To eliminate CSF1 release from cholinergic neurons, including axotomized motoneurons, we crossed $Chat^{iREScre/+}$ with $csf1^{f/f}$ animals. This manipulation has been shown to greatly attenuate the ventral horn microglial response to PNI (Rotterman et al., 2019).

We also crossed $Chat^{iREScre/+}$ animals with $bdnf^{f/f}$, mice to remove BDNF expression from motoneurons after injury. In this case, the *bdnf* gene was deleted from motoneurons throughout development. To delete *bdnf* more specifically in adult motoneurons, we used tamoxifen inducible "single-neuron labeling with inducible CreER-mediated knockout" (SLICK) mice. Specifically, mice of the SLICK-A line were crossed to $bdnf^{f/f}$ mice. SLICK-A mice express YFP and tamoxifen-inducible cre in subsets of neurons controlled by the *thy1* promoter (Young et al., 2008). When treated with tamoxifen, cre recombinase is activated in YFP+ neurons and eliminates expression of floxed genes. Thus, after tamoxifen treatment, YFP+ axotomized motoneurons (expressing cre) can be compared with YFP- axotomized motoneurons (not expressing cre) within the same animal (Young et al., 2008; Wilhelm et al., 2012; Zhu et al., 2016). All animals were injected with FB bilaterally and underwent sciatic cut/ligation surgeries as described. All analyses on KCC2 depletion were performed 14 days after nerve surgeries. The animals were perfusion-fixed with 4% paraformaldehyde as explained before and spinal cord sections immunolabeled for NeuN and KCC2, as explained

A summary of the mice used to generate experimental genotypes can be found in Table 4.1. Mice carrying $csf1^{f/f}$ alleles were generously donated by Dr. Jean X. Jiang (University of

Texas, San Antonio, TX). BDNF-floxed mice were generously donated by Dr. Michael Sendtner (Universität Würzburg, Würzburg, Germany).

4.3.2 Pharmacological block of TrkB activation: ANA-12 treatment

Wild type animals were treated continuously from injury to euthanasia with ANA-12, a competitive TrkB antagonist, or vehicle. ANA-12 was prepared in DMSO (30%), PEG300 (30%), and sterile saline (40%) at 2 mg/mL, and delivered (0.5 µl/hour) intraperitoneally (i.p) using an ALZET-2002 mini-osmotic pump. This rate was chosen to deliver the same concentration of ANA-12 per 12 hours as when administered twice daily with i.p. injections (Ambrogini et al., 2013; Chen et al., 2015). The use of osmotic pumps allows maintenance of a more constant concentration of the drug throughout the treatment period. Pumps were filled with ANA-12 or vehicle and primed in sterile saline overnight at 37°C. Pumps were implanted in the animals at the time of nerve cut/ligation (ANA12, n = 6; vehicle, n = 4) or sham surgery (ANA12, n = 4). They were brought from warm saline and immediately inserted into the peritoneal cavity, being careful not to disturb internal organs. The wound was closed in layers and animals were monitored daily to insure pump stability. Osmotic pumps were implanted the same day of nerve surgeries. Experiments were as above, we first retrogradely labeled LG motoneurons with Fast Blue and one week later performed a unilateral sciatic nerve cut/ligation paradigm followed 14 days later by perfusion-fixation with paraformaldehyde and the spinal cord sections were immunostained with KCC2 and NeuN. Prior to perfusion-fixation 14 days later, pumps were removed, weighed, and evacuated with a needle to ensure the drug was properly delivered. All pumps had expelled the expected volume of drug.

A subset of animals (n = 2 per group: sham-vehicle, sham-ANA-12, injury-vehicle, injury-ANA-12) was utilized to confirm the effectiveness of the ANA-12 treatment by testing phosphorylation of extracellular signal–regulated kinases (pERK), a downstream effector of TrkB activation known to increase in the spinal cord after nerve injury (Wang et al., 2004), with

Western blots. Animals were treated with ANA-12 or vehicle (as above) but underwent bilateral sham or sciatic nerve cut/ligations to increase the pERK signal. Seven days post-injury, the animals were euthanized and rapidly perfused with ice-cold saline, and the lumbar spinal cords were extracted and flash frozen. The tissue was homogenized in phosphatase-inhibitory lysis buffer (10 mM Hepes, pH 7.4, 50 mM NaF, 50 mM NaCl, 5 mM EDTA, 5 mM EGTA, 0.1% Triton X, 1 mM Na_3VO_4, 10 uM leupeptin, and 1 mM phenylmethylsulfonyl fluoride, PMSF, 25KIU/ml aprotinin) and centrifuged (13,000G at 4°C) to separate lysate. The pellet was discarded and cell lysates preserved at -80°C until the samples were assayed for protein concentration and processed for PAGE. Protein concentration was determined with the BioRad DC protein assay (cat# 5000116) at 750 nm. Protein standard dilutions were prepared in buffer containing the protease inhibitors (see above). Forty micrograms of protein from each sample was loaded onto BioRad 10% polyacrylamide precast gels (50 µl wells, cat# 456-0834) and BioRad Kaleidoscope protein molecular weight markers (cat# 161-0375) were loaded into at least one well on each gel. After electrophoresis, Western blotting was carried out overnight at 4°C onto PVDF membranes (BioRad cat# 162-0177) using 150 mA constant current. Primary rabbit antibodies against Phospho-p44/42 mitogen-activated protein kinase (pMAPK) also known as extracellular signal–regulated kinases (pERK) (Thr202/Thr204) (1:1000; rabbit polyclonal; Cell Signaling Technology Cat# 9101; RRID: AB_331646) and β actin (1:5000; rabbit polyclonal; Novus Cat# NB600-503) were utilized. The secondary antibody in all cases was HRP-conjugated donkey anti-rabbit, (1:5000; GE Healthcare Cat# GENA934; RRID:AB_2722659) and protein immunostaining was revealed using chemiluminescence (Clarity ECL western substrate, BioRad cat# 170-5061). β-actin was used as a loading control. The membrane was stripped using Re-Blot Plus, Strong Solution (Millipore cat# 2504) prior to re-probing with anti β-actin.

4.3.3 Pharmacogenetic TrkB Inactivation

F616A mice carry a mutation in the TrkB receptor that makes it sensitive to specific inhibition by the small molecule inhibitor 1-(1,1-dimethylethyl)-3-(1-naphthalenylmethyl)-1H-pyrazolo[3,4-d]pyrimidin-4-amine,PP1 analog (1NMPP1). We used these animals to block TrkB activation by administering 1NMPP1 following protocols well validated in the literature (Chen et al., 2005). Briefly, three days prior to nerve injury, F616A animals were switched from normal drinking water to drinking water with 1NMPP1 (5 μM, 0.01% DMSO) or vehicle. Animals were monitored twice daily to ensure proper hydration and adequate access to the water. They underwent standard FB retrograde labeling of the LG motor pool and unilateral sciatic nerve cut/ligation injuries. Fourteen days after injury, animals were perfusion fixed for KCC2 analyses.

4.4 Results

4.4.1 KCC2 depletion is independent of microglia.

To examine whether microglia-BDNF is involved in KCC2 loss from axotomized motoneurons, we used *Cx3cr1*$^{CreERT/+}$ :: *bdnf*$^{f/f}$ animals in which *bdnf* is removed specifically from microglia by cre recombination after tamoxifen treatment. All animals (n = 5 WT, 6 *Cx3cr1*^{CreERT2}) were analyzed 14 days after injury. KCC2 downregulation in axotomized motoneurons was similar in wild type animals and those with microglia-specific deletion of BDNF (Figure 4.1A). We compared injured and non-injured motoneurons in both wild-types and *Cx3cr1*$^{CreERT/+}$ :: *bdnf*$^{f/f}$ animals using a two-way ANOVA and found there were significant differences according only to injury, but not to genotype or their interaction (Statistical Table 4.1A). Deletion of BDNF from microglia had no effect on the downregulation of KCC2 after axotomy.

To further examine a possible role of microglia independent of BDNF, we attenuated the microglial reaction in the ventral horn by removing the colony stimulating factor 1 gene (*csf1*)

from motoneurons using *csf1* floxed alleles and a Chat-iRES-Cre mouse line expressing cre in choline acetyltransferase-expressing neurons (including all motoneurons). This manipulation was previously shown to prevent ventral horn microgliosis while preserving dorsal horn microglia activation after sciatic nerve injury (Rotterman et al., 2019), and we replicated this effect (Figure 4.1B). As in WT animals, *Chat* $^{iREScre/+}$ :: *csf1* $^{f/f}$ animals and *Chat* $^{+/+}$ :: *csf* $^{f/f}$ (n = 5 per group) expressed high levels of KCC2-IR on the cell body of motoneurons contralateral to injury, while motoneurons axotomized after sciatic nerve cut/ligation were similarly depleted in animals of both genotypes. Two-way ANOVA revealed KCC2 depletions dependent on injury, with no effect of genotype or interaction between the two (Statistical Table 4.1B). Thus, attenuating the microglia reaction in the ventral horn after nerve injury did not alter motoneuron KCC2 downregulation after axotomy (Figure 4.1C). We used animals of both sexes (n = 2 females, 3 males per group), and they similarly lose KCC2 with or without ventral horn microglia activation. In conclusion, mechanisms that deplete KCC2 on spinal cord motoneurons following axotomy are independent of microglia in both sexes. This is different from mechanisms inducing KCC2 depletion in dorsal horn neurons following nerve injuries, which involve sex-dependent microglia activation (Mapplebeck et al., 2017).

4.4.2 KCC2 depletion is independent of motoneuron-BDNF.

In addition to microglial induction of BDNF release, axotomized motoneurons increase BDNF expression after nerve injuries (Kobayashi et al., 1996; Al-Majed et al., 2000; Al-Majed et al., 2004). To determine whether autocrine BDNF signaling may induce KCC2 downregulation in axotomized motoneurons, we utilized *Chat* $^{iRES\text{-}Cre/+}$ *:: bdnf* $^{f/f}$ mice to knock out *bdnf* from all cholinergic neurons. Removal of BDNF from motoneurons did not impact baseline KCC2 levels or KCC2 decrease after axotomy (Figure 4.2A). We compared *Chat* $^{iRES\text{-}Cre/+}$ *:: bdnf* $^{f/+}$ (n = 4) and *Chat* $^{+/+}$ *:: bdnf* $^{f/f}$ animals (n = 4) and found no significant difference in KCC2-IR levels between uninjured motoneurons and similar statistically significant reductions in injured motoneurons

in animals of both genotypes. As with other groups, two-way ANOVA revealed only injury predicted KCC2 loss (Statistical Table 4.1C).

In these experiments, all cholinergic neurons lacked BDNF throughout development, raising the possibility of compensatory mechanisms developing to regulate KCC2. To circumvent this potential pitfall, we analyzed a cohort of animals using "single-neuron labeling with inducible CreER-mediated knock-out" or SLICK mice. We specifically used the SLICK-A line that we have used previously to delete *bdnf* in a cell-specific manner (Krakowiak et al., 2015). In these animals, YFP and $CreER^{T2}$ are constitutively expressed under the control of the *thy1* promoter in sparse populations of neurons, including some motoneurons (Figure 4.2B). $CreER^{T2}$ is activated in the presence of tamoxifen, which we administered in adulthood, thereby eliminating developmental confounds. This technique has the added advantage of allowing internal controls since only YFP+ cells have the capacity of cre recombination, leaving YFP- populations unaffected. We crossed these animals with $bdnf^{f/f}$ animals, treated them with tamoxifen, and retrogradely labeled LG motoneurons with Fast Blue (FB) prior to bilateral sciatic cut/ligation. Thus, all FB+ cells are axotomized LG motoneurons, but only YFP+ and FB+ motoneurons have undergone cre recombination removing BDNF expression. Due to the sparse YFP/cre expression of motoneurons, 10 YFP/cre+ neurons per animal were not feasible even after doing bilateral injections and axotomy to increase the number of FB/YFP/cre-expressing motoneurons. Membrane KCC2-IR was measured in 2 to 10 FB/YFP+ motoneurons per animal (4.23 ± 2.75 average neurons/animal ± SD) to obtain each animal average and compared to similar numbers of FB/non-YFP (cre-) neurons (n = 2-10 neurons, average 4.22 ± 3.35). We compared SLICK :: $bdnf^{+/+}$ animals (n = 3 animals) with SLICK :: $bdnf^{f/f}$ animals (n = 5 animals) all treated with tamoxifen prior to Fast Blue retrograde labeling and bilateral sciatic nerve cut and ligation. There was no significant difference in KCC2 levels between injured FB+/YFP+ and FB+/YFP- motoneurons (with or without cre, respectively) in either genotype 14 days after injury (Figure 4.2B,C; Statistical Table 4.1D). Removing BDNF from adult

motoneurons did not prevent KCC2 downregulation, similar to the lack of effects of removing BDNF from all motoneurons throughout development.

4.4.3 KCC2 depletion is independent of TrkB activation.

Removing BDNF from either of the two main sources in the spinal cord after injury did not have any effects on KCC2 regulation, but it is still possible that another source could compensate for motoneuron or microglial BDNF. Moreover, removal of BDNF could also be compensated for by upregulation of neurotrophin-4/5, another ligand of TrkB (Huang and Reichardt, 2003). It has also been shown that ligand-independent autophosphorylation of TrkB receptors can occur (Zaccaro et al., 2001). We therefore blocked the TrkB receptor directly with either the competitive TrkB antagonist ANA-12 (Cazorla et al., 2011) or by utilizing the F616A mutant pharmacogenetic system (Chen et al., 2005).

In ANA-12 experiments, mini-osmotic pumps were used to continuously deliver the drug or vehicle intraperitoneally into wild-type animals, starting at the time of injury and until euthanasia (14 days). Systemic ANA-12 delivered via intraperitoneal injections has been shown to cross the blood brain barrier and effectively inhibit TrkB four hours post-injection (Cazorla et al., 2011). The concentration of ANA-12 in the pump was adjusted such that we delivered 1 ng per hour into the animal. ANA-12 actions were confirmed with western blot by probing for extracellular signal-regulated kinase phosphorylation (pERK), a target of TrkB activation and kinase activity (Wilkerson and Mitchell, 2009). In animals treated with vehicle, pERK expression was increased in the spinal cord of injured animals compared to sham-vehicle treated animals. This change was attenuated with ANA-12 treatment (Figure 4.3A). There was no difference in pERK signal between sham and cut ligated animals treated with ANA-12.

To assess any effects of ANA-12 treatment on KCC2 downregulation, we implemented the same quantitative analyses used before on the cell bodies of bilaterally labeled LG motoneurons 14 days following unilateral sciatic nerve cut/ligation. Thus, we compared KCC2

on FB LG motoneurons ipsilateral and contralateral to the injury. In addition, one cohort of animals (n = 4) was treated with ANA-12 but underwent a sham injury in one side. In sham control animals, no significant differences in KCC2 membrane immunofluorescence were found on the sham side compared to the contralateral side, and the levels of KCC2-IR was comparable to all control motoneurons in previous experiments. This suggests that basal expression of KCC2 was not affected by ANA-12 treatment. In injured animals we found similar reductions of KCC2 on injured motoneurons in animals treated with either vehicle (n = 4) or with ANA-12 (n = 6) compared to control motoneurons (Figure 4.3B). Two-way ANOVA revealed significant effects of side, treatment, and an interaction between the two. However, this was due to the inclusion of a sham group within the injury parameter. Post-hoc *Bonferroni t tests* confirmed there were no significant differences in sham injured and intact motoneurons. There were also no reductions in KCC2 levels between injured neurons treated with ANA12 or vehicle (Statistical Table 4.1F). In conclusion, ANA-12 treatment did not prevent KCC2 downregulation in axotomized motoneurons or impact KCC2 levels in intact neurons.

ANA-12 is a partial competitive antagonist of TrkB (Chen et al., 2015) and therefore we cannot assume block of ligand binding to be complete. To obtain further proof of a lack of a role for TrkB in KCC2 downregulation, we blocked TrkB kinase activity (and thus signaling) utilizing F616A mutant mice. F616A animals express a TrkB mutation with a single base substitution that makes it sensitive to the kinase inhibitor 1NMPP1 (Chen et al., 2005). 1NMPP1 was administered in the drinking water using established protocols that prevent TrkB downstream signaling (Chen et al., 2005; Wang et al., 2009; Rantamaki et al., 2011). In agreement with ANA-12 experiments, in F616A animals treated with normal drinking water (n = 3) and 1NMPP1 (n = 6) had no differences in uninjured FB LG motoneurons. Two-way ANOVA showed that downregulation of KCC2 was also found after injury in FB LG motoneurons regardless of treatment (Statistical Table 4.1F, Figure 4.3C). Taken together, the results in ANA-12 treated

animals and F616A animals allow us to conclude that KCC2 downregulation in axotomized motoneurons is independent of TrkB signaling.

4.5 Discussion

KCC2 regulation on peripherally axotomized motoneurons occurs independent of microglia and BDNF/TrkB signaling.

KCC2 regulation after PNI differs between motoneurons and dorsal horn interneurons.

Like motoneurons, dorsal horn spinal neurons (more specifically nociceptive Lamina I neurons) decrease KCC2 following nerve injuries, resulting in disinhibition and behavioral hyperalgesia (Coull et al., 2003; Coull et al., 2005). Unlike motoneurons, dorsal horn neurons are fully contained within the CNS and are not directly injured or axotomized after PNI. Instead, signals from injured sensory afferents trigger the activation of a pathway involving microglia and TrkB activation that depletes KCC2 in neighboring neurons, at least in males (Tsuda et al., 2003; Coull et al., 2005; Trang et al., 2009; Beggs et al., 2012; Trang et al., 2012; Sorge et al., 2015). Dorsal horn neurons in female mice also decrease KCC2 but through a different mechanism that has not yet been well elucidated (Mapplebeck et al., 2018). Independent of sex, the changes in KCC2 occur quickly following injury—most typically a constriction of the nerve—and are likely due to changes in KCC2 phosphorylation and membrane trafficking. In axotomized motoneurons, however, KCC2 is downregulated at the transcriptional level and it takes 2-3 weeks for complete loss of the protein from the membrane, likely because of slow protein turnover (See Chapter 3).

Another major distinction between spinal motoneurons after PNI and mechanisms described in other models is a differential dependence on microglia and BDNF. Activated microglia quickly surround the cell bodies of axotomized motoneurons after injury (Aldskogius,

2011) that, similar to microglia in the dorsal horn, could be involved in regulating KCC2 expression through local BDNF release on the motoneuron surface. It should be noted that while studies investigating the microglia-BDNF-TrkB mechanism discuss it as an ATP-stimulated release of BDNF from P2X4R+ microglia, recent evidence from RNAseq experiments has shown that, both in healthy spinal cord (Matcovitch-Natan et al., 2016; Fernandez-Zafra et al., 2019) and following peripheral nerve injury (Denk et al., 2016; Tay et al., 2018) BDNF RNA is not expressed microglia at significant levels. While studies from the de Koninck lab have clearly illustrated a relationship between microglia stimulation with ATP and signaling through the TrkB receptor on dorsal horn neurons, they have not confirmed direct release of BDNF from microglia alone. Studies directly reporting BDNF expression within microglia have done so using antibodies that have not been validated (Wang et al., 2012; Zhang et al., 2014; Taylor et al., 2016; Xu et al., 2019). It is possible that P2X4R+ microglia (at least in male mice) are responsible for inducing changes in other cell types such as astrocytes and thus that microglia represent an intermediate step in the process of decreasing KCC2 from motoneuron membranes after axotomy. Astrocytes have also been shown to release BDNF after PNI (Qian et al., 2018) and in a model of demyelinating disease (Fulmer et al., 2014), though, again with antibodies that aren't validated. However in culture, astrocytes have been shown to release BDNF as measured with solution hybridization and ELISA (Wu et al., 2004). Given that microglia and astrocytic activation are tightly related (Pascual et al., 2012; Yang et al., 2012; Liddelow et al., 2017) it is possible that astrocytic release of BDNF, concurrent with or induced by microgliosis, induces KCC2 loss in the dorsal horn. However, our data show that TrkB is not involved, and thus that BDNF release from any source is not likely responsible for KCC2 loss.

Regardless of whether BDNF is directly released from microglia or is a downstream pathway of microglial activation, our results negate the hypothesis that microglia play a role in KCC2 depletion on spinal motoneurons following axotomy. Microglia activation phenotypes are different depending on the distance from injured cells (Perego et al., 2011) and the type of injury

(Hu et al., 2007; Taylor and Sansing, 2013). They can also have distinct phenotypes in proximal CNS regions independent of injury (Lawson et al., 1990), making it possible that dorsal and ventral horn microglia may have very different responses to PNI. Although activation of microglia in the dorsal horn is also dependent on CSF1, this time released from injured primary afferents (Guan et al., 2016), the release of BDNF following microglial activation was shown to specifically depend on microglia P2X4 receptors activated by ATP released from the central terminals of overactive sensory afferents (Beggs et al., 2012). Ventral horn microglia also upregulate several classes of purinergic receptor after nerve injury (Kobayashi et al., 2012), but their exact roles have not yet been investigated. Although ventral horn microgliosis is also dependent on CSF1 released by axotomized motoneurons (Rotterman et al., 2019), some features of the microglia reaction to nerve injury differ between the dorsal and ventral horn (Rotterman et al., 2019).

Another significant difference is the type of nerve injury leading to activation of microglia. Dorsal horn studies are focused on models of partial ligation of the sciatic nerve known to cause well-characterized hyperalgesia (Bennett and Xie, 1988), while we studied the consequences of full transection of the nerve in which we don't observe any obvious pain-like behavioral phenotypes. One study comparing the phenotype of dorsal horn microglia in these two types of injuries found many significant differences (Hu et al., 2007). Clearly, the response of microglia in the ventral horn is not involved in the downregulation of KCC2 from motoneurons after nerve transections and is thus different from the well-established role of dorsal horn microglia after hyperalgesia-inducing nerve injuries.

KCC2 downregulation differs in motoneurons following PNI or spinal cord injury

BDNF is transiently upregulated in motoneurons following axotomy (Kobayashi et al., 1996; Al-Majed et al., 2000a; Al-Majed et al., 2004), and the release of BDNF is key in treatments that enhance motor axon regeneration and functional recovery following injury (Al-

Majed et al., 2000a; Al-Majed et al., 2000b; English et al., 2007; Wilhelm et al., 2012; English et al., 2013; Krakowiak et al., 2015). However, based on the results of our experiments showing little effect on the loss of KCC2 after axotomy after knocking out the *bdnf* gene in motoneurons, either through development or selectively in adults before injury, along with blocking TrkB signaling with ANA-12 or in the F616A mice, we conclude that BDNF/TrkB mechanisms are not involved in the regulation of KCC2 expression in axotomized motoneurons after PNI.

BDNF has been implicated in the reduction of KCC2 inducing spasticity after spinal cord injury, but as discussed in the introduction, this regulation is not clear. Unlike PNI, most models of spinal cord injury investigate motoneurons caudal to the trauma, and their axons remain intact in the periphery. While they also lose KCC2 after injury, this change is relatively fast and minor relative to our axotomized motoneurons (Boulenguez et al., 2010). A post-translational mechanism has been proposed to explain this effect, indicating that KCC2 downregulation was dependent on the loss of descending serotonergic inputs and 5HT2A receptor activity (Bos et al., 2013). In fact, 5HT2 pharmacological activation was found to increase KCC2 membrane content and hyperpolarize the chloride equilibrium (Bos et al., 2013). However following PNI, descending serotonin tone should not be affected and the mechanism of KCC2 downregulation we have shown in Chapter 3 is best related to altered gene expression than KCC2 trafficking. Therefore the mechanism down regulating motoneuron KCC2 after PNI is distinct from previous mechanisms suggested for KCC2 downregulation in motoneurons after SCI.

4.6 Tables and Figures

Table 4.1 Mouse strains used in Chapter 4

Mouse Strain	Stock No.	References
$Cx3cr1^{creER/+}$	RRID:IMSR_JAX: 020940	Goldman et al., 2013
CSF^{ff}	Donated by Dr. Jean X. Jiang, University of Texas, San Antonio, TX	Harris et al. 2012
SLICK-A	RRID:IMSR_JAX:007606	Young et al., 2008
F616A	RRID: MSR_JAX:022363	Chen et al., 2005
$ChAT^{iRES-cre/+}$	RRID:IMSR_JAX: 006410	Rossi et al., 2011

Statistical Table 4.1

	Data Reference	Data Structure	Type of Test	Statistical Significance
A	4.1A	Normal Distribution	**Two-way ANOVA** Side; $F_{(1,19)} = 37.293$; $p < 0.001$ Genotype; $F_{(1,19)} = 0.0715$; $p = 0.792$ Interaction; $F_{(1,19)} = 0.336$; $p = 0.569$	
	WT (Intact) vs. WT (cut/ligated) Cx3cr1$^{CreERT/+}$:: *bdnf*$^{f/f}$ (Intact) Cx3cr1$^{CreERT/+}$:: *bdnf*$^{f/f}$ (cut/ligated)		*Post hoc* Bonferroni *Post hoc* Bonferroni *Post hoc* Bonferroni	$p = 0.005$ $p > 0.999$ $p < 0.001$
B	4.1C	Normal Distribution	**Two-way ANOVA** Side; $F_{(1,19)} = 25.611$; $p < 0.001$ Genotype; $F_{(1,19)} = 3.665$; $p = 0.074$ Interaction; $F_{(1,19)} = 2.541$; $p = 0.131$	
	Chat$^{+/+}$:: *csf1*$^{f/f}$ (Intact) vs. Chat$^{+/+}$:: *csf1*$^{f/f}$ (cut/ligated) Chat$^{iREScre/+}$:: *csf1*$^{f/f}$ (Intact) Chat$^{iREScre/+}$:: *csf1*$^{f/f}$ (cut/ligated)		*Post hoc* Bonferroni *Post hoc* Bonferroni *Post hoc* Bonferroni	$p < 0.001$ $p = 0.074$ $p < 0.001$
C	4.2A	Normal Distribution	**Two-way ANOVA** Side; $F_{(1,17)} = 22.070$; $p < 0.001$ Genotype; $F_{(1,17)} = 2.417$; $p = 0.142$ Interaction; $F_{(1,17)} = 0.545$; $p = 0.473$	
	Chat$^{iREScre/+}$:: *bdnf*$^{f/+}$ (Intact) vs. Chat$^{iREScre/+}$:: *bdnf*$^{f/+}$ (cut/ligated) Chat$^{iREScre/+}$:: *bdnf*$^{f/f}$ (Intact) Chat$^{iREScre/+}$:: *bdnf*$^{f/f}$ (cut/ligated)		*Post hoc* Bonferroni *Post hoc* Bonferroni *Post hoc* Bonferroni	$p = 0.008$ $p = 0.382$ $p = 0.002$
D	4.2C	Normal Distribution	**Two-way ANOVA** Genotype; $F_{(1,12)} = 0.443$; $p = 0.518$ Cre/YFP; $F_{(1,12)} = 0.00489$; $p = 0.945$ Interaction; $F_{(1,12)} = 0.0157$; $p = 0.902$	
E	4.3B	Normal Distribution Unequal Variance	**Two-way ANOVA** Side; $F_{(1,27)} = 6.474$; $p = 0.018$ Treatment; $F_{(2,27)} = 13.095$; $p < 0.001$ Interaction; $F_{(2,27)} = 7.289$; $p = 0.004$	
	Intact ANA12 vs Sham ANA12 Intact VEH Injured VEH Intact ANA12 Injured ANA12		*Post hoc* Bonferroni *Post hoc* Bonferroni *Post hoc* Bonferroni *Post hoc* Bonferroni *Post hoc* Bonferroni	$p = 0.576$ $p > 0.999$ $p = 0.003$ $p > 0.999$ $p = 0.006$
F	4.3C	Normal Distribution	**Two-way ANOVA** Side; $F_{(1,17)} = 35.783$; $p < 0.001$ Treatment; $F_{(1,17)} = 0.935$; $p = 0.350$ Interaction; $F_{(1,,17)} = 1.325$; $p = 0.269$	
	Intact VEH vs Injured VEH Intact 1NMPP1 Injured 1NMPP1		*Post hoc* Bonferroni *Post hoc* Bonferroni *Post hoc* Bonferroni	$p = 0.002$ $p = 0.470$ $p < 0.001$

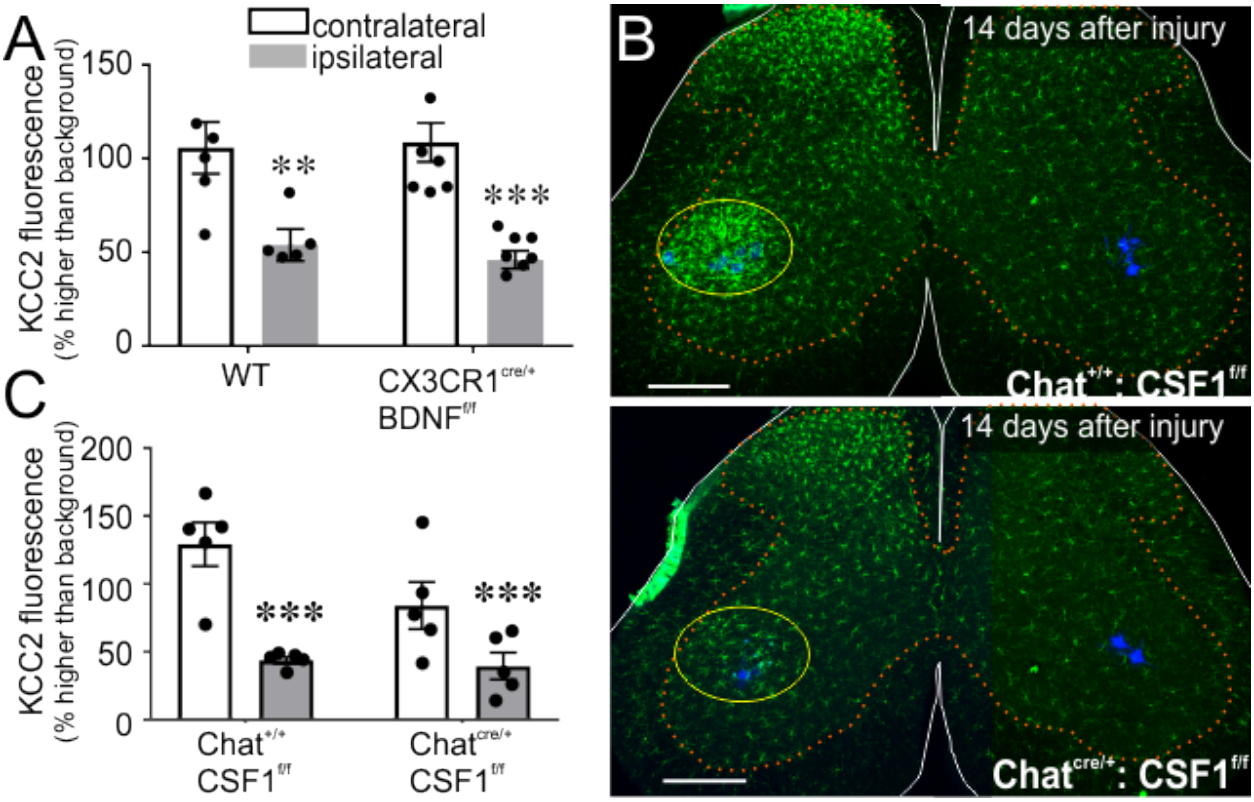

Figure 4.1 KCC2 depletion occurs independent of microgliosis. A) Relative KCC2 depletion in WT and Cx3cr1 BDNF KO animals 14 days after cut/ligation. Genotype had no effect on KCC2 levels in motoneurons contralateral or ipsilateral to injury (Statistical Table 4.1A). Removing BDNF from microglia had no impact on KCC2 expression. **B**) Lumbar spinal cord sections from animals expressing normal CSF1 (top) and with CSF1 removed from motoneurons (bottom) 14 days after cut/ligation. *Chat*$^{iREScre/+}$ *:: csf1*$^{f/f}$ animals (bottom image) exhibit normal microgliosis in the dorsal horn but have the microglial reaction to injury greatly attenuated in the ventral horn compared to *Chat*$^{I+/+}$ *:: csf1*$^{f/f}$ (top image). Scale bars = 200 μm. **C**) KCC2 immunofluorescence 14 days after sciatic cut/ligation in *csf1*$^{f/f}$ animals. Preventing microgliosis in the ventral horn had no impact on KCC2 within intact or injured motoneurons (Statistical Table 4.1B). Error bars = SEM; ** p ≤0.01, *** p ≤ 0.001.

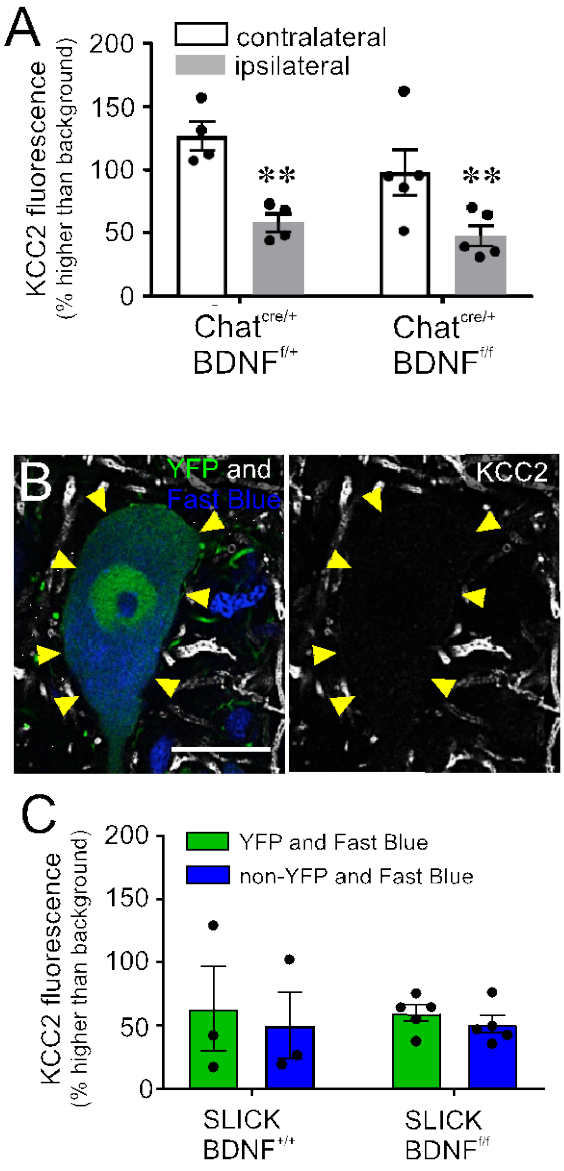

Figure 4.2 Knockout of motoneuron BDNF does not impact KCC2 downregulation. **A)** KCC2 immunoreactivity in *Chat*$^{iREScre/+}$ *:: bndf*$^{f/f}$ motoneurons 14 days after sciatic cut/ligation. Removal of BDNF from motoneurons throughout development had no impact on KCC2-IR in motoneurons ipsilateral or contralateral to injury. The same baseline levels and depletion were observed regardless of genotype. (Statistical Table 4.1C; ** $p \leq 0.01$). **B**) SLICK: BDNF$^{f/f}$ LG motoneurons following tamoxifen treatment, 14 days after sciatic nerve cut/ligation. YFP+ neurons express cre and have *bdnf* excised with tamoxifen treatment. KCC2 is extensively

removed from the somatic membrane in response to injury even after BDNF KO in adulthood. **C**) Quantification of KCC2 downregulation on ligated cre+ (YFP+) and cre- (YFP-) motoneurons after tamoxifen treatment and bilateral sciatic cut/ligation (n = 4.23 ± 2.75 YFP+ and 4.22 ± 3.35 YFP- motoneurons/animal). There is no difference between cre+ (green) and cre- (blue) motoneuron loss of KCC2 regardless of BDNF KO (Statistical Table 4.1D). Error bars = SEM. Removing motoneuron BDNF production had no impact on KCC2 expression or downregulation following peripheral axotomy.

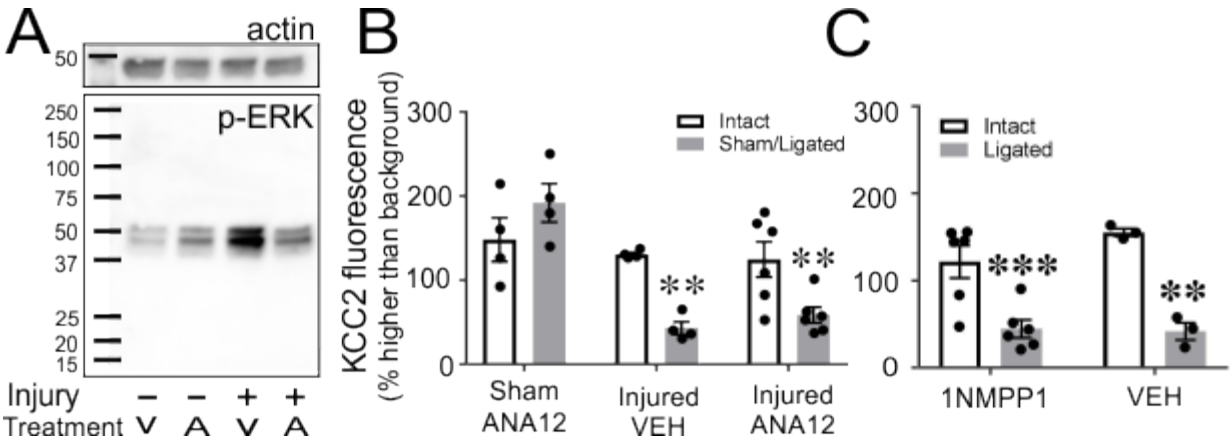

Figure 4.3 Systemic blockade of TrkB does not attenuate KCC2 downregulation. A) Western blots of pERK (bottom) and B-actin (top) from lumbar tissue 7 days after bilateral sciatic cut/ligation or sham surgery. Animals were exposed to ANA12 (a partial TrkB antagonist) or vehicle continuously from time of surgery to euthanasia. In sham animals exposed to ANA12, there is a slight increase in pERK. However, there was a much larger amount of pERK in vehicle-treated animals that underwent sciatic cut/ligation; this was not seen in injured animals treated with ANA12. Thus, ANA12 prevented the normal increase in TrkB signaling that typically occurs after injury. **B**) KCC2-IR on LG motoneurons of WT animals treated with ANA12 or vehicle through mini osmotic pumps 14 days after unilateral sciatic sham surgery or cut/ligation. Neither exposure to ANA12 nor sham surgery altered KCC2 levels in intact motoneurons, and motoneurons with their axons cut and ligated had the same depletion of KCC2 regardless of exposure to ANA12 (Statistical Table 4.1E). **C**) KCC2-IR on motoneurons of F616A animals 14 days after peripheral cut/ligation. Animals were given 1NMPP1 or vehicle prior to surgery, through time of euthanasia. F616A animals have a mutated TrkB receptor such that when exposed to 1NMPP1 cannot autophosphorylate or signal. There was no difference in KCC2 presence or loss regardless of treatment (Statistical Table 4.1F). Preventing TrkB signaling did not alter KCC2 protein expression or loss after injury. (** $p \leq 0.01$, *** $p \leq 0.001$). Error bars = SEM.

4.7 References

Al-Majed AA, Brushart TM, Gordon T (2000) Electrical stimulation accelerates and increases expression of BDNF and trkB mRNA in regenerating rat femoral motoneurons. Eur J Neursoci 12:4381-4390.

Al-Majed AA, Tam SL, Gordon T (2004) Electrical stimulation accelerates and enhances expression of regeneration-associated genes in regenerating rat femoral motoneurons. Cell Mol Neurobiol 24:379-402.

Bennett ML, Bennett FC, Liddelow SA, Ajami B, Zamanian jL, Fernhoff NB, Mulinyawe SB, Bohlen CJ, Adil A, Tucker A, Weissman IL, Chang EF, Li GH, Grant GA, Hayden Gephart MG, Barres BA (2015) New tools for studying microglia in the mouse and human CNS. PNAS:1-9.

Bos R, Sadlaoud K, Boulenguez P, Buttigieg D, Liabeuf S, Brocard C, Haase G, Bras H, Vinay L (2013) Activation of 5-HT2A receptors upregulates the function of the neuronal K-Cl cotransporter KCC2. PNAS 110:348-353.

Boulenguez P, Liabeuf S, Bos R, Bras H, Jean-Xavier C, Brocard C, Stil A, Darbon P, Cattaert D, Delpire E, Marsala M, Vinay L (2010) Down-regulation of the potassium chloride cotransporter KCC2 contributes to spasticity after spinal cord injury. Nat. Med. 16:302-307.

Boyce VS, Park J, Gage FH, Mendell LM (2012) Differential effects of brain-derived neurotrophic factor and neurotrophin-3 on hindlimb function in paraplegic rats. Eur J Neursoci 35:221-232.

Cazorla M, Premont J, Mann A, Girard N, Kellendonk C, Rognan D (2011) Identification of a low-molecular weight TrkB antagonist with anxiolytic and antidepressant activity in mice. J Clin Invest 121:1846-1857.

Chen L, Gao X, Zhao S, Hu W, Chen J (2015) The Small-Molecule TrkB Agonist 7, 8-Dihydroxyflavone Decreases Hippocampal Newborn Neuron Death After Traumatic Brain Injury. J Neuropath Exp Neur 74:557-567.

Chen X, Ye H, Kuruvilla R, Ramanan N, Scangos KW, Zhang C, Johnson NM, England PM, Shokat KM, Ginty DD (2005) A chemical-genetic approach to studying neurotrophin signaling. Neuron 46:13-21.

Coull JA, Beggs S, Boudreau D, Boivin D, Tsuda M, Inoue K, Gravel C, Salter MW, De Koninck Y (2005) BDNF from microglia causes the shift in neuronal anion gradient underlying neuropathic pain. Nature 438:1017-1021.

Denk F, Crow M, Didangelos A, Lopes DM, McMahon SB (2016) Persistent Alterations in Microglial Enhancers in a Model of Chronic Pain. Cell Rep 15:1771-1781.

Elmore MR, Najafi AR, Koike MA, Dagher NN, Spangenberg EE, Rice RA, Kitazawa M, Matusow B, Nguyen H, West BL, Green KN (2014) Colony-stimulating factor 1 receptor signaling is necessary for microglia viability, unmasking a microglia progenitor cell in the adult brain. Neuron 82:380-397.

Fernandez-Zafra T, Gao T, Jurczak A, Sandor K, Hore Z, Agalave NM, Su J, Estelius J, Lampa J, Hokfelt T, Wiesenfeld-Hallin Z, Xu X, Denk F, Svensson CI (2019) Exploring the transcriptome of resident spinal microglia after collagen antibody-induced arthritis. Pain 160:224-236.

Ferrini F, De Koninck Y (2013) Microglia control neuronal network excitability via BDNF signalling. Neural Plast 2013:429815.

Fulmer CG, VonDran MW, Stillman AA, Huang Y, Hempstead BL, Dreyfus CF (2014) Astrocyte-derived BDNF supports myelin protein synthesis after cuprizone-induced demyelination. J Neurosci 34:8186-8196.

Funakoshi H, Frisen J, Barbany G, Timmusk T, Zachrisson O, Verge VM, Persson H (1993) Differential expression of mRNAs for neurotrophins and their receptors after axotomy of the sciatic nerve. J Cell Biol 123:455-465.

Goldmann T, Wieghofer P, Muller PF, Wolf Y, Varol D, Yona S, Brendecke SM, Kierdorf K, Staszewski O, Datta M, Luedde T, Heikenwalder M, Jung S, Prinz M (2013) A new type of microglia gene targeting shows TAK1 to be pivotal in CNS autoimmune inflammation. Nat Neurosci 16:1618-1626.

Guan Z, Kuhn J, Wang X, Colquitt B, Solorzano C, Vaman S, Guan A, Evans-Reinsch Z, Braz J, Devor M, Abboud-Werner S, Lanier L, Lomvardas S, Basbaum A (2016) Injured sensory neuron-derived CSF1 induces microglial proliferation and DAP12-dependent pain. Nat Neurosci 19:94-101.

Harris SE, MacDougall M, Horn D, Woodruff K, Zimmer SN, Rebel VI, Farjardo R, Feng JQ, Gluhak-Heinrich J, Harris MA, Abbound Werner S (2012) Meox2Cre-mediated disruption of CSF-1 leads to osteopetrosis and osteocyte defects. Bone 1:42-53

Hu P, Bembrick AL, Keay KA, McLachlan EM (2007) Immune cell involvement in dorsal root ganglia and spinal cord after chronic constriction or transection of the rat sciatic nerve. Brain Behav Immun 21:599-616.

Huang EJ, Reichardt LF (2003) Trk receptors: roles in neuronal signal transduction. Annu Rev Biochem 72:609-642.

Kaila K, Price TJ, Payne JA, Puskarjov M, Voipio J (2014) Cation-chloride cotransporters in neuronal development, plasticity and disease. Nat Rev Neurosci 15:637-654.

Kang SK, Johnston MV, Kadam SD (2015) Acute TrkB inhibition rescues phenobarbital-resistant seizures in a mouse model of neonatal ischemia. Eur J Neursoci 42:2792-2804.

Kobayashi NR, Bedard AM, Hincke MT, Tetzlaff W (1996) Increased expression of BDNF and trkB mRNA in rat facial motoneurons after axotomy. Eur J Neursoci 8:1018-1029.

Kourdougli N, Pellegrino C, Renko JM, Khirug S, Chazal G, Kukko-Lukjanov TK, Lauri SE, Gaiarsa JL, Zhou L, Peret A, Castren E, Tuominen RK, Crepel V, Rivera C (2017) Depolarizing gamma-aminobutyric acid contributes to glutamatergic network rewiring in epilepsy. Ann Neurol 81:251-265.

Krakowiak J, Liu C, Papudesu C, Ward PJ, Wilhelm JC, English AW (2015) Neuronal BDNF signaling is necessary for the effects of treadmill exercise on synaptic stripping of axotomized motoneurons. Neural Plast 2015:392591.

Lawson LJ, Perry VH, Dri P, Gordon S (1990) Heterogeneity in the distribution and morphology of microglia in the normal adult mouse brain. Neuroscience 39:151-170.

Lee-Hotta S, Uchiyama Y, Kametaka S (2019) Role of the BDNF-TrkB pathway in KCC2 regulation and rehabilitation following neuronal injury: A mini review. Neurochem Int 128:32-38.

Liddelow SA et al. (2017) Neurotoxic reactive astrocytes are induced by activated microglia. Nature 541:481-487.

Ludwig A, Uvarov P, Pellegrino C, Thomas-Crusells J, Schuchmann S, Saarma M, Airaksinen MS, Rivera C (2011a) Neurturin evokes MAP-K dependent upregulation of Egr4 and KCC2 in developing neurons. Neural Plast 1-8

Ludwig A, Uvarov P, Soni S, Thomas-Crusells J, Airaksinen MS, Rivera C (2011b) Early growth response 4 mediates BDNF induction of potassium chloride cotransporter 2 transcription. J Neurosci 31;644-649

Mapplebeck JC, Beggs S, Salter MW (2017) Molecules in pain and sex: a developing story. Mol Brain 10:9.

Matcovitch-Natan O et al. (2016) Microglia development follows a stepwise program to regulate brain homeostasis. Science (New York, NY) 353:aad8670.

Medina I, Friedel P, Rivera C, Kahle KT, Kourdougli N, Uvarov P, Pellegrino C (2014) Current view on the functional regulation of the neuronal K(+)-Cl(-) cotransporter KCC2. Front Cell Neurosci 8:27.

Miletic G, Miletic V (2008) Loose ligation of the sciatic nerve is associated with TrkB receptor-dependent decreases in KCC2 protein levels in the ipsilateral spinal dorsal horn. Pain 137:532-539.

Neeper SA, Gomez-Pinilla F, Choi J, Cotman CW (1996) Physical activity increases mRNA for brain-derived neurotrophic factor and nerve growth factor in rat brain. Brain Res 726:49-56.

Pascual O, Ben Achour S, Rostaing P, Triller A, Bessis A (2012) Microglia activation triggers astrocyte-mediated modulation of excitatory neurotransmission. Proc Natl Acad Sci USA 109:E197-205.

Perego C, Fumagalli S, De Simoni MG (2011) Temporal pattern of expression and colocalization of microglia/macrophage phenotype markers following brain ischemic injury in mice. Journal of neuroinflammation 8:174.

Puskarjov M, Ahmad F, Kaila K, Blaesse P (2012) Activity-dependent cleavage of the K-Cl cotransporter KCC2 mediated by calcium-activated protease calpain. J Neurosci 32:11356-11364.

Qian C, Tan D, Wang X, Li L, Wen J, Pan M, Li Y, Wu W, Guo J (2018) Peripheral Nerve Injury-Induced Astrocyte Activation in Spinal Ventral Horn Contributes to Nerve Regeneration. Neural Plast 2018:8561704.

Rantamaki T, Vesa L, Antila H, Di Lieto A, Tammela P, Schmitt A, Lesch KP, Rios M, Castren E (2011) Antidepressant drugs transactivate TrkB neurotrophin receptors in the adult rodent brain independently of BDNF and monoamine transporter blockade. PloS one 6:e20567.

Rivera C, Voipio J, Thomas-Crusells J, Li H, Emri Z, Sipila S, Payne JA, Minichiello L, Saarma M, Kaila K (2004) Mechanism of activity-dependent downregulation of the neuron-specific K-Cl cotransporter KCC2. J Neurosci 24:4683-4691.

Rivera C, Li H, Thomas-Crusells J, Lahtinen H, Viitanen T, Nanobashvili A, Kokaia Z, Airaksinen MS, Voipio J, Kaila K, Saarma M (2002) BDNF-induced TrkB activation down-regulates the K+-Cl- cotransporter KCC2 and impairs neuronal Cl- extrusion. J Cell Biol 159:747-752.

Rossi J, Balthasar N, Olson D, Scott M, Berglund E, Lee CE, Choi MJ, Lauzon D, Lowell BB, Elmquist JK (2011) Melanocortin-4 receptors expressed by cholinergic neurons regulate energy balance and glucose homeostasis. Cell Metab 2:195-204

Rotterman TM, Akhter ET, Lane AR, MacPherson KP, Garcia VV, Tansey MG, Alvarez FJ (2019) Spinal motor circuit synaptic plasticity after peripheral nerve injury depends on microglia activation and a CCR2 mechanism. J Neurosci 32:3412–3433

Shulga A, Thomas-Crusells J, Sigl T, Blaesse A, Mestres P, Meyer M, Yan Q, Kaila K, Saarma M, Rivera C, Giehl KM (2008) Posttraumatic GABA(A)-mediated [Ca2+]i increase is essential for the induction of brain-derived neurotrophic factor-dependent survival of mature central neurons. J Neurosci 28:6996-7005.

Tay TL, Sagar, Dautzenberg J, Grun D, Prinz M (2018) Unique microglia recovery population revealed by single-cell RNAseq following neurodegeneration. Acta Neuropathol Cummun 6:87.

Tay TL, Mai D, Dautzenberg J, Fernandez-Klett F, Lin G, Sagar, Datta M, Drougard A, Stempfl T, Ardura-Fabregat A, Staszewski O, Margineanu A, Sporbert A, Steinmetz LM, Pospisilik JA, Jung S, Priller J, Grun D, Ronneberger O, Prinz M (2017) A new fate mapping system reveals context-dependent random or clonal expansion of microglia. Nat Neurosci 20:793-803.

Taylor AM, Castonguay A, Ghogha A, Vayssiere P, Pradhan AA, Xue L, Mehrabani S, Wu J, Levitt P, Olmstead MC, De Koninck Y, Evans CJ, Cahill CM (2016) Neuroimmune Regulation of GABAergic Neurons Within the Ventral Tegmental Area During Withdrawal from Chronic Morphine. Neuropsycholpharmacol 41:949-959.

Taylor RA, Sansing LH (2013) Microglial responses after ischemic stroke and intracerebral hemorrhage. Clin Dev Immunol 2013:746068.
Uvarov P, Ludwig A, Markkanen M, Pruunsild P, Kaila K, Delpire E, Timmusk T, Rivera C, Airaksinen MS (2007) A novel N-terminal isoform of the neuron-specific K-Cl cotransporter KCC2. J Biol Chem 282:30570-30576
Wang LN, Yang JP, Zhan Y, Ji FH, Wang XY, Zuo JL, Xu QN (2012) Minocycline-induced reduction of brain-derived neurotrophic factor expression in relation to cancer-induced bone pain in rats. J Neurosci Res 90:672-681.
Wang X, Ratnam J, Zou B, England PM, Basbaum AI (2009) TrkB signaling is required for both the induction and maintenance of tissue and nerve injury-induced persistent pain. J Neurosci 29:5508-5515.
Wilhelm JC, Xu M, Cucoranu D, Chmielewski S, Holmes T, Lau KS, Bassell GJ, English AW (2012) Cooperative roles of BDNF expression in neurons and Schwann cells are modulated by exercise to facilitate nerve regeneration. J Neurosci 32:5002-5009.
Wilkerson JE, Mitchell GS (2009) Daily intermittent hypoxia augments spinal BDNF levels, ERK phosphorylation and respiratory long-term facilitation. Exp Neurol 217:116-123.
Wu H, Friedman WJ, Dreyfus CF (2004) Differential regulation of neurotrophin expression in basal forebrain astrocytes by neuronal signals. J Neurosci Res 76:76-85.
Xu X, Fu S, Shi X, Liu R (2019) Microglial BDNF, PI3K, and p-ERK in the Spinal Cord Are Suppressed by Pulsed Radiofrequency on Dorsal Root Ganglion to Ease SNI-Induced Neuropathic Pain in Rats. Pain Res Manag 2019:5948686.
Yang H, Feng GD, Liang Z, Vitale A, Jiao XY, Ju G, You SW (2012) In vitro beneficial activation of microglial cells by mechanically-injured astrocytes enhances the synthesis and secretion of BDNF through p38MAPK. Neurochem Int 61:175-186.
Young P, Qiu L, Wang D, Zhao S, Gross J, Feng G (2008) Single-neuron labeling with inducible Cre-mediated knockout in transgenic mice. Nat Neurosci 11:721-728.
Zaccaro MC, Ivanisevic L, Perez P, Meakin SO, Saragovi HU (2001) p75 Co-receptors regulate ligand-dependent and ligand-independent Trk receptor activation, in part by altering Trk docking subdomains. J Biol Chem 276:31023-31029.
Zhang HH, Zhang XQ, Xue QS, Yan L, Huang JL, Zhang S, Shao HJ, Lu H, Wang WY, Yu BW (2014) The BDNF/TrkB signaling pathway is involved in heat hyperalgesia mediated by Cdk5 in rats. PloS one 9:e85536.
Zhou HY, Chen SR, Byun HS, Chen H, Li L, Han HD, Lopez-Berestein G, Sood AK, Pan HL (2012) N-methyl-D-aspartate receptor- and calpain-mediated proteolytic cleavage of K+-Cl- cotransporter-2 impairs spinal chloride homeostasis in neuropathic pain. J Biol Chem 287:33853-33864.
Zhu X, Ward PJ, English AW (2016) Selective Requirement for Maintenance of Synaptic Contacts onto Motoneurons by Target-Derived trkB Receptors. Neural Plast 2016:2371893.
Ziemlinska E, Kugler S, Schachner M, Wewior I, Czarkowska-Bauch J, Skup M (2014) Overexpression of BDNF increases excitability of the lumbar spinal network and leads to robust early locomotor recovery in completely spinalized rats. PloS one 9:e88833.

Chapter 5: KCC2 regulation by a muscle-derived signal

5.1 Abstract

Previous work has extensively described the role that neural activity, as modulated by exercise or pharmacological interference in the periphery, has on motoneuron properties, both independent of and after, neural injury. In this chapter we investigate the role motoneuron activity has on regulating KCC2. Specifically, we tested the activity of the muscle controlled through the neuromuscular junction (NMJ) and found that, unlike in animals that had regeneration prevented with ligation, animals in which axon regeneration was enabled had recovery of KCC2. The degree of KCC2 expression was correlated with the degree of NMJ reinnervation. We also illustrate that modulating neuromuscular activity through exercise or blockade of NMJ signaling had no significant effect on KCC2 protein levels. In fact, KCC2 protein expression was best correlated with the presence of NMJs and not the muscular response. These findings lead to the conclusion that KCC2 is likely regulated through an activity-independent retrograde signal from the muscle that precedes the functional reconnection of neuromuscular synapses after regeneration.

5.2 Introduction

In the previously described experiments, the sciatic nerve was cut and ligated to prevent regeneration and eliminate potentially confounding peripheral factors that may influence KCC2 expression. In these animals we did not observe KCC2 recovery, even at the longest survival times examined. However, in cranial motoneurons axotomized but not ligated during nerve injury, it has been shown that KCC2 expression and IPSP reversal potentials recover to normal levels after extended periods of time (Takata et al., 1990; Toyoda et al., 2003). In these experiments it was unclear if KCC2 recovery was dependent on muscle reinnervation (Tatetsu et al., 2012) or merely time after injury (Takata et al., 1990). Thus, we decided to test the hypothesis that KCC2 recovery may be directly related to reconnection of regenerating axons with the muscle. We completed a similar time course as described in Chapter 3, but in animals

in which we allowed regeneration by repairing the cut nerve with fibrin glue. We then compared KCC2 recovery with neuromuscular junction (NMJ) reinnervation. We found a correlation between the two, which led to the hypothesis that KCC2 restoration may be dependent on a retrograde signal originating in the muscle that may or may not be dependent on NMJ function. To investigate whether KCC2 recovery and muscle reinnervation are causally related, we decided to speed up muscle reinnervation by exercising the animals.

Exercise is known to accelerate motor axon growth (English et al., 2014; Gordon and English, 2016) and to revert synaptic changes that occur after axotomy in a motoneuron-BDNF dependent way (Krakowiak et al., 2015). Exercise also impacts the physiology of intact motoneurons by modifying motoneuron dendritic and NMJ structure, increasing protein synthesis, and inducing a hyperpolarized resting membrane potential, as reviewed in (Gardiner et al., 2006). Exercise can operate through changes in descending drive, increased activity at the level of the spinal cord circuitry, and/or increased coupling with muscle activity. In the case of axotomized motoneurons, the last explanation is supported by studies that show that functionally decoupling motoneurons from muscle induces changes in motoneuron excitability similar to those that occur after nerve injury (Czeh et al., 1978; Sattelle et al., 1983; Nakanishi et al., 2005). Motoneuron excitability increases after applying tetrodotoxin (TTX) to the nerve, or botulinum toxin or alpha-bungarotoxin to the muscle. Respectively, these manipulation block action potentials from reaching the NMJ, prevent the release of acetylcholine from presynaptic motor terminals, and prevent neurotransmitter binding at NMJ postsynaptic acetylcholine receptors.

Activity of the muscle, rather than activity of the nerve, is critical for maintaining intact motoneuron excitability. If nerves are stimulated distal to a TTX cuff, allowing propagation of an action potential to the muscle but not to the cell body, the changes induced by TTX exposure are rescued. However, stimulation central to the TTX cuff, allowing propagation of activity back to the cell body but not the muscle, does not preserve motoneuron properties (Czeh et al., 1978).

The central importance of NMJ neurotransmission is further confirmed by the dramatic effect of alpha-bungarotoxin on motoneuron excitability, which best replicates changes occurring after axotomy compared to the relatively minor changes following botulinum toxin exposure (Nakanishi et al., 2005). While both treatments block evoked NMJ neurotransmission, botulinum toxin allows spontaneous "mini" or single vesicle release of acetylcholine (Pastor et al., 1997), whereas alpha-bungarotoxin binds postsynaptic nAChR's irreversibly and completely (Chang and Lee, 1963). It is possible that nicotinic receptor activation after the spontaneous release of single acetylcholine-carrying vesicles is enough to trigger retrograde signals that maintain normal motoneuron excitability properties. Similar experiments have not yet been performed to test the influence of NMJ function on KCC2 expression on the motoneuron cell body.

In the dorsal horn, exercise ameliorates KCC2 deletion after nerve injury. Following a chronic constriction nerve injury in female rats, exercise attenuates KCC2 loss in the dorsal horn and reduces mechanical allodynia (Cobianchi et al., 2010; Cobianchi et al., 2014; Lopez-Alvarez et al., 2015; Grace et al., 2016). Treadmill training also attenuated microgliosis; the authors tied this finding to decreased expression of BDNF in dorsal microglia (Lopez-Alvarez et al., 2015), but they did so by using an antibody against BDNF protein that has not been verified for specificity. In previous chapters we showed that KCC2 regulation in axotomized motoneurons is independent of BDNF and microglia, but on the other hand, KCC2 expression and function is known to be modulated by a variety of posttranslational mechanisms influenced by neural activity and synaptic drive (Medina et al., 2014; Come et al., 2019). It is clear that exercise can modulate activity and KCC2 in many neural populations, raising the possibility that it may impact KCC2 on axotomized motoneurons as well, independent of muscle reinnervation.

To test a possible role of exercise on motoneuron KCC2 expression, we treadmill-trained mice and analyzed recovery at different time points after injury. Only females were used because the type of exercise protocol necessary to effect axon regeneration is sex dependent (Wood et al.,

2012). To test the effect of exercise alone, we performed analyses of KCC2 recovery before muscle reinnervation. We also hypothesized that if KCC2 is recovered by muscle reinnervation, and not just by mechanisms solely dependent on exercise or time after injury, then we should observe an acceleration of KCC2 recovery at time points in which we increase muscle reinnervation in an exercise dependent manner. If KCC2 and exercise were both associated with motor axon regeneration, it would be of high interest to clarify any possible relationships between them. Finally, to test the influence of NMJ neurotransmission in maintaining KCC2 expression in motoneurons we chronically blocked postsynaptic muscle nicotinic acetylcholine receptors (nAChR's) with alpha-bungarotoxin in intact, non-injured motoneurons.

5.3 Methods

5.3.1 Animals

Fast Blue was administered uni- or bilaterally in adult animals as described in general methods. For the time course of KCC2 restoration, $CX3CR1^{GFP/+}$ animals underwent unilateral sciatic nerve transection/repair as described in Chapter 2 and were euthanized at 21, 28 or 60 days after injury. Data from $CX3CR1^{GFP/+}$ sham and cut/ligated animals 21, 28, and 60 days after injury are included in the analysis below for comparison. All other animals utilized were WT and underwent a unilateral sciatic nerve transection/repair prior to euthanasia 14, 28, or 35 days after injury, as described below.

5.3.2 Exercise paradigm

All animals utilized for exercise experiments were female, as exercise effects have been shown to be sex-dependent (Wood et al., 2012). All animals underwent FB and sciatic nerve transection/repair prior to beginning an interval training paradigm known to be effective for enhancing motoneuron axon regeneration in female mice (Sabatier et al., 2008). On the third day after sciatic nerve transection/repair, animals were placed on a treadmill and run at high

intensity (33.3 cm/min) for four bouts of two minutes, with five minutes of rest in between. A cohort of untrained animals was placed on the treadmill without it turned on for the same total amount of time daily. This protocol was repeated five days a week for two weeks.

5.3.3 Alpha-bungarotoxin administration

In order to investigate a role of muscle activity in motoneuron KCC2 regulation, we blocked binding of postsynaptic nicotinic acetylcholine receptors (nAChR's) using alpha-bungarotoxin. Following FB administration, adult male and female animals underwent unilateral intramuscular injections of vehicle or alpha-bungarotoxin conjugated to AlexaFluor-555 (αBTX-555) every 48 hours until euthanasia (5 µl, 0.1 µg/µl in physiological saline). This concentration was selected as it is known to be sufficient for chronic NMJ blockage (Nakanishi et al., 2005). We confirmed the effective block of the NMJ with electromyography in a subset of animals, as described below.

5.3.4 Motor endplate quantification

To confirm the degree of successful muscle reinnervation or degree of alpha-bungarotoxin blockade, LG muscles were harvested from sciatic nerve transection/repair animals and post-fixed overnight prior to cryoprotection in 30% sucrose. Cryostat sections were cut at 25 µm thickness and collected onto glass slides. For all exercised and αBTX -555 animals, the intact (untreated) muscle was also collected and processed. In some animals (n= 2 in 14 day exercised and unexercised groups, n = 1 in 28 day exercised and unexercised groups), the immunohistochemistry failed in the muscle contralateral to injury. If no VAChT or axon labeling could be seen even though the sciatic nerve was intact, the animal was removed from muscle analyses because the reliability of reinnervation could not be confirmed.

For animals in which the restoration of neuromuscular synapses was studied, slides were washed and incubated for 1 hour with 10% normal donkey serum. Then they were incubated

overnight at room temperature with alpha-bungarotoxin conjugated to AlexaFluor®-555 (αBTX -555, Invitrogen cat# B35451, 1:100) and primary antibodies against neurofilament-H (NF-H) and vesicular acetylcholine transporter (VAChT) (Table 5.1). NF-H and VAChT label presynaptic axon terminals by binding the cytoskeleton in thick motor axons and synaptic vesicles contained within the motor nerve terminal, respectively. VAChT immunoreactivity was revealed with Cy5-conjugated secondary antibodies and NF-H with Fluorescein (FITC)-conjugated antibodies (dilution 1:100, see Table 5.2). In animals treated with αBTX-555, muscles were harvested and sectioned as described above. Then, sections were washed prior to 2 hour exposure to alpha-bungarotoxin conjugated to FITC (αBTX-FITC, Invitrogen cat# B13422, 1:100). αBTX-FITC allowed us to identify receptors that were not previously bound by αBTX-555, and thus marked nAChRs that were newly synthesized.

All sections were mounted with Vectashield. Fifty motor endplates per animal were imaged for quantification with an Olympus FLUOVIEW FV1000 Confocal microscope (20X). Motor endplates were designated as reinnervated or not for repaired muscles (Figure 5.1B) and fully, partially, or not blocked (Figure 5.4A) for bungarotoxin or saline treated muscles. Fully and partially blocked NMJ's were pooled for analysis.

5.3.6 Electromyography

To determine the degree of successful muscle reinnervation and blockade of muscle activity for exercise and alpha-bungarotoxin treated animals, respectively, we measured direct muscle (M) responses generated by stimulating the sciatic nerve, using electromyography (EMG), in subsets of animals just prior to euthanasia. In anesthetized animals, the sciatic nerve was exposed just distal to its exit from the pelvis. Stimulating tungsten needle electrodes were placed on either side of the nerve. Bipolar fine wire electrodes (California Fine Wire Company, Grover Beach, CA) were placed into the ipsilateral LG muscle with a 25 gauge hypodermic needle and connected to differential amplifiers. Monophasic constant voltage electrical pulses

were applied to the nerve at increasing intensity (0.1 ms pulse, 3 second inter-pulse interval) and compound muscle action potentials were sampled at 10 kHz. The data were visualized and recorded using custom software written in LabVIEW (National Instruments, Austin, TX). The average rectified voltage within the duration of this triphasic action potential was measured as described in detail elsewhere (Sabatier et al., 2011) and the maximal muscle response amplitude (M-max) was measured. Three-second inter-pulse intervals were utilized, as this has been shown to avoid muscle fatigue (English et al., 2007). At least two trials per side were conducted with varied placement of stimulating electrodes, and the average M-Max of these trials was used for analysis. Recordings were made from the leg ipsilateral to injury as well as from the contralateral limb, which acted as an internal control. The order of stimulus was randomized. For animals treated with alpha-bungarotoxin, recordings were also made from the muscles in the plantar footpad to validate that the placement of the stimulating electrodes was effective in activating muscle innervated by the sciatic nerve but not affected by the bungarotoxin blockade.

5.4 Results

5.4.1 KCC2 restoration is dependent on muscle reinnervation

In order to determine whether KCC2 is restored after injury, we performed a time-series in which we compared somatic membrane KCC2 levels between animals in which we cut and ligated the sciatic nerve (to prevent regeneration) or facilitated regeneration by nerve repair (n = 4-5 per time point). Spinal cords containing FB-labeled LG motoneurons were examined at 21, 28 and 60 days after injury. In nerve repaired animals, by 60 days, KCC2 on the somatic membrane was restored (Figure 5.1A) and significant differences in KCC2 protein expression on the cell body membrane of FB-labeled LG motoneurons were found between cut/ligated motoneurons at 60 days and those with regeneration allowed (Two-way ANOVA; Figure 5.1B; Statistical Table 5.1A). When compared with intact motoneurons, no differences were found in KCC2-IR of motoneurons of repaired animals, whereas the ligated animals maintained KCC2

loss (One-way ANOVA; Statistical Table 5.1A) indicating that, with time, KCC2 returned to normal levels in animals when regeneration had occurred.

To investigate whether motoneuron KCC2 restoration was correlated with successful reinnervation of neuromuscular junctions (NMJs), and not just a product of the act of axon regeneration, LG muscles from repaired animals were collected and examined for reinnervation of vacated motor endplates by regenerated motor axons and presynaptic motor nerve terminals. Postsynaptic acetylcholine receptors were labeled with αBTX-555, and any co-localized motor nerve terminals were identified using antibodies against neurofilament-H, and VAChT (Figure 5.1C). We expected minimal reinnervation of NMJs at 21 days, some limited reinnervation at 28 days and significant reinnervation by 60 days based on previous data from the English lab. Within and across times, the proportion of reinnervated NMJs was variable, and this allowed us to correlate average NMJ motor axon occupancy rates with the average levels of KCC2 in the cell body (Figure 5.1D). We found a statistically significant correlation between reinnervation and KCC2 on the soma membrane (Statistical Table 5.1B), indicating that KCC2 recovery in axotomized motoneurons is associated the successful reinnervation of NMJs.

5.4.2 KCC2 depletion occurs independent of exercise

Exercise has been well established as a method for improving peripheral regeneration of motoneurons (Gordon and English, 2016). It also helps to regulate spasticity and neuropathic pain symptoms following SCI, in which neurons are not disconnected with the muscle but presumably receive more central drive, which helps normalize firing rates (Côté et al., 2014; Detloff et al., 2014; Chopek et al., 2015; Côté et al., 2017). Exercise was able to revert depletions of KCC2 in motoneurons after spinal cord injury (Côté et al., 2014; Tashiro et al., 2015). Thus, we decided to test two hypotheses: that KCC2 may be regulated by exercise independent of muscle reinnervation, and that increased reinnervation speed induced by exercise would restore KCC2 levels to pre-injury levels more quickly than in animals in which regeneration speed was

normal. We tested the first hypothesis, that exercise may regulate KCC2 prior to muscle reinnervation, by looking at 14 days post injury when minimal reinnervation was expected whether animals were exercised or not. In fact, a very low percentage of NMJs was similarly found in exercised (n = 7) and unexercised (n = 4) animals at 14 days (Figure 5.2A), 1.9 ± 3 (average ± SD) and 2.5 ± 5 %, respectively.

Surprisingly, at 28 (n = 4/group) and 35 days (n=2/group) after injury, the time points in which we expected exercise to enhance regeneration, we also did not detect statistically significant differences in muscle reinnervation between exercised and unexercised groups (Statistical Table 5.1 C). Statistics were not run on the 35 day group, since at the time of writing, a sufficient number of animals had not been examined. However, with n = 2 the differences between exercised and non-exercised animals is minimal; both show reinnervation in over 80% of NMJs indicating that reinnervation has been largely completed by this time. In contrast, there was a strong trend toward higher reinnervation at 28 days in exercised animals (21 ± 16% NMJ re-occupancy in unexercised vs 50 ± 27% in exercised animals, n = 4/group). This trend did not reach significance because of high interanimal variability in both exercised and non-exercised animals (Statistical table 5.1C, Figure 5.2A). High variability is not uncommon in these types of studies (McGregor et al., 2019) but resulted in reduced statistical power in our comparisons. We found that n = 6 will be required to reach power = 0.8 with this amount of variability and α = 0.05 and these experiments will be completed after the writing of this document.

To correlate NMJ re-occupancy with recovery of NMJ function, we performed further analyses of correlations between the degrees of reinnervation in animals 28 days after injury and their ability to produce muscle responses measured with EMG (Figure 5.2B). In these animals (n = 4 unexercised, n = 3 exercised due to one EMG failure), there was a significant improvement in the recovery of the muscle response in animals that were exercised (Statistical table 5.1D, Figure 5.2B). The degree of muscle reinnervation and maximal muscle response were not well correlated, indicating that the NMJ's, even if intact and expressing immunoreactivity to a

synaptic vesicle antigen (VAChT), may not have yet been fully functional (Statistical table 5.1E, Figure 5.2C). However, given the increased number of animals needed to reach sufficient power, this trend may become significant when the group is completed. Interestingly, the slope of the regression line of endplate reoccupation to M-Max is less than one, suggesting that the recovery of M-responses lags with respect to NMJ reinnervation. This might be a reflection of NMJ maturation after re-establishing synaptic contact. It should be noted that percent of reinnervation is based on NMJs with either partial or complete coverage by VAChT-IR motor end-plates. It is quite possible that NMJs with partial VAChT-IR coverage are not yet fully functional or that, while we took pains to avoid muscle fatigue, the nascent synapses can not follow repeated activation. This would cause the M-max of partially reinnervated muscles to be an underestimate of the amount of reinnervation.

At both 14 and 28 days after injury, the KCC2-IR was similarly depleted between exercised and unexercised groups (Figure 5.3A,B; Statistical Table 5.1F, G). At 14 days after injury (n = 4 unexercised, n = 7 exercised), two-way ANOVA revealed only injury status predicted the level of KCC2, indicating that exercise does not impact KCC2 levels before regeneration. Given that exercise is thought to increase BDNF in the spinal cord, this finding further supports our previous conclusions that KCC2 downregulation is not dependent on BDNF-TrkB. Interestingly, exercised animals 28 days after injury (n = 5/group), after exercise has ceased for two weeks, may exhibit an increase in KCC2 fluorescence overall. Two-way ANOVA revealed the contralateral (control) side of exercised animals had significantly higher level of KCC2-IR when compared to unexercised controls, whereas injured motoneurons were not different from unexercised control motoneurons (Statistical Table 5.G). This indicates that both the ipsilateral and contralateral levels of KCC2-IR were higher than expected, but exercised animals showed a similar difference between sides ipsilateral and contralateral to injury (an average 54.7 ± 39% depletion compared to a depletion of 45 ± 44% in unexercised animals) that was significant when examined with a t-test (Statistical Table 5.G). The possibility that there

could be a delayed effect of exercise on KCC2 should be further investigated in the future and may be resolved with the planned additional animals.

One way to overcome interanimal variability is to directly correlate average KCC2 levels with NMJ reinnervation (Figure 5.3C) and M-max (Figure 5.3D) in individual animals. When this was done we found a significant correlation (linear regression) between KCC2 fluorescence on motoneuron somatic membrane and NMJ re-occupancy, but not between KCC2 and M responses (Statistical Table 5.1H, I). Thus, the presence of axons in muscles at or near the NMJ is more important than the functional maturation of the synapses when examining KCC2 recovery on the motoneuron cell body.

5.4.3 KCC2 depletion and alpha-bungarotoxin

To further explore the connection between NMJ function and KCC2 regulation, we blocked NMJ function in intact muscles using alpha-bungarotoxin, a permanent antagonist of postsynaptic nicotinic acetylcholine receptors in the muscle. We first performed a pilot experiment to prove the feasibility of blocking the NMJ by injecting animals unilaterally with either saline or alpha-bungarotoxin conjugated to Alexa-555 (αBTX-555) (n = 2/group). Forty-eight hours later, we tested the maximal muscle response (M-max, as measured through EMG) that could be elicited through stimulation of the sciatic nerve and confirmed binding of the post-synaptic nAChR's with IHC.

Following muscle extraction and standard sectioning, we applied fresh αBTX-FITC to muscle sections. This αBTX-FITC would only bind to nicotinic receptors not occupied by αBTX-555 injected 48 hours earlier. "Unbound" NMJs refer to those NMJs with no αBTX-555 labeling and strong labeling with αBTX-FITC; "partially bound" indicate NMJs with mostly αBTX-555 and some weak αBTX-FITC; "bound" NMJs are those that show only αBTX-555 and no αBTX-FITC (Figure 5.4A). Saline injected muscles had virtually no previously bound receptors (0% fully bound, 5 ± 7% partially bound, potentially due to contamination of the Hamilton syringe

with αBTX-555). Alpha-bungarotoxin treated muscles had 71 ± 27% % partially bound NMJs 48 hours after αBTX-555 injections. No muscle showed all NMJs completely bound—at least some new receptors were always visible in some NMJs. While these unbound receptors could be receptors that failed to bind the αBTX-555 injected initially, it is more likely they reflect "de novo" insertion of receptors between the time of αBTX—555 injection and euthanasia of the animal.

Even partial binding of nAChR's in the LG was sufficient to reduce the muscle response drastically. Plateaus in both the M-max of the LG and foot-pad muscles were used to confirm maximal stimulation of the nerve. In saline injected animals, the ipsilateral and contralateral LG produced the same M-max (100 ± 11.6%, average ± SD; Figure 5.4C), whereas muscles injected with αBTX-555 had M-max reduced to 14.6% and 63.0% of the M-max recorded from the un-injected LG muscle of the same animal (Figure 5.4D). These data confirmed that we were able to attenuate the activity in the muscle with alpha-bungarotoxin.

In a second set of animals (n = 3) we injected the LG with αBTX-555 every 48 hours for 14 days. Multiple injections resulted in 100% of NMJ's at least partially bound by αBTX-555 (Figure 5.4B). In these animals we did not perform EMGs, but based on our pilot data this level of αBTX-555 is expected to cause substantial silencing of the NMJ. In these animals, we compared the levels of somatic KCC2 on FB+ LG motoneurons ipsilateral and contralateral to the injection (Figure. 5.4E). Alpha-bungarotoxin silencing of the NMJ did not impact KCC2 levels in intact motoneurons (Figure 5.4F; Statistical Table 5.1J). We therefore conclude that, in agreement with our correlation between M-response and KCC2 recovery, KCC2 downregulation is not related to NMJ function. In other words, functional disconnection of the NMJ is not sufficient to induce KCC2 loss from spinal motoneurons.

5.5 Discussion

Motoneuron properties that are lost after injury, such as rheobase, distribution of ion channels, and most synaptic contacts, are restored by reinnervation of the muscle (Eccles et al., 1958; Kuno et al., 1974; Nishimura et al., 1992; Iwahashi et al., 1994; Romer et al., 2014). We have shown that KCC2 is similarly restored after muscle reinnervation. It was possible that this observed increase in KCC2 was tied to increases in motoneuron activity (driven by reestablishment of synaptic contacts with the muscle that induce the motoneuron to fire or simulate the surrounding circuitry via sensory stimulation from regenerated afferents), so we decided to test the hypothesis that KCC2 upregulation may be triggered by more activity using an exercise paradigm shown previously to impact motoneuron regeneration.

Exercise has been shown to alter motoneuron excitability transiently in healthy human populations by both altering presynaptic inhibition (Bongiovanni and Hagbarth, 1990; Macefield et al., 1991) and changing the excitability of alpha motoneurons themselves (Duchateau et al., 2002; Andersen et al., 2003; Racinais et al., 2007). In uninjured animals, exercise-induced changes include a hyperpolarized resting membrane potential and faster action potential rise-times, but not changes in rheobase or input resistance (Beaumont and Gardiner, 2003). However, in experimental conditions, whether exercise makes motoneurons more or less excitable depends on the injury and exercise paradigm used (reviwed in Gardiner et al., 2006). As reviewed above, PNI itself induces many changes in motoneurons and exercise can improve their regeneration and functionality. Motoneuron activity is essential in this enhancement; if motoneuron activity is blocked during training, the effects of exercise are prevented as well (Jaiswal et al., 2017).

Very recently, KCC2 regulation has also been tied to neuron excitability through a direct coupling between KCC2 expression and expression of Task-3 K+ channels. These K+ channels control the set point of the membrane potential and the input resistance of hippocampal neurons (Goutierre et al., 2019). Interestingly, Task-3 K+ channels are downregulated after

axotomy of hypoglossal motoneurons, changing their excitability and resting membrane potential (Gonzalez-Forero et al., 2007). It is possible that KCC2 and voltage-gated ion channels controlling motoneuron excitability are coregulated and/or that they are complementary mechanisms for modulating motoneuron firing after injury. Unfortunately, there have been no electrophysiological studies of motoneurons following exercise with PNI specifically that could help explain the dynamics between these factors further. However, there have been many investigations following various spinal cord injury models that show exercise enhances recovery of motoneuron excitability to normal basal levels. This is also associated with a hyperpolarization of the resting membrane potential (Beaumont and Gardiner, 2003). However, given that we saw no changes in KCC2 prior to reinnervation, regardless of exercise exposure, it is unlikely that exercise alone modulates KCC2 in motoneurons axotomized peripherally.

In our model, the best predictor of KCC2 presence was NMJ presence, independent of muscle response or NMJ activity. The importance of the nerve-muscle functional coupling is highlighted by the development of axotomy-like changes in excitability that are induced by blocking spontaneous neuromuscular neurotransmission in the absence of injury with tetrodotoxin or alpha-bungarotoxin (Czeh et al., 1978; Nakanishi et al., 2005). These results support the hypothesis that motoneuron electrical properties are maintained by retrograde signals from muscle informing the existence of functional connections. However, we found that blocking the muscle's ability to respond to motor axon synapses had no impact on KCC2; muscles ipsilateral to injection had the same KCC2 on the somatic membrane as those contralateral to injection.

Given these data, it seems likely that a signal from the muscle—independent of activity—is responsible for the recovery of KCC2 after injury. However, it should also be noted that we did not confirm full block of NMJ post-synaptic receptors; it is possible that even a small amount of activation may be sufficient to maintain KCC2 or induce its expression. Additional experiments may need to be performed in which alpha-bungarotoxin is injected more regularly, or

continuously with a pump. However, these are challenging experiments due to the possibility of systemic effects, which could induce a large number of pleiotropic outcomes, making interpretation of the data more complex. Our dosage protocol was highly specific and did not seem to impact animal health; the fact that no trend was seen in KCC2 loss suggests that the treatment was not effective in reducing KCC2 on the membrane of motoneurons.

In this chapter, we have illustrated that KCC2 presence on axotomized motoneurons is not affected by increasing activity with exercise. While this is surprising based on previous literature describing exercise modulation of KCC2 (Lopez-Alvarez et al., 2015; Tashiro et al., 2015; Lee-Hotta et al., 2019), this finding is consistent with our previous conclusions that KCC2 on axotomized motoneurons is not regulated by BNDF/TrkB signaling. Many of the effects of exercise on both motoneurons and other cell populations are thought to occur by altering BDNF signaling (Gomez-Pinilla et al., 2002; Wilhelm et al., 2012; Almeida et al., 2015; Krakowiak et al., 2015; Sabatier and English, 2015; Tashiro et al., 2015) and thus KCC2's independence from exercise supports our hypothesis that a different mechanism is regulating it after axotomy. Instead, KCC2 is dependent solely on the physical presence of neuromuscular junctions, indicating that presynaptic activity from the motor axons themselves, or—most likely—an activity-independent signal from the muscle, is modulating KCC2's restoration. In the first case, it could be argued that the acetylcholine release at the motor end plate could trigger a retrograde, cell-autonomous signal independent of the activation of the postsynaptic receptors. This possibility could be tested by application of TTX, to prevent action potentials from invading the motoneuron synapse, or with application of botulinum toxin to prevent release of acetylcholine by degrading SNARE complexes and the synaptic machinery of the presynaptic active zone (Czeh et al., 1978; Nakanishi et al., 2005). However, this presynaptic release of acetylcholine would not fully explain the good correlations we demonstrated between NMJ physical reinnervation and recovery of KCC2 in the cell body of motoneurons. This observation argues in favor of an activity-independent trophic signal from the muscle. Whatever the

mechanism, KCC2's close dependence on connection with the muscle reinforces that its recovery is a phenomenon closely associated with reinnervation, and this relationship will be the most interesting area of future study.

5.6 Tables and Figures

Table 5.1 Primary antibodies utilized for immunohistochemistry (IHC) in Chapter 5.

Antigen	Immunogen	Host/type	Manufacturer	RRID #	Dilution
Neurofilament-H	Purified neurofilament-H from bovine brain	Chicken/ polyclonal	Aves catalog #NFH	NA	1:500
Guinea pig: VAChT	Recombinant protein; rat VAChT; aa 475-530	Guinea pig/ polyclonal	Synaptic Systems Catalog #139105	NA	1:500

Table 5.2 Secondary antibodies utilized for immunohistochemistry (IHC) in Chapter 5.

Antigen	Manufacturer	RRID#
Cyanine Cy™5 (Cy5 α Guinea Pig)	Jackson ImmunoResearch Labs Cat# 706-175-148	RRID:AB_2340462

Statistical Table 5.1

	Data Reference	Data Structure	Type of Test	Statistical Significance
A	5.1B	Normal Distribution	**Two-way ANOVA** Day; $F_{(2,19)} = 4.28$; $p = 0.029$ Injury; $F_{(1,19)} = 6.73$; $p = 0.0178$ Interaction; $F_{(2,19)} = 2.78$; $p = 0.088$	
	Ligated vs Repaired			
	21 days		*Post hoc* Bonferroni	$p = 0.308$
	28 days		*Post hoc* Bonferroni	$p > 0.999$
	60 days		*Post hoc* Bonferroni	$p = 0.0195$
			One-way ANOVA $F_{(2,9)} = 4.28$; $p = 0.049$	
	Intact vs			
	60 day ligated		*Post hoc* Bonferroni	$p = 0.0498$
	60 day repaired		*Post hoc* Bonferroni	$p = 0.979$
B	5.1D	Normal Distribution	**Linear Regression** $F_{(1,11)} = 17.03$; $p = 0.0017$ $y = 0.818x + 43.45$; $R^2 = 0.608$	
	KCC2 fluorescence and NMJ Reinnervation			
C	5.2A	Normal Distribution	**Two-Way ANOVA** Day; $F_{(2,13)} = 33.0$; $p < 0.0001$ Treatment; $F_{(1,13)} = 2.29$; $p = 0.155$ Interaction; $F_{(2,13)} = 1.81$; $p = 0.203$	
	Exercised vs Unexercised		**One-tailed paired t tests**	
	14 days post injury			$t = 0.86$; $p = 0.430$

	28 days post injury			t = 1.83; p = 0.117
D	5.2C **M-max exercised vs** Unexercised	Normal Distribution	**<u>One-tailed t test</u>**	 t = 4.57; p = 0.003
E	5.2D **M-max and NMJ Reinnervation**	Normal Distribution	**<u>Linear Regression</u>** $F_{(1,5)} = 1.85$; p = 0.232 y = 0.308x + 0.085; $R^2 = 0.27$	
F	5.3A **Unexercised Contralateral vs** Unexercised ipsilateral Exercised contralateral Exercised ipsilateral	Normal Distribution	**<u>Two-Way ANOVA</u>** Treatment; $F_{(1,18)}$ =0.768; p = 0.392 Side; $F_{(1,18)}$ = 50.1; p = 50.1 Interaction; $F_{(1,18)}$ = 0.471; p = 0.471 *Post hoc* Bonferroni *Post hoc* Bonferroni *Post hoc* Bonferroni	 p = 0.0025 p > 0.999 p < 0.0001
G	5.3B **Unexercised Contralateral vs** Unexercised ipsilateral Exercised contralateral Exercised ipsilateral **Exercised Contralateral vs** Exercised ipsilateral	Normal Distribution	**<u>Two-Way ANOVA</u>** Treatment; $F_{(1,16)}$ =15.1; p = 0.0013 Side; $F_{(1,16)}$ = 45.64; p < 0.0013 Interaction; $F_{(1,18)}$ = 0.163; p = 0.69 *Post hoc* Bonferroni *Post hoc* Bonferroni *Post hoc* Bonferroni **<u>One-tailed t-test</u>**	 p = 0.0011 p = 0.0239 p = 0.177 t = 3.053 p = 0.019
H	5.3D **KCC2 and NMJ Reinnervation**	Normal Distribution	**<u>Linear Regression</u>** $F_{(1,13)}$ = 37.6; p < 0.0001 y = 1.32X + 40.9; $R^2 = 0.743$	
I	5.3C **KCC2 and M-max**	Normal Distribution	**<u>Linear Regression</u>** $F_{(1,7)}$ = 5.26 p = 0.0555 y = 1.67x + 54.8; $R^2 = 0.429$	
J	5.4F **Injected vs uninjected**	Normal Distribution	**<u>One-tailed paired t-test</u>**	 t = 0.0237; p = 0.387

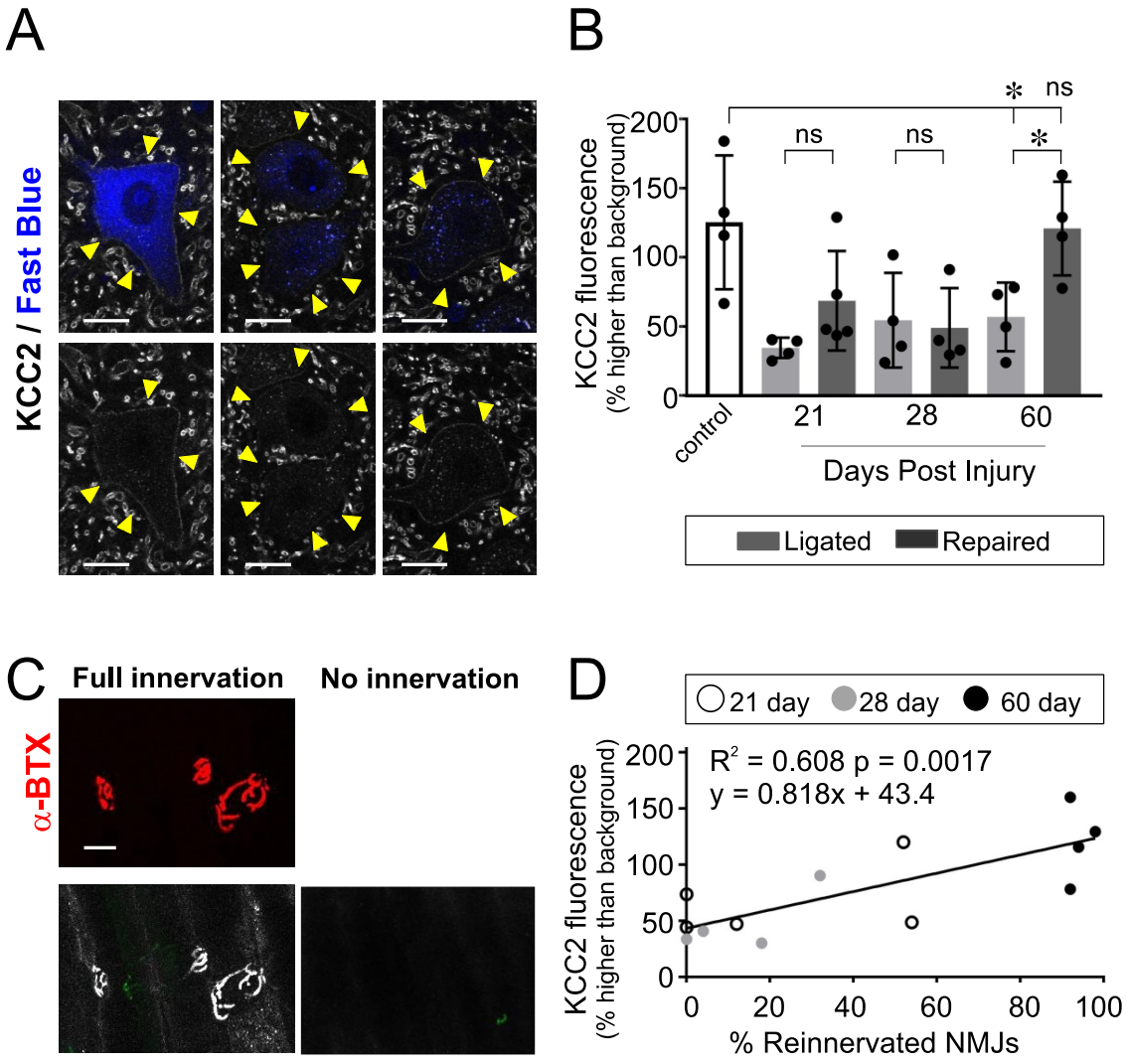
A
KCC2 / Fast Blue
B
KCC2 fluorescence
(% higher than background)
200
150
100
50
0
ns
ns
*
*
ns
control
21
28
60
Days Post Injury
Ligated
Repaired
C
Full innervation
No innervation
α-BTX
D
21 day
28 day
60 day
R² = 0.608 p = 0.0017
y = 0.818x + 43.4
KCC2 fluorescence
(% higher than background)
200
150
100
50
0
0
20
40
60
80
100
% Reinnervated NMJs

Figure 5.1 KCC2 restoration is correlated with muscle reinnervation. CX3CR1$^{EGFP/+}$ animals underwent unilateral sciatic nerve injury and were allowed to survive for various time points. **A**) Representative images of FB+ motoneurons after sham surgery or 60 days after sciatic nerve cut/ligation or transection/repair. Yellow arrows surround motoneuron somata. KCC2 loss is maintained in animals with regeneration prevented but is restored in animals with regeneration allowed. Scale bar = 20 μm **B**) Time course of KCC2 downregulation and recovery in CX3CR1$^{EGFP/+}$ animals with a sciatic nerve cut/ligation or transection/repair. KCC2 protein levels are restored by 60 days post injury in repaired, but not ligated, animals (Statistical Table 5.1A; * $p \leq 0.05$, ** $p \leq 0.01$). Error bars = SEM. **C)** Representative motor endplates in the LG muscle following sciatic nerve transection/repair. Acetylcholine receptors were labeled with α-bungarotoxin (red, α-BTX) and motor axons and presynaptic terminals were identified by antibodies against neurofilament-H (NF, green) and the vesicular acetylcholine transporter (VAChT, white). Scale bar = 10 μm. Endplates with overlapping acetylcholine receptors and VAChT were designated as reinnervated. **D**) Correlation between average KCC2 immunoreactivity and neuromuscular junction (NMJ) reinnervation of individual animals (circles) color-coded for time after injury. Animals with higher levels of reinnervation of the LG have higher levels of KCC2 fluorescence on LG motoneurons (Statistical Table 5.1B).

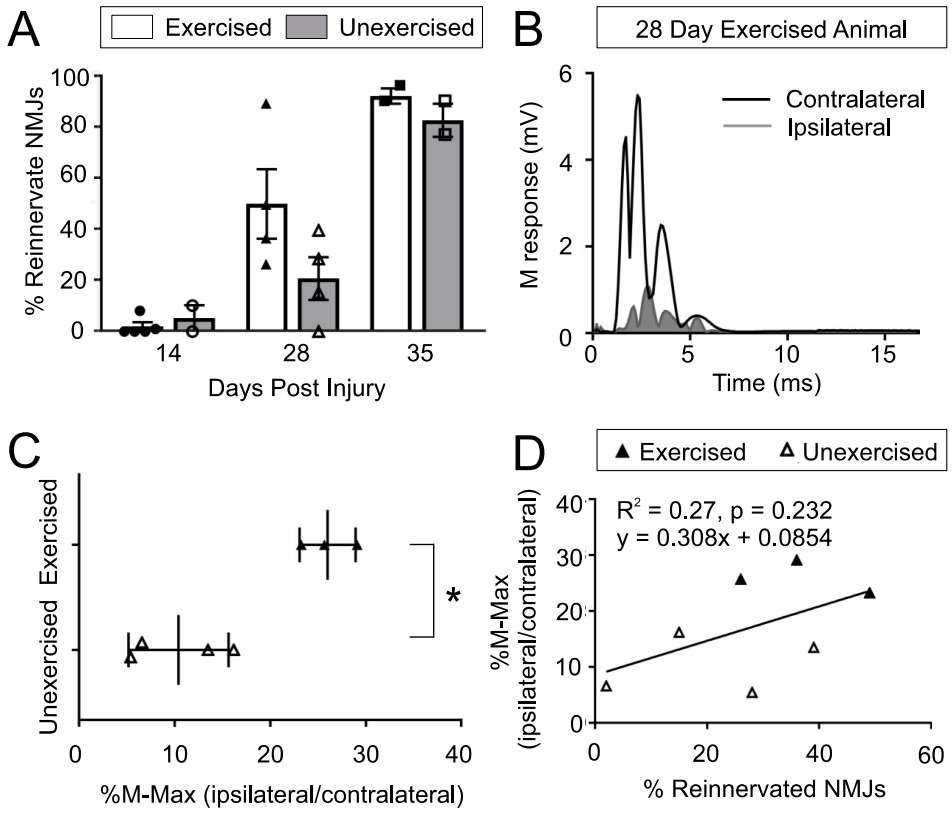

Figure 5.2 Exercise improves functional muscle recovery. Wild type female animals underwent unilateral sciatic transection/repair and were either treadmill trained (exercised) or unexercised. Points are average values for individual animals **A**) Neuromuscular NMJ re-occupancy of the LG muscles following injury. Exercised did not significantly improve neuromuscular reinnervation, but regeneration did get better with time (Statistical Table 5.1C) Error bars = SD. **B)** Representative muscle response traces from an injured (ipsilateral) and uninjured (contralateral) LG muscle following a sciatic nerve transection/repair. **C)** Average maximal muscle response (M-Max) values of exercised and unexercised animals 28 days following injury. Exercise improved the M-Max recovery (Statistical Table 5.1D). Data are represented as the average injured muscle's response as a percentage of the contralateral side with line at the mean. **D**) Correlation between NMJ reinnervation and M-max of individual animals. Higher levels of NMJ re-occupancy are not significantly statistically correlated with increased muscle responses (Statistical Table 5.1E).

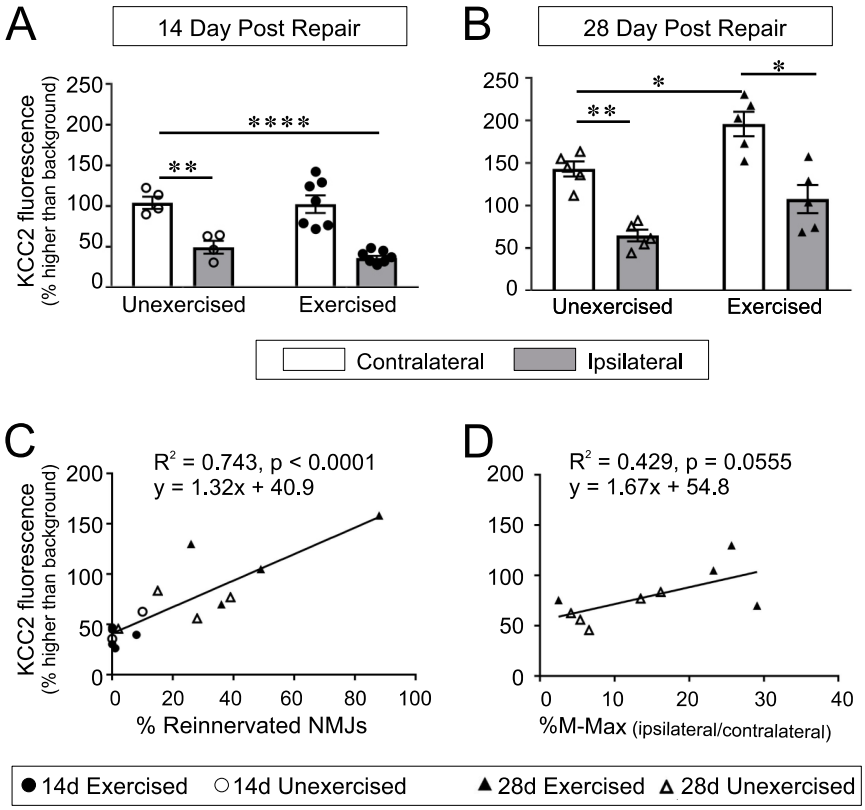

Figure 5.3 KCC2-IR is correlated with NMJ re-occupancy. Wild type female animals underwent unilateral sciatic transection/repair and were either treadmill trained (exercised) or not (unexercised). Circles/triangles are averages of individual animals **A,B**) KCC2-IR on motoneuron somata 14 (**A**) or 28 (**B**) days after injury. Only injury predicted KCC2 levels at 14 days (Statistical Table 5.1F), but there was an unexpected interaction between exercise and KCC2 at 28 days, with exercised animals showing higher than expected KCC2-IR in both motoneurons ipsilateral and contralateral to injury (Statistical Table 5.1G). However, there is still a statistically significant reduction in motoneuron KCC2 ipsilateral relative to contralateral to injury in exercised animals. Error bars = SE. **C**) Correlation between NMJ reinnervation and KCC2 reinnervation of individual animals. Higher levels of NMJ re-occupancy are correlated with increased levels of KCC2 on the soma (Statistical Table 5.1H). **D)** Correlation between KCC2-IR and M-Max. M-Max does not predict levels of KCC2 on motoneurons (Statistical Table 5.1I)

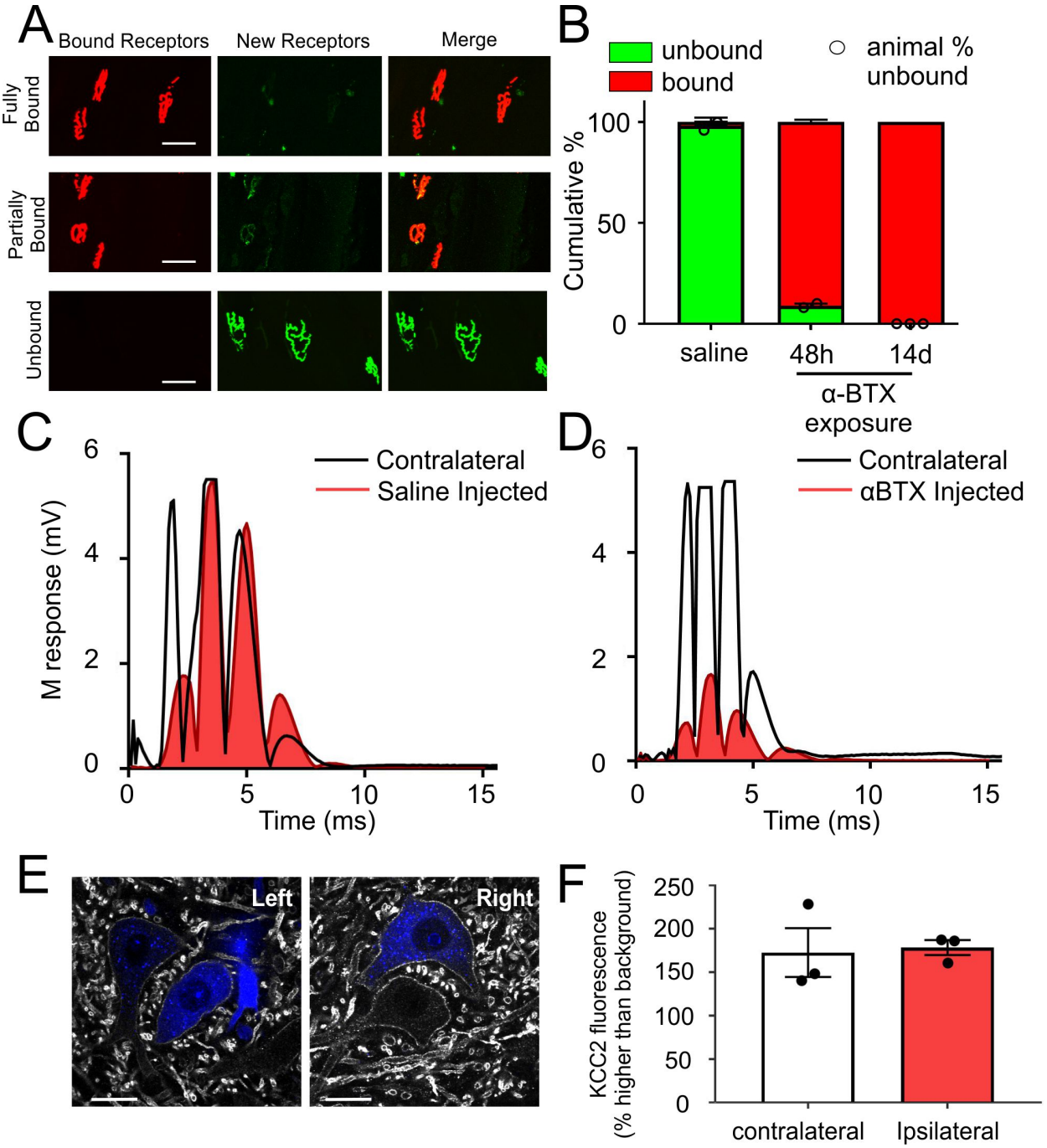
A
Bound Receptors
New Receptors
Merge
Fully Bound
Partially Bound
Unbound
B
unbound
bound
animal % unbound
Cumulative %
100
50
0
saline
48h
14d
α-BTX exposure
C
Contralateral
Saline Injected
M response (mV)
6
4
2
0
0
5
10
15
Time (ms)
D
Contralateral
αBTX Injected
6
4
2
0
0
5
10
15
Time (ms)
E
Left
Right
F
KCC2 fluorescence (% higher than background)
250
200
150
100
50
0
contralateral
Ipsilateral

Figure 5.4 Blocking NMJ activity alone does not induce KCC2 loss. A) Representative images of neuromuscular junctions (NMJs) within LG muscles 48 hours after injection with alpha-bungarotoxin conjugated to AlexaFluor-555 (top two rows) or saline (bottom row) after incubation with alpha-bungarotoxin conjugated to FITC. Alexa-555 (red) bound receptors were still bound 48 hours after the initial injection. Green labeling indicates receptors that were not previously bound by alpha-bungarotoxin in vivo, either because the animal was not exposed to it (saline injected), because the bungarotoxin did not completely fill the muscle, or because some or all of the receptors were replaced within that time frame. Scale bars = 20 μm. **B**) Quantification of postsynaptic receptor binding in LG muscles of saline injected animals, animals euthanized 48 hours after initial alpha-bungarotoxin injection, or 14 days after initial injection of alpha-bungarotoxin, after receiving injections every 48 hours. No animals had all completely bound postsynaptic nAChR's, but the majority of NMJs were at least partially bound in both the 48 hour and 14 day alpha-bungarotoxin treated animals. **C**, **D**) Representative muscle responses of saline treated (**C**) and alpha-bungarotoxin treated (**D**) LG muscles 48 hours after injection. Black traces are from contralateral muscles. Red traces are from injected muscles. Animals injected with alpha-bungarotoxin showed significantly diminished muscle responses on the injected side despite only partial binding of receptors. **E**) Representative images of KCC2 on LG motoneurons from animals after two weeks of bungarotoxin exposure. Scale bar = 20 μm. **F**) Quantification of KCC2-IR on motoneuron somata ipsilateral and contralateral exposure to alpha-bungarotoxin injections. Long-term blockade of postsynaptic signaling did not impact KCC2 protein levels on the motoneuron somata (Statistical Table 5.1J). Error bars = SD.

5.7 References

Almeida C, DeMaman A, Kusuda R, Cadetti F, Ravanelli MI, Queiroz AL, Sousa TA, Zanon S, Silveira LR, Lucas G (2015) Exercise therapy normalizes BDNF upregulation and glial hyperactivity in a mouse model of neuropathic pain. Pain 156:504-513.

Andersen B, Westlund B, Krarup C (2003) Failure of activation of spinal motoneurones after muscle fatigue in healthy subjects studied by transcranial magnetic stimulation. J Physiol 551:345-356.

Beaumont E, Gardiner PF (2003) Endurance training alters the biophysical properties of hindlimb motoneurons in rats. Muscle Nerve 27:228-236.

Bichler EK, Carrasco DI, Rich MM, Cope TC, Pinter MJ (2007) Rat motoneuron properties recover following reinnervation in the absence of muscle activity and evoked acetylcholine release. J Physiol 585:47-56.

Bongiovanni LG, Hagbarth KE (1990) Tonic vibration reflexes elicited during fatigue from maximal voluntary contractions in man. J Physiol 423:1-14.

Chang CC, Lee CY (1963) Isolation of neurotoxins from the venom of Bungarus Multicinctus and their modes of neuromuscular blocking action. Arch Int Pharmacodyn 144:241-257

Chopek JW, Sheppard PC, Gardiner K, Gardiner PF (2015) Serotonin receptor and KCC2 gene expression in lumbar flexor and extensor motoneurons posttransection with and without passive cycling. J Neurophysiol 113:1369-1376.

Cobianchi S, de Cruz J, Navarro X (2014) Assessment of sensory thresholds and nociceptive fiber growth after sciatic nerve injury reveals the differential contribution of collateral reinnervation and nerve regeneration to neuropathic pain. Exp Neurol 255:1-11.

Cobianchi S, Marinelli S, Florenzano F, Pavone F, Luvisetto S (2010) Short- but not long-lasting treadmill running reduces allodynia and improves functional recovery after peripheral nerve injury. Neuroscience 168:273-287.

Come E, Heubl M, Schwartz EJ, Poncer JC, Levi S (2019) Reciprocal Regulation of KCC2 Trafficking and Synaptic Activity. Front Cell Neurosci 13:48.

Côté MP, Gandhi S, Zambrotta M, Houle JD (2014) Exercise modulates chloride homeostasis after spinal cord injury. J Neurosci 34:8976-8987.

Côté MP, Murray M, Lemay MA (2017) Rehabilitation Strategies after Spinal Cord Injury: Inquiry into the Mechanisms of Success and Failure. J Neurotrauma 34:1841-1857.

Czeh G, Gallego R, Kudo N, Kuno M (1978) Evidence for the maintenance of motoneurone properties by muscle activity. J Physiol 281:239-252.

Detloff MR, Smith EJ, Molina DQ, Ganzer PD, Houlé JD (2014) Acute exercise prevents the development of neuropathic pain and the sprouting of non-peptidergic (GDNF- and artemin-responsive) c-fibers after spinal cord injury. Exp Neurol 255:38-48.

Duchateau J, Balestra C, Carpentier A, Hainaut K (2002) Reflex regulation during sustained and intermittent submaximal contractions in humans. J Physiol 541:959-967.

Eccles JC, Libet B, Young RR (1958) The behaviour of chromatolysed motoneurones studied by intracellular recording. J Physiol 143:11-40.

English AW, Wilhelm JC, Ward PJ (2014) Exercise, neurotrophins, and axon regeneration in the PNS. Physiol (Bethesda, Md) 29:437-445.

English AW, Cucoranu D, Mulligan A, Sabatier M (2009) Treadmill training enhances axon regeneration in injured mouse peripheral nerves without increased loss of topographic specificity. J Comp Neurol 517:245-255.

English AW, Chen Y, Carp JS, Wolpaw JR, Chen XY (2007) Recovery of electromyographic activity after transection and surgical repair of the rat sciatic nerve. J Neurophysiol 97:1127-1134.

Gardiner P, Dai Y, Heckman CJ (2006) Effects of exercise training on alpha-motoneurons. J Appl Physiol 101:1228-1236.

Gomez-Pinilla F, Ying Z, Roy RR, Molteni R, Edgerton VR (2002) Voluntary exercise induces a BDNF-mediated mechanism that promotes neuroplasticity. J Neurophysiol 88:2187-2195.

Gordon T, English AW (2016) Strategies to promote peripheral nerve regeneration: electrical stimulation and/or exercise. Eur J Neursoci 43:336-350.

Goutierre M, Al Awabdh S, Donneger F, Francois E, Gomez-Dominguez D, Irinopoulou T, Menendez de la Prida L, Poncer JC (2019) KCC2 Regulates Neuronal Excitability and Hippocampal Activity via Interaction with Task-3 Channels. Cell Rep 28:91-103.e107.

Grace PM, Fabisiak TJ, Green-Fulgham SM, Anderson ND, Strand KA, Kwilasz AJ, Galer EL, Walker FR, Greenwood BN, Maier SF, Fleshner M, Watkins LR (2016) Prior voluntary wheel running attenuates neuropathic pain. Pain 157:2012-2023.

Iwahashi Y, Furuyama T, Inagaki S, Morita Y, Takagi H (1994) Distinct regulation of sodium channel types I, II and III following nerve transection. Brain Res Mol Brain Res 22:341-345.

Jaiswal PB, Tung JK, Gross RE, English AW (2017) Motoneurons activity is required for enhancements in functional recovery after peripheral nerve injury in exercised female mice. J Neurosci Res.

Krakowiak J, Liu C, Papudesu C, Ward PJ, Wilhelm JC, English AW (2015) Neuronal BDNF signaling is necessary for the effects of treadmill exercise on synaptic stripping of axotomized motoneurons. Neural Plast 2015:392591.

Kuno M, Miyata Y, Munoz-Martinez EJ (1974) Properties of fast and slow alpha motoneurones following motor reinnervation. J Physiol 242:273-288.

Lee-Hotta S, Uchiyama Y, Kametaka S (2019) Role of the BDNF-TrkB pathway in KCC2 regulation and rehabilitation following neuronal injury: A mini review. Neurochem Int 128:32-38.

Lopez-Alvarez VM, Modol L, Navarro X, Cobianchi S (2015) Early increasing-intensity treadmill exercise reduces neuropathic pain by preventing nociceptor collateral sprouting and disruption of chloride cotransporters homeostasis after peripheral nerve injury. Pain 156:1812-1825.

Macefield G, Hagbarth KE, Gorman R, Gandevia SC, Burke D (1991) Decline in spindle support to alpha-motoneurones during sustained voluntary contractions. J Physiol 440:497-512.

McGregor CE, Irwin AM, English AW (2019) The Val66Met BDNF Polymorphism and Peripheral Nerve Injury: Enhanced Regeneration in Mouse Met-Carriers Is Not Further Improved With Activity-Dependent Treatment. Neurorehabil Neural Rep 33:407-418.

Medina I, Friedel P, Rivera C, Kahle KT, Kourdougli N, Uvarov P, Pellegrino C (2014) Current view on the functional regulation of the neuronal K(+)-Cl(-) cotransporter KCC2. Front Cell Neurosci 8:27.

Nakanishi ST, Cope TC, Rich MM, Carrasco DI, Pinter MJ (2005) Regulation of motoneuron excitability via motor endplate acetylcholine receptor activation. J Neurosci 25:2226-2232.

Nishimura Y, Asahara T, Yamamoto T, Tanaka T (1992) Observations on morphology and electrophysiological properties of the normal and axotomized facial motoneurons in the cat. Brain Res 596:305-310.

Park S, Liu C, Ward PJ, Jaiswal PB, English AW (2019) Effects of repeated 20Hz electrical stimulation on functional recovery following peripheral nerve injury. Neurorehabilitation & Neural Repair.

Pastor AM, Moreno-Lopez B, De La Cruz RR, Delgado-Garcia JM (1997) Effects of botulinum neurotoxin type A on abducens motoneurons in the cat: ultrastructural and synaptic alterations. Neuroscience 81:457-478.

Racinais S, Girard O, Micallef JP, Perrey S (2007) Failed excitability of spinal motoneurons induced by prolonged running exercise. J Neurophysiol 97:596-603.

Romer SH, Dominguez KM, Gelpi MW, Deardorff AS, Tracy RC, Fyffe RE (2014) Redistribution of Kv2.1 ion channels on spinal motoneurons following peripheral nerve injury. Brain Res 1547:1-15.
Sabatier MJ, English AW (2015) Pathways Mediating Activity-Induced Enhancement of Recovery From Peripheral Nerve Injury. Exercise and sport sciences reviews 43:163-171.
Sabatier MJ, Redmon N, Schwartz G, English AW (2008) Treadmill training promotes axon regeneration in injured peripheral nerves. Exp Neurol 211:489-493.
Sabatier MJ, To BN, Nicolini J, English AW (2011) Effect of axon misdirection on recovery of electromyographic activity and kinematics after peripheral nerve injury. Cells Tissues Organs 193:298-309.
Sattelle DB, Harrow ID, Hue B, Pelhate M, Gepner JI, Hall LM (1983) α-Bungarotoxin Blocks Excitatory Synaptic Transmission between Cercal Sensory Neurones and Giant Interneurone 2 of the Cockroach, Peripianeta Americana. Jounal of Experimental Biology 107:473-489.
Takata M, Tomomune N, Nagahama T, Tomioka S, Nakajo N (1990) Synaptic efficacy of inhibitory synapses and repetitive firing in the reinnervating trigeminal and hypoglossal motoneurons. Neuroscience 36:785-792.
Tashiro S, Shinozaki M, Mukaino M, Renault-Mihara F, Toyama Y, Liu M, Nakamura M, Okano H (2015) BDNF Induced by Treadmill Training Contributes to the Suppression of Spasticity and Allodynia After Spinal Cord Injury via Upregulation of KCC2. Neurorehabil Neural Rep 29:677-689.
Tatetsu M, Kim J, Kina S, Sunakawa H, Takayama C (2012) GABA/glycine signaling during degeneration and regeneration of mouse hypoglossal nerves. Brain Res 1446:22-33.
Toyoda H, Ohno K, Yamada J, Ikeda M, Okabe A, Sato K, Hashimoto K, Fukuda A (2003) Induction of NMDA and GABAA receptor-mediated Ca2+ oscillations with KCC2 mRNA downregulation in injured facial motoneurons. The J Neurophysiol 89:1353-1362.
Wilhelm JC, Xu M, Cucoranu D, Chmielewski S, Holmes T, Lau KS, Bassell GJ, English AW (2012) Cooperative roles of BDNF expression in neurons and Schwann cells are modulated by exercise to facilitate nerve regeneration. J Neurosci 32:5002-5009.
Wood K, Wilhelm JC, Sabatier MJ, Liu K, Gu J, English AW (2012) Sex differences in the effectiveness of treadmill training in enhancing axon regeneration in injured peripheral nerves. Dev Neurobiol 72:688-698.

Chapter 6: General Discussion & Future Directions

We have shown the potassium chloride co-transporter KCC2 is significantly and consistently depleted in spinal motoneurons following peripheral axotomy. This occurs at the transcriptional level, independent of BDNF/TrkB signaling and microglia, which is notably different than what has previously been described in other models. While it is still unclear what is regulating KCC2 depletion, it is probable that a signal from the periphery—likely from the muscle or terminal Schwann cells—is controlling the downregulation, and eventual restoration, of KCC2 following regeneration. While we hypothesized that this signal was likely activity dependent, the findings that KCC2 was not affected by exercise prior to regeneration, was not correlated with increased muscle response as measured by EMG, and was not affected by functional blockade of the NMJ did not support this hypothesis. Instead, KCC2 appears to be restored based on the physical presence of the NMJ rather than it's functionality. Future studies are needed to address whether this physical connection with the muscle is responsible for maintaining KCC2 in intact conditions and/or whether there is another injury signal inducing KCC2 loss. This difference in KCC2 regulatory mechanisms between dorsal horn neurons and motoneurons after PNI is excellent news for groups targeting the microglia/BDNF/TrkB pathway to prevent neuropathic pain. It also bodes well for the potential of manipulating KCC2 loss to investigate its impacts on regeneration without inducing pain; the two processes are not likely to interfere with each other.

Irrespective of what is modulating KCC2, future studies need to investigate the consequence of KCC2 loss in spinal motoneurons following PNI. While evidence from the brainstem and spinal cord (reviewed below) suggests that changes in motoneuron KCC2 after injury can have large functional consequences, and we have shown that KCC2 protein expression is tightly linked to the regenerative state in spinal motoneurons, this does not guarantee that its loss has a physiological impact on spinal motoneurons or on their regeneration after injury. Whether by impairing the mechanism of KCC2 downregulation or

influencing KCC2 expression in another way, the functional significance of KCC2 depletion after PNI should become a priority.

6.1 Mechanisms of KCC2 depletion on spinal motoneurons following PNI

Aside from BDNF, there are numerous neurotrophic factors and signals from peripheral cells that interact with, or travel through, motor axons. In intact adult motoneurons, BDNF is the predominant neurotrophin transported from the muscle (Koliatsos et al., 1993; Verhovshek et al., 2013). However, given our evidence that eliminating BDNF from microglia and motoneurons, preventing TrkB signaling, and exercising animals, which increases BDNF production (Gomez-Pinilla et al., 2002; Wu et al., 2011; Tashiro et al., 2015), all have no affect on KCC2, it is more likely that a non-BDNF retrograde signal from the muscle or a signal from the Schwann cells myelinating their axons is responsible for maintaining KCC2. Rather than searching for individual retrograde signals to target, future studies should begin addressing this possibility by utilizing peripheral manipulations to target activity-independent signaling from the periphery—such as by blocking retrograde transport in motoneuron axons or knocking out the ability of muscles or Schwann cells to perform exocytosis. Unfortunately, while single proteins have been identified that can interfere with muscle exocytosis in *c. elegans* (AEX-1) (Doi and Iwasaki, 2002) and drosophila (F-actin) (Tran et al., 2015), similar in vivo experiments in mammals have not been performed. However, Schwann cell exocytosis can be prevented by knockdown of the small GTP-ase RAb27a (Blott and Griffiths, 2002; Chen et al., 2012) and there are well-characterized blockers of axonal retrograde transport. These include brefeldin A (Campenot et al., 2003), and colchicine (Schwab and Thoenen, 1983), which could both be applied in a cuff around the nerve of interest. Brefeldin A may be toxic to spinal motoneurons (Kikuchi et al., 2003), whereas colchicine has been used previously to successfully block axonal transport when applied through a peripheral cuff for at least eight days (Cangiano and Fried, 1977), making it a better candidate for these experiments.

We have shown that KCC2 is restored after reconnection with the muscle, but it is possible there are different signals for inducing KCC2 downregulation and it's restoration. In this case, interfering with signaling from the muscle in intact nerves may not induce KCC2 downregulation at all. A "positive" injury signal, rather than the lack of a constitutively transported signal, could also be responsible for changing *kcc2* gene transcription. After injury there are significant increases in glial derived neurotrophic factor (GDNF) (Zahavi et al., 2015), leukemia inhibitory factor (LIF) and ciliary neurotrophic factor (CNTF) secreted from Schwann cells peripherally (Sendtner et al., 1997). The role of these factors could be investigated by blocking exocytosis and/or retrograde transport following axotomy rather than in only intact nerves.

Transport-dependent signals are not the only signs of injury that can affect transcription within the motoneuron cell body. In addition to astrocytic activation (Qian et al., 2018), withdrawal of synapses from motoneurons cell bodies, and the eventual influx of peripheral immune cells (Rotterman et al., 2019) that all occur with a slower time course than KCC2 loss, there is also a large influx of calcium that immediately follows axotomy (Strautman et al., 1990). It is this calcium influx that may be responsible for triggering many regeneration-associated genes (RAGs) (Mar et al., 2014). To date, there have been no studies investigating the full motoneuron transcriptome changes following peripheral axotomy. Those studies investigating RAGs in motoneurons have generally focused on subsets of genes whose upregulation are known to be associated with regeneration, rather than trying to find new targets or look at those that are downregulated after injury, such as *kcc2* (reviewed (Shin and Cho, 2017)).

Regardless of whether KCC2 expression is regulated by a positive or negative injury signal, the detailed mechanisms inducing these changes must also be illuminated. A full transcriptome analysis could illuminate new pathways that may be related to KCC2 downregulation, and would be beneficial for more fully understanding the changes in motoneurons following axotomy generally. However, several other mechanisms have already

been implicated in KCC2 regulation in other systems. We have shown that KCC2 depletion occurs independent from miRNA's (see Appendix 1) but after injury, changes in transcriptional repressor REST-RE-1 (Yeo et al., 2009), nitric oxide (NO) signaling (Yassin et al., 2014), and/or alterations in serotonergic signaling (Mahadevan and Woodin, 2016) have been shown to affect KCC2 expression. Of these, REST-RE-1 and serotonin have not been investigated in the ventral horn after PNI. However, nitric oxide is well known to be upregulated in motoneurons after axotomy and may be an intermediary between injury signals and the induction of other shifts towards hyperexcitability in motoneurons (Reviewed in (Gonzalez-Forero and Moreno-Lopez, 2014)). Both REST-RE-1 and NO will be difficult to manipulate independently; REST is involved in the expression of many neuronal proteins (Thiel et al., 2015) and it's dysregulation in the development of many cancers (Huang and Bao, 2012). Nitric oxide is also involved in numerous neuronal cell processes and its disruption in neurons after injury causes significant death of sensory, motor, and interneurons (Keilhoff et al., 2002, 2003). Interruption of inducible nitric oxide also impairs regeneration (Levy et al., 2001) and while it is possible that impaired KCC2 depletion contributes to this outcome, parsing its role from the other outcomes of NO disruption would be difficult. Before pursuing these questions it is essential to determine *if* and *what* KCC2 depletion after injury contributes to regeneration.

6.2 The impact of KCC2 loss on spinal motoneurons following spinal cord injury and brainstem motoneurons after PNI

Following spinal cord injury (SCI) in adults, motoneurons below the level of injury partially lose KCC2 (Boulenguez et al., 2010; Chopek et al., 2015). Unlike after axotomy, these motoneurons are not directly injured during SCI and their axons remain intact in the peripheral nerve. A post-translational mechanism has been proposed to explain this effect, indicating that KCC2 downregulation was dependent on the loss of descending serotonergic inputs and 5HT2A receptor activity (Bos et al., 2013). The downregulation of KCC2, as measured in just the cell

body, was estimated to be around 20% (but may be better preserved on the dendrites). This lead to a small but significant increase in the reversal potential of chloride of only 5 mV in adult rats (Murray et al., 2011) that was sufficient to generate significant disinhibition and spasticity. After SCI, motoneuron excitability and spasticity can be rectified with enhancers of KCC2 activity (Sanchez-Brualla et al., 2017), suggesting that enough KCC2 remains on the surface of the motoneurons to rescue the animal from spasticity. We see a nearly complete loss of KCC2 from the somatic membrane of spinal motoneurons following peripheral axotomy, and their serotonergic input is presumably intact.

KCC2 regulation in SCI and PNI injured motoneurons differ in mechanism and completeness, but KCC2 in axotomized spinal motoneurons closely resembles that of axotomized brainstem motoneurons. Following PNI of the vagal nerve, KCC2 mRNA was diminished in the DMV by three days after vagal nerve axotomy in young rats (Nabekura et al., 2002). DMV neurons innervate postganglionic parasympathetic neurons rather than skeletal muscle, but these findings were later recapitulated in facial (Toyoda et al., 2003; Kim et al., 2018) and hypoglossal (Tatetsu et al., 2012) motoneurons following transection of the respective peripheral nerves. Several of these studies speculated that the eventual return of KCC2 mRNA (Toyoda et al., 2003) and protein (Tatetsu et al., 2012; Kim et al., 2018) they observed was tied to regeneration, but none analyzed this directly or whether it was dependent on successful target reinnervation. It is likely that if these studies had performed similar correlations as we described in Chapter 5, the restoration of KCC2 in these motoneurons would also have been closely correlated with the degree of successful reinnervation.

Rather than focusing on KCC2 regulation, the previous studies in the brainstem focused on the physiological impact of KCC2 loss during the weeks following axotomy. In contrast to the relatively small shift in E_{GABA} following SCI, after axotomy of adult facial motoneurons, E_{GABA} depolarizes by almost 19 mV (Toyoda et al., 2003). This change, driven by the loss of KCC2, seems to induce a state in which GABAergic transmission is a direct driver of activity. Loss of

KCC2 was coupled with increased calcium levels and firing in response to GABA exposure in slice preparations of axotomized DMV motoneurons (Nabekura et al., 2002) and with spontaneous calcium oscillations in axotomized facial motoneurons that were driven by depolarizations dependent on activation of $GABA_A$ and NMDA receptors (Toyoda et al., 2003).

Given how drastic the loss of KCC2 is on the spinal cord, it is likely GABA-driven activity induces firing in regenerating motoneurons. However, it important to consider that while brainstem and spinal motoneurons both innervate muscle, the circuitry surrounding them is vastly different and responses to injury may not always be equivalent across motoneuron populations. Whereas facial (Vaughan, 1994; Kim et al., 2018), like spinal motoneurons (Alvarez et al., 2011; Rotterman et al., 2019) have small decreases in gephyrin+ (GABA/glycinergic) synapses following peripheral axotomy, hypoglossal motoneurons do not lose inhibitory synapses (Sumner, 1975; Tatetsu et al., 2012). Interestingly, inhibitory synapses on facial motoneurons increase in size and GABA content following axotomy (Vaughan, 1994). While this has not been investigated on spinal motoneurons following PNI, it is possible that they also shift their inhibitory synapse phenotype or strength following injury. Many inhibitory synapses in the spinal cord are mixed GABA/glycine synapses, and they shift from predominantly GABAergic to predominantly glycinergic during postnatal development (Gao et al., 2001; Gonzalez-Forero and Alvarez, 2005). Adult spinal motoneurons predominantly receive inhibition from glycinergic synapses (Alvarez et al., 1997) but could revert to GABAergic mechanisms after axotomy. Postsynaptic $GABA_A$ synaptic currents have much slower decay times than glycinergic synapses (Alvarez, 2017), allowing for longer depolarizations in the context of diminished KCC2 expression and high internal chloride. This might be necessary for NMDA activation as shown in brainstem axotomized motoneurons. Calcium entry by NMDA receptors and voltage-gated calcium channels could trigger or maintain gene expression that promotes regeneration. Thus, the exact consequences of KCC2 loss on motoneurons in the spinal cord must be elucidated and the impacts of regeneration described in our model specifically.

6.3 Does increased inhibitory synaptic activity promote motor axon regeneration after PNI?

A direct link has yet to be made between inhibitory synapse depolarization and regeneration, but there is clear evidence that chloride-driven activity is important for axon sprouting in other central neurons (Sernagor et al., 2010; Nakajima and Marunaka, 2016; Kourdougli et al., 2017). While KCC2 levels are low during development, high internal chloride and long-lasting GABAergic depolarizations drive neurite outgrowth while glutamatergic activation is insufficient to do so (Sernagor et al., 2010). High intracellular chloride and GABA-receptor driven activity are also essential for regeneration in non-nociceptive dorsal root ganglia cells (Pieraut et al., 2007; Modol et al., 2014), and regenerating spinal motoneurons make many changes to increase their excitability generally, like increased input resistance, decreased rheobase, and changes in action potential dynamics (Kuno et al., 1974; Huizar et al., 1977; Gustafsson, 1979; Gustafsson and Pinter, 1984; Gonzalez-Forero et al., 2007). Given that activity-dependent treatments are known to enhance regeneration (Al-Majed et al., 2000a; Al-Majed et al., 2000b; English et al., 2007; English et al., 2009; Udina et al., 2011), and motoneuron activity is essential for the pro-regenerative effects of exercise (Jaiswal et al., 2017), it is possible that KCC2 depletion on motoneurons resulting in enhanced "excitatory" drive from GABA/glycine synapses may further promote motoneuron firing and calcium entry, contributing to regeneration.

Activity driven by GABA/glycine has yet to be studied on axotomized adult spinal motoneurons, so it is unclear whether these motoneurons become depolarized to the same degree as has been shown in the brainstem. However, inhibitory synapses are preferentially preserved on axotomized motoneurons (Linda et al., 2000; Alvarez et al., 2011; Rotterman et al., 2019) so it is feasible they are driving activity. Interestingly, studies on axotomized spinal neurons have illustrated that manipulations decreasing retention of "inhibitory" synapses

(defined by electron microscopy or immunohistochemistry) decrease motoneuron regeneration, while those that preserve more inhibitory synapses correlated with greater speed of motor function recovery (Oliveira et al., 2004; Berg et al., 2012). The authors of these studies suggest this correlation could be due to better "focusing" of the motoneuron on regeneration than firing, but neither considered that the function of these inhibitory synapses may be altered by KCC2 depletion.

Internal chloride is also dependent on the activation of NKCC1, and a recent study analyzed motor axon regeneration following sciatic nerve injury after pharmacologically blocking NKCC1 activity with bumetamide (Modol et al., 2015). In this study, bumetamide was applied systemically and the number of motoneurons retrogradely labeled with Fluoro-Gold 14 mm distal to the lesion was estimated. Although fewer motoneurons were retrogradely labeled in bumetamide-treated animals, suggesting bumetamide may have interfered with regeneration, the differences compared to controls were not significant, which does not support the idea that elevated intracellular chloride is important for regeneration. If chloride influx and efflux mechanisms are both blocked in axotomized motoneurons due to bumetamide treatment and KCC2-depletion respectively, then opening of chloride channels due to inhibitory synapse activity should move chloride toward E_{Cl^-}, preventing any accumulation. Thus, if NKCC1 was the only chloride accumulating mechanism in motoneurons, blocking NKCC1 should prevent any putative benefits of elevated chloride in axon regeneration. However, there is some evidence that NKCC1 transport function is inactivated in mature spinal motoneurons (Kanaka et al., 2001; Delpy et al., 2008) and that motoneurons can accumulate chloride through alternative pathways including the anion exchanger, AE3 (Gonzalez-Islas et al., 2009) which is upregulated after spinal cord injury (Ryge et al., 2010; Wienecke et al., 2010). NKCC1 function is tightly regulated (Kahle and Delpire, 2016) and it is possible that axotomy causes reactivation of NKCC1 transport. It is also possible that alternative mechanisms are upregulated in the presence or absence of NKCC1 activity and contribute to accumulating chloride inside motoneurons.

When tested in the brainstem, GABA clearly depolarizes axotomized motoneurons, implying effective chloride accumulation above its equilibrium. Much work needs to be done elucidating chloride transport mechanisms in normal and axotomized motoneurons, but critically, studies must first address the significance of changes in inhibitory synapse function due to elevated internal chloride for motoneuron regeneration.

6.4 Future strategies for investigating the importance of altered KCC2 and inhibitory signaling in axotomized motoneurons

The ideal strategy for investigating the impact of KCC2 on regeneration would to block KCC2 loss, but until a precise mechanism for KCC2 is resolved this approach is unfeasible. Overexpression of KCC2 is another potential strategy. However, KCC2 is too large to insert into commonly used AAV vectors for motoneuron transection and gene manipulation from the periphery. It is also not guaranteed that overexpression of KCC2 would overcome the regulatory mechanisms preventing gene transcription. Before investing more resources in understanding the regulation of KCC2 in this system, future studies should determine whether the observed decreases in KCC2 impact the injured motoneurons' responses to typically inhibitory synapses and what the roles of these inhibitory synapses in injury are more generally. To answer the first question, calcium imaging in mice that allow GCAMP imaging motoneurons within in spinal cord slices ($Chat^{iREScre/+}$ :: GCAMP mice) or patching motoneurons after axotomy would allow comparisons of uninjured and axotomized motoneuron responses to GABA and glycine. Traditional slice physiology is difficult to perform in the adult spinal cord, but it is feasible (Mitra and Brownstone, 2012) and in collaboration with the Perrault lab we have obtained proof-of-principle for the GCAMP recording strategy in young animals. In either case, the optimal strategy will be to puff GABA or glycine onto specifically the injured motoneurons while recording so that the impact of other changes in circuitry may be minimized.

Addressing the role of retained GABA/glycine synapses in regeneration after injury may be more difficult. One option is to increase the inhibitory tone of the whole CNS using a GABA receptor agonist like a benzodiazepine, or inversely, antagonizing these "inhibitory" receptors with gabazine, bicuculline, or strychnine throughout the regenerative period and observing the impacts of this on functional recovery following PNI. It will be important to confirm that there are no differences in overall movement or exercise patterns in these treated mice and to confirm no direct action of treatment on KCC2 expression. Diazepam, a benzodiazepine, has been reported to attenuate the KCC2 depletion usually found in neonates after ischemia (Ma et al., 2014), and ethanol, another GABA receptor agonist, exposure has been shown to increase KCC2 expression in the neonatal hippocampus (Silvestre de Ferron et al., 2017). While both of these studies investigated immature neurons, it will be important to consider whether the interventions themselves impact KCC2 in injured adult motoneurons, especially given that they return to a less-mature phenotype following injury.

6.5 High chloride promotes regeneration in axotomized sensory neurons

Injury to the periphery does not affect motoneurons in isolation. Sensory neurons with cell bodies in the dorsal root ganglia are also axotomized and also become hyperexcitable after PNI. Somatic sensory neurons are pseudounipolar and extend both central and peripheral axonal processes that, respectively, enter the spinal cord through dorsal roots or innervate peripheral organs after exiting through spinal nerves. Axotomy of the peripheral branch, but not of the central branch, triggers changes in gene expression in DRG cell somata and initiation of a regenerative program that shifts these neurons towards hyperexcitability (DeFrancesco-Lisowitz et al., 2015). These alterations include changes in sodium and potassium voltage-gated channel composition that mimic many of the features already reviewed in axotomized motoneurons (see (Navarro et al., 2007)).

One major difference between DRG neurons and motoneurons is that adult DRG neurons normally maintain a high internal chloride concentration in their cell body, peripheral, and central branches (Alvarez-Leefmans et al., 1988; Valverde et al., 1996; Sung et al., 2000) as a result of high expression of NKCC1 and lack of KCC2 (Alvarez-Leefmans et al., 2001; Mao et al., 2012). In spinal neurons, the reversal potential of $GABA_A$ receptors is typically near -70 mV (Coull et al., 2003), whereas in DRG neurons it is around -35 mV (Alvarez-Leefmans et al., 1988; Sung et al., 2000; Chen et al., 2014) and -19 mV after injury (Pieraut et al., 2007). Thus, internal chloride increases in the cell bodies of DRG neurons two-fold after axotomy, from 31 to 68 mM (Pieraut et al., 2007). This accumulation is due to increased NKCC1 phosphorylation and trafficking to the membrane, which occurs rapidly (3 days after injury) without changes at the transcriptional level. NKCC1 phosphorylation and increased chloride concentration correlate with increases in neurite outgrowth, while blocking NKCC1 or abolishing the chloride gradient (manipulating external chloride) diminishes sensory axon growth (Pieraut et al., 2007; Modol et al., 2015) in medium- and large-sized cutaneous and muscle sensory afferents. Interestingly, it has minimal effects on regeneration of nociceptors (Pieraut et al., 2007; Modol et al., 2015). Instead, increased activity in these cells contributes to hyperalgesia by propagating pain signals to the brain that are normally blocked at the spinal cord level (reviewed in (Treede, 2016)). Thus, mammalian DRG neurons embody the dual nature of changes in chloride, with both positive (enhances regeneration) and negative (hyperalgesia) outcomes. It needs to be proven whether high chloride in motoneurons may similarly enhance regenerative capacity.

6.6 Conclusions

It is important to consider the possibility that while KCC2 depletion in the adult spinal cord can be maladaptive in some conditions—like development of spasticity after spinal cord injury, and hyperalgesia in many injury states—KCC2 downregulation might be beneficial in other situations, such as peripheral axon regeneration. Through this dissertation we have

illustrated that KCC2 on axotomized spinal motoneurons is regulated in a manner distinct from mechanisms previously described after PNI in other cell types and on motoneurons after spinal cord injury. It is important to take lessons from these other models about potential implications for the loss in KCC2 we observe, but it is also necessary to investigate each observation in the context in which it is found. It is unlikely that such a consistent phenomenon as chloride dysregulation after injury would persist through evolution if it purely caused neuronal dysfunction. Perhaps chloride-facilitate regeneration will explain why KCC2 disruption after injury is so reliable and difficult to prevent.

6.7 References

Alvarez FJ, Titus-Mitchell HE, Bullinger KL, Kraszpulski M, Nardelli P, Cope TC (2011) Permanent central synaptic disconnection of proprioceptors after nerve injury and regeneration. I. Loss of VGLUT1/IA synapses on motoneurons. J Neurophysiol 106:2450-2470.

Alvarez-Leefmans FJ, Gamino SM, Giraldez F, Nogueron I (1988) Intracellular chloride regulation in amphibian dorsal root ganglion neurones studied with ion-selective microelectrodes. J Physiol 406:225-246.

Alvarez-Leefmans FJ, Leon-Olea M, Mendoza-Sotelo J, Alvarez FJ, Anton B, Garduno R (2001) Immunolocalization of the Na(+)-K(+)-2Cl(-) cotransporter in peripheral nervous tissue of vertebrates. Neuroscience 104:569-582.

Berg A, Zelano J, Stephan A, Thams S, Barres BA, Pekny M, Pekna M, Cullheim S (2012) Reduced removal of synaptic terminals from axotomized spinal motoneurons in the absence of complement C3. Exp Neurol 237:8-17.

Blott EJ, Griffiths GM (2002) Secretory lysosomes. Nat Rev Mol Cell Biol 3:122-131.

Boulenguez P, Liabeuf S, Bos R, Bras H, Jean-Xavier C, Brocard C, Stil A, Darbon P, Cattaert D, Delpire E, Marsala M, Vinay L (2010) Down-regulation of the potassium chloride cotransporter KCC2 contributes to spasticity after spinal cord injury. Nat. Med. 16:302-307.

Campenot RB, Soin J, Blacker M, Lund K, Eng H, MacInnis BL (2003) Block of slow axonal transport and axonal growth by brefeldin A in compartmented cultures of rat sympathetic neurons. Neuropharmacol 44:1107-1117.

Cangiano A, Fried JA (1977) The production of denervation-like changes in rat muscle by colchicine, without interference with axonal transport or muscle activity. J Physiol 265:63-84.

Chen G, Zhang Z, Wei Z, Cheng Q, Li X, Li W, Duan S, Gu X (2012) Lysosomal exocytosis in Schwann cells contributes to axon remyelination. Glia 60:295-305.

Chen JT, Guo D, Campanelli D, Frattini F, Mayer F, Zhou L, Kuner R, Heppenstall PA, Knipper M, Hu J (2014) Presynaptic GABAergic inhibition regulated by BDNF contributes to neuropathic pain induction. Nat Comm 5:5331.

Chopek JW, Sheppard PC, Gardiner K, Gardiner PF (2015) Serotonin receptor and KCC2 gene expression in lumbar flexor and extensor motoneurons posttransection with and without passive cycling. J Neurophysiol 113:1369-1376.

Coull JA, Boudreau D, Bachand K, Prescott SA, Nault F, Sik A, De Koninck P, De Koninck Y (2003) Trans-synaptic shift in anion gradient in spinal lamina I neurons as a mechanism of neuropathic pain. Nature 424:938-942.

DeFrancesco-Lisowitz A, Lindborg JA, Niemi JP, Zigmond RE (2015) The neuroimmunology of degeneration and regeneration in the peripheral nervous system. Neuroscience.

Delpy A, Allain AE, Meyrand P, Branchereau P (2008) NKCC1 cotransporter inactivation underlies embryonic development of chloride-mediated inhibition in mouse spinal motoneuron. J Physiol 586:1059-1075.

Doi M, Iwasaki K (2002) Regulation of retrograde signaling at neuromuscular junctions by the novel C2 domain protein AEX-1. Neuron 33:249-259.

Gomez-Pinilla F, Ying Z, Roy RR, Molteni R, Edgerton VR (2002) Voluntary exercise induces a BDNF-mediated mechanism that promotes neuroplasticity. J Neurophysiol 88:2187-2195.

Gong L, Wu J, Zhou S, Wang Y, Qin J, Yu B, Gu X, Yao C (2016) Global analysis of transcriptome in dorsal root ganglia following peripheral nerve injury in rats. Biochem Bioph Res Co 478:206-212.

Gonzalez-Forero D, Moreno-Lopez B (2014) Retrograde response in axotomized motoneurons: nitric oxide as a key player in triggering reversion toward a dedifferentiated phenotype. Neuroscience 283:138-165.
Gonzalez-Islas C, Chub N, Wenner P (2009) NKCC1 and AE3 appear to accumulate chloride in embryonic motoneurons. J Neurophysiol 101:507-518.
Huang Z, Bao S (2012) Ubiquitination and deubiquitination of REST and its roles in cancers. FEBS Lett 586:1602-1605.
Jaiswal PB, Tung JK, Gross RE, English AW (2017) Motoneuron activity is required for enhancements in functional recovery after peripheral nerve injury in exercised female mice. J Neurosci Res.
Kahle KT, Delpire E (2016) Kinase-KCC2 coupling: Cl- rheostasis, disease susceptibility, therapeutic target. J Neurophysiol 115:8-18.
Kanaka C, Ohno K, Okabe A, Kuriyama K, Itoh T, Fukuda A, Sato K (2001) The differential expression patterns of messenger RNAs encoding K-Cl cotransporters (KCC1,2) and Na-K-2Cl cotransporter (NKCC1) in the rat nervous system. Neuroscience 104:933-946.
Keilhoff G, Fansa H, Wolf G (2002) Neuronal nitric oxide synthase is the dominant nitric oxide supplier for the survival of dorsal root ganglia after peripheral nerve axotomy. J Chem Neuroanat 24:181-187.
Keilhoff G, Fansa H, Wolf G (2003) Nitric oxide synthase, an essential factor in peripheral nerve regeneration. Cell Mol Biol (Noisy-le-Grand, France) 49:885-897.
Kikuchi S, Shinpo K, Tsuji S, Yabe I, Niino M, Tashiro K (2003) Brefeldin A-induced neurotoxicity in cultured spinal cord neurons. J Neurosci Res 71:591-599.
Koliatsos VE, Clatterbuck RE, Winslow JW, Cayouette MH, Price DL (1993) Evidence that brain-derived neurotrophic factor is a trophic factor for motor neurons in vivo. Neuron 10:359-367.
Kourdougli N, Pellegrino C, Renko JM, Khirug S, Chazal G, Kukko-Lukjanov TK, Lauri SE, Gaiarsa JL, Zhou L, Peret A, Castren E, Tuominen RK, Crepel V, Rivera C (2017) Depolarizing gamma-aminobutyric acid contributes to glutamatergic network rewiring in epilepsy. Ann Neurol 81:251-265.
Levy D, Kubes P, Zochodne DW (2001) Delayed peripheral nerve degeneration, regeneration, and pain in mice lacking inducible nitric oxide synthase. J Neuropath Exp Neur 60:411-421.
Li S, Xue C, Yuan Y, Zhang R, Wang Y, Wang Y, Yu B, Liu J, Ding F, Yang Y, Gu X (2015) The transcriptional landscape of dorsal root ganglia after sciatic nerve transection. Sci. Rep. 5:16888.
Linda H, Shupliakov O, Ornung G, Ottersen OP, Storm-Mathisen J, Risling M, Cullheim S (2000) Ultrastructural evidence for a preferential elimination of glutamate-immunoreactive synaptic terminals from spinal motoneurons after intramedullary axotomy. J Comp Neurol 425:10-23.
Ma JY, Zhang SP, Guo LB, Li YM, Li Q, Wang SQ, Liu HM, Wang C (2014) KCC2 expression changes in Diazepam-treated neonatal rats with hypoxia-ischaemia brain damage. Brain Res 1563:22-30.
Mahadevan V, Woodin MA (2016) Regulation of neuronal chloride homeostasis by neuromodulators. J Physiol.
Mao S, Garzon-Muvdi T, Di Fulvio M, Chen Y, Delpire E, Alvarez FJ, Alvarez-Leefmans FJ (2012) Molecular and functional expression of cation-chloride cotransporters in dorsal root ganglion neurons during postnatal maturation. J Neurophysiol 108:834-852.
Mar FM, Bonni A, Sousa MM (2014) Cell intrinsic control of axon regeneration. EMBO Rep 15:254-263.
Mariotti R, Bentivoglio M (1996) Botulinum toxin induces nitric oxide synthase activity in motoneurons. Neurosci Lett 219:25-28.

Mitra P, Brownstone RM (2012) An in vitro spinal cord slice preparation for recording from lumbar motoneurons of the adult mouse. The J Neurophysiol 107:728-741.
Modol L, Cobianchi S, Navarro X (2014) Prevention of NKCC1 phosphorylation avoids downregulation of KCC2 in central sensory pathways and reduces neuropathic pain after peripheral nerve injury. Pain 155:1577-1590.
Modol L, Santos D, Cobianchi S, Gonzalez-Perez F, Lopez-Alvarez V, Navarro X (2015) NKCC1 Activation Is Required for Myelinated Sensory Neurons Regeneration through JNK-Dependent Pathway. J Neurosci 35:7414-7427.
Nakajima KI, Marunaka Y (2016) Intracellular chloride ion concentration in differentiating neuronal cell and its role in growing neurite. Biochem Bioph Res Co 479:338-342.
Navarro X, Vivo M, Valero-Cabre A (2007) Neural plasticity after peripheral nerve injury and regeneration. Progress in neurobiology 82:163-201.
Novikov L, Novikova L, Kellerth JO (1995) Brain-derived neurotrophic factor promotes survival and blocks nitric oxide synthase expression in adult rat spinal motoneurons after ventral root avulsion. Neurosci Lett 200:45-48.
Oliveira AL, Thams S, Lidman O, Piehl F, Hokfelt T, Karre K, Linda H, Cullheim S (2004) A role for MHC class I molecules in synaptic plasticity and regeneration of neurons after axotomy. Proc Natl Acad Sci USA 101:17843-17848.
Pieraut S, Laurent-Matha V, Sar C, Hubert T, Mechaly I, Hilaire C, Mersel M, Delpire E, Valmier J, Scamps F (2007) NKCC1 phosphorylation stimulates neurite growth of injured adult sensory neurons. J Neurosci 27:6751-6759.
Ray P, Torck A, Quigley L, Wangzhou A, Neiman M, Rao C, Lam T, Kim JY, Kim TH, Zhang MQ, Dussor G, Price TJ (2018) Comparative transcriptome profiling of the human and mouse dorsal root ganglia: an RNA-seq-based resource for pain and sensory neuroscience research. Pain 159:1325-1345.
Rotterman TM, Akhter ET, Lane AR, MacPherson KP, Garcia VV, Tansey MG, Alvarez FJ (2019) Spinal motor circuit synaptic plasticity after peripheral nerve injury depends on microglia activation and a CCR2 mechanism. J Neurosci.
Ryge J, Winther O, Wienecke J, Sandelin A, Westerdahl AC, Hultborn H, Kiehn O (2010) Transcriptional regulation of gene expression clusters in motor neurons following spinal cord injury. BMC Genomics 11:365.
Schwab ME, Thoenen H (1983) Mechanism of uptake and retrograde axonal transport of noradrenaline in sympathetic neurons in culture: reserpine-resistant large dense-core vesicles as transport vehicles. J Cell Biol 96:1538-1547.
Sendtner M, Gotz R, Holtmann B, Thoenen H (1997) Endogenous ciliary neurotrophic factor is a lesion factor for axotomized motoneurons in adult mice. J Neurosci 17:6999-7006.
Sernagor E, Chabrol F, Bony G, Cancedda L (2010) GABAergic control of neurite outgrowth and remodeling during development and adult neurogenesis: general rules and differences in diverse systems. Front Cell Neurosci 4:11.
Shin JE, Cho Y (2017) Epigenetic Regulation of Axon Regeneration after Neural Injury. Mol Cells 40:10-16.
Silvestre de Ferron B, Vilpoux C, Kervern M, Robert A, Antol J, Naassila M, Pierrefiche O (2017) Increase of KCC2 in hippocampal synaptic plasticity disturbances after perinatal ethanol exposure. Addict Biol 22:1870-1882.
Strautman AF, Cork RJ, Robinson KR (1990) The distribution of free calcium in transected spinal axons and its modulation by applied electrical fields. J Neurosci 10:3564-3575.
Sung KW, Kirby M, McDonald MP, Lovinger DM, Delpire E (2000) Abnormal GABAA receptor-mediated currents in dorsal root ganglion neurons isolated from Na-K-2Cl cotransporter null mice. J Neurosci 20:7531-7538.
Tashiro S, Shinozaki M, Mukaino M, Renault-Mihara F, Toyama Y, Liu M, Nakamura M, Okano H (2015) BDNF Induced by Treadmill Training Contributes to the Suppression of

Spasticity and Allodynia After Spinal Cord Injury via Upregulation of KCC2. Neurorehabil Neural Rep 29:677-689.
Thiel G, Ekici M, Rossler OG (2015) RE-1 silencing transcription factor (REST): a regulator of neuronal development and neuronal/endocrine function. Cell Tissue Res 359:99-109.
Tran DT, Masedunskas A, Weigert R, Ten Hagen KG (2015) Arp2/3-mediated F-actin formation controls regulated exocytosis in vivo. Nat Commun 6:1-10
Treede RD (2016) Gain control mechanisms in the nociceptive system. Pain 157:1199-1204.
Valverde MA, Bond TD, Hardy SP, Taylor JC, Higgins CF, Altamirano J, Alvarez-Leefmans FJ (1996) The multidrug resistance P-glycoprotein modulates cell regulatory volume decrease. EMBO J 15:4460-4468.
Verhovshek T, Rudolph LM, Sengelaub DR (2013) Brain-derived neurotrophic factor and androgen interactions in spinal neuromuscular systems. Neuroscience 239:103-114.
Wienecke J, Westerdahl AC, Hultborn H, Kiehn O, Ryge J (2010) Global gene expression analysis of rodent motor neurons following spinal cord injury associates molecular mechanisms with development of postinjury spasticity. J Neurophysiol 103:761-778.
Wu W, Li L, Yick LW, Chai H, Xie Y, Yang Y, Prevette DM, Oppenheim RW (2003) GDNF and BDNF alter the expression of neuronal NOS, c-Jun, and p75 and prevent motoneuron death following spinal root avulsion in adult rats. J Neurotrauma 20:603-612.
Wu SY, Wang TF, Yu L, Jen CJ, Chuang JI, Wu FS, Wu CW, Kuo YM (2011) Running exercise protects the substantia nigra dopaminergic neurons against inflammation-induced degeneration via the activation of BDNF signaling pathway. Brain Behav Immun 25:135-146.
Yassin L, Radtke-Schuller S, Asraf H, Grothe B, Hershfinkel M, Forsythe ID, Kopp-Scheinpflug C (2014) Nitric oxide signaling modulates synaptic inhibition in the superior paraolivary nucleus (SPN) via cGMP-dependent suppression of KCC2. Front Neural Circuit 8:65.
Yeo M, Berglund K, Augustine G, Liedtke W (2009) Novel Repression of Kcc2 Transcription by REST-RE-1 Controls Developmental Switch in Neuronal Chloride. 29:14652-14662.
Zahavi EE, Ionescu A, Gluska S, Gradus T, Ben-Yaakov K, Perlson E (2015) A compartmentalized microfluidic neuromuscular co-culture system reveals spatial aspects of GDNF functions. J Cell Sci 128:1241-1252.

Appendix 1: Regulation of KCC2 by miRNA's

A.1 Abstract

Micro-RNA's (miR's) have recently become an area of increased interest in the field of peripheral nerve injury. MiR's have important roles in development and disease-states as post-transcriptional regulators of various genes. MiR-92, specifically, is now an area of interest for labs studying KCC2 in models of development and memory. However, miR-92 has not been investigated in axotomized motoneurons, while other miR's are implicated in motoneuron axonal regeneration (Sun et al., 2013; Nagata et al., 2014). Here, we remove the ability of a subpopulation of motoneurons to produce miR's to determine whether miR upregulation following injury may be responsible for the loss of KCC2. Though our knockout of DICER, an essential protein for miR production, was successful, KCC2 was still downregulated in injured neurons. Thus, after peripheral axotomy, micro-RNA's are not responsible for regulating KCC2 on spinal motoneurons

A.2 Introduction

Several recent studies have highlighted the relationship between microRNA-92 (miR-92) and KCC2 in developing cerebellar neurons (Barbato et al., 2010), spinal neurons challenged with peripheral inflammation (Zhang et al., 2017), and adult hippocampal neurons (Vetere et al., 2014). In each case, microRNA-92 and KCC2 had an inverse relationship. Overexpression of miRNA92 induced a reduction in KCC2 protein that caused a depolarization of the chloride reversal potential; inhibition of microRNA-92 shifted KCC2 expression and the chloride gradient the opposite direction (Barbato et al., 2010). A similar phenomenon was described in bladder-associated dorsal horn neurons that become sensitized and hyperexcitable in a model of cystitis-induced neuropathic pain. Inflammation challenge induced *de novo* expression of miR-92b-3p followed by a decrease in both KCC2 expression and the vesicular GABA transporter (vGAT), that could be blocked by sponging the miR, indicating it can regulate both the pre and post synaptic GABAergic levels (Zhang et al., 2017).

Micro-RNA's generally are becoming targets for treatment of many diseases (Ruberti et al., 2012). Many miRNA's are up regulated after PNI, in both neurons and Schwann cells (Sohn and Park, 2018) but miR-92 upregulation has not specifically been reported after PNI. MiR-128 and miR-124, specifically, are implicated in axon generation, though this effect is dependent on a decrease in miR-124 (Nagata et al., 2014) and an increase in miR-128 (Sun et al., 2013). Because of this myriad of potential miR targets, rather than use a narrow approach by targeting only miR-92, we decided to eliminate the production of all miRNA's by knocking out DICER, a protein essential for their production, in a subset of adult neurons prior to injury.

Previous evidence has shown that microRNA's are relatively stable (Bail et al., 2010), but a host of miRNA's are induced after neural injury (Pan et al., 2017). In another inducible DICER KO study, after five days of tamoxifen treatment and sciatic nerve injury, outcomes became much worse in DICER KO's (Wu et al., 2012). We tested in our model if KCC2 loss after axotomy would be prevented in DICER KO motoneurons in parallel to this reported worse regeneration.

A.3 Methods

A.3.1 Animals

Adult SLICK:: DICER$^{f/f}$ or SLICK:: DICER$^{+/+}$ animals were utilized as described in Table A.1.

A.3.2 Animal procedures

Adult animals underwent tamoxifen treatment and bilateral Fast Blue injection followed by bilateral sciatic cut/ligation as described in Chapter 2. Animals were allowed to survive for 14 days after nerve injury prior to standard euthanasia. Both lumbar and thoracic tissue was harvested for IHC processing. Lumbar tissue, containing FB+ cells, was used for standard KCC2 quantification. Thoracic tissue was used to confirm successful recombination in the expected YFP+ cells because the antigen retrieval used to aid in KCC2 antibody penetration made the antibody to DICER nonspecific.

A.3.2 Histology, immunohistochemistry and DICER KO quantification

An antibody against raised against a synthetic peptide corresponding to human DICER (mouse monoclonal, Abcam #ab14601; 1:500 dilution) was utilized to confirm DICER KO from YFP+ cells in the thoracic spinal cord. Thoracic tissue was incubated with primary antibodies overnight and revealed with a mouse secondary antibody (as described in Chapter 2). DICER antibody was also utilized in the lumbar tissue sections, but became nonspecific following the antigen retrieval procedure used to improve KCC2 antibody penetration, so it was not quantified.

All sections were imaged with standard confocal microscopy. In the ventral horn of thoracic spinal cord sections, YFP+ and YFP- neurons resembling the size and shape of motoneurons were quantified for cytoplasmic DICER immunoreactivity using FIJI. Neurons were identified with NeuN and classified as YFP+ or YFP-, and then five samples of 9 um^2 areas within the cytoplasm were taken in the Cy3 (DICER) channel. Due to limited numbers of YFP+ cells, neurons for all animals with the same genotype (n = 2-4 YFP+ and 2-4 YFP- per animal) were pooled for comparison.

With the exception of NeuN, lumbar sections containing injured FB+ motoneurons underwent standard IHC and KCC2 quantification using FIJI. Due to limited number of FB+/YFP+ motoneurons, ten motoneurons per animal was not feasible, so the all YFP+/FB+ neurons were imaged (n = 2-9 per animal) and animal KCC2-IR averages were calculated from these YFP+ neurons and the equivalent number of YFP-/FB+ neurons found in that animal.

A.4 Results

A.4.1 KCC2 regulation occurs independently from miRNA upregulation after PNI

As expected, SLICK:: $DICER^{+/+}$ animals (n=2) had no difference in DICER-IR between YFP+ and YFP- neurons. However, SLICK:: $DICER^{f/f}$ animals (n = 3) did have lower DICER-IR in YFP+ compared to control (YFP-) neurons (Figure A.1A-C; Statistical Table A.1A). Due to the

limited number of YFP+ cells, individual motoneurons were used (single points in graph) rather than animal averages in analysis. Despite successful KO in SLICK:: DICER$^{f/f}$ YFP+ cells, there was no difference in KCC2-IR on injured motoneurons regardless of YFP expression or genotype (Figure A.1D-H; Statistical Table A.1B). Thus, upregulation of miR's is not responsible for KCC2 loss after peripheral axotomy of spinal motoneurons.

A.5 Discussion

While miR's have been shown to be important in axon development (Hancock et al., 2014), and axon regeneration (Wu et al., 2012) as well as neuropathic pain development (reviewed in (Lopez-Gonzalez et al., 2017) they do regulate KCC2 on motoneurons after injury. All of these previous KCC2-related studies focused on sensory neurons, sensory-associated neurons in the spinal cord, or whole nerves (containing both sensory and motoneuron axons). Previous studies have illustrated that DICER is essential for motoneuron development (Chen and Wichterle, 2012) and survival. DICER KO in adult motoneurons (using a VAChT-cre driven line) results in progressive neurodegeneration (Haramati et al., 2010). We observed no clear signs of motoneuron stress following DICER KO in our motoneurons, but this may have become evident at longer intervals after tamoxifen treatment. Motoneuron loss began at 7 weeks post KO in the Haramati et al., (2010) study.

In our model, though we had a loss of DICER in YFP+ motoneurons, we observe no difference in the regulation of KCC2 after injury. It should be noted that the loss of DICER-IR was not as clear-cut as we would have hoped; some motoneurons showed a clear loss, while others had relatively normal DICER immunofluorescence (Figure 1A-C). This variability may have been the result of incomplete recombination in the DICER locus. Nevertheless, we didn't observe KCC2 preservation in any population of YFP+/FB+ motoneurons. Thus, it is unlikely that upregulation of injury-associated miRNA's, including our candidate miRNA (mir-92) (Fedeli et al., 2016), controls KCC2 in adult spinal motoneurons. Instead, KCC2 is more likely

downregulated through direct gene regulation, maybe through transcription factors like REST-RE-1 (Yeo et al., 2009) or an alternative pathway as discussed in Chapter 6.

A.6 Tables and Figures

Table A.1. Animals utilized in Appendix.

Mouse Strain	Stock No.	References
$DICER^{f/f}$	JAX: 006366	(Harfe et al., 2005)

Statistical Table A.1

	Data Reference	Data Structure	Type of Test	Statistical Significance
A	A.1C	Normal Distribution	**Two-Way ANOVA** Genotype; $F_{(1,28)} = 3.49$; $p = 0.072$ YFP status; $F_{(1,28)} = 3.49$; $p = 0.072$ Interaction; $F_{(1,28)} = 0.01$; $p = 0.92$	
	SLICK non-YFP vs		*Post hoc* Bonferroni	$p = 0.668$
	SLICK YFP		*Post hoc* Bonferroni	$p = 0.522$
	SLICK $DICER^{ff}$ non-YFP		*Post hoc* Bonferroni	$p = 0.04$
	SLICK $DICER^{ff}$ YFP			
B	A.1H	Normal Distribution	**Two-Way ANOVA** Genotype; $F_{(1,10)} = 16.67$; $p = 0.100$ YFP Status; $F_{(1,10)} = 3.28$; $p = 0.0022$ Interaction; $F_{(1,10)} = 0.00054$; $p = 0.98$	
	SLICK $DICER^{+/+}$ non-YFP vs		*Post hoc* Bonferroni	$p = 0.793$
	SLICK $DICER^{+/+}$ YFP+		*Post hoc* Bonferroni	$p = 0.047$
	SLICK $DICER^{f/f}$ non-YFP		*Post hoc* Bonferroni	$p = 0.418$
	SLICK $DICER^{f/f}$ YFP+			
	SLICK $DICER^{+/+}$ non-YFP vs		**One-tailed paired t-test**	$t = 1.41$ $p = 0.147$
	SLICK $DICER^{+/+}$ YFP+			
	SLICK $DICER^{f/f}$ non-YFP vs		**One-tailed paired t-test**	$t = 1.96$ $p = 0.0721$
	SLICK $DICER^{f/f}$ YFP+			

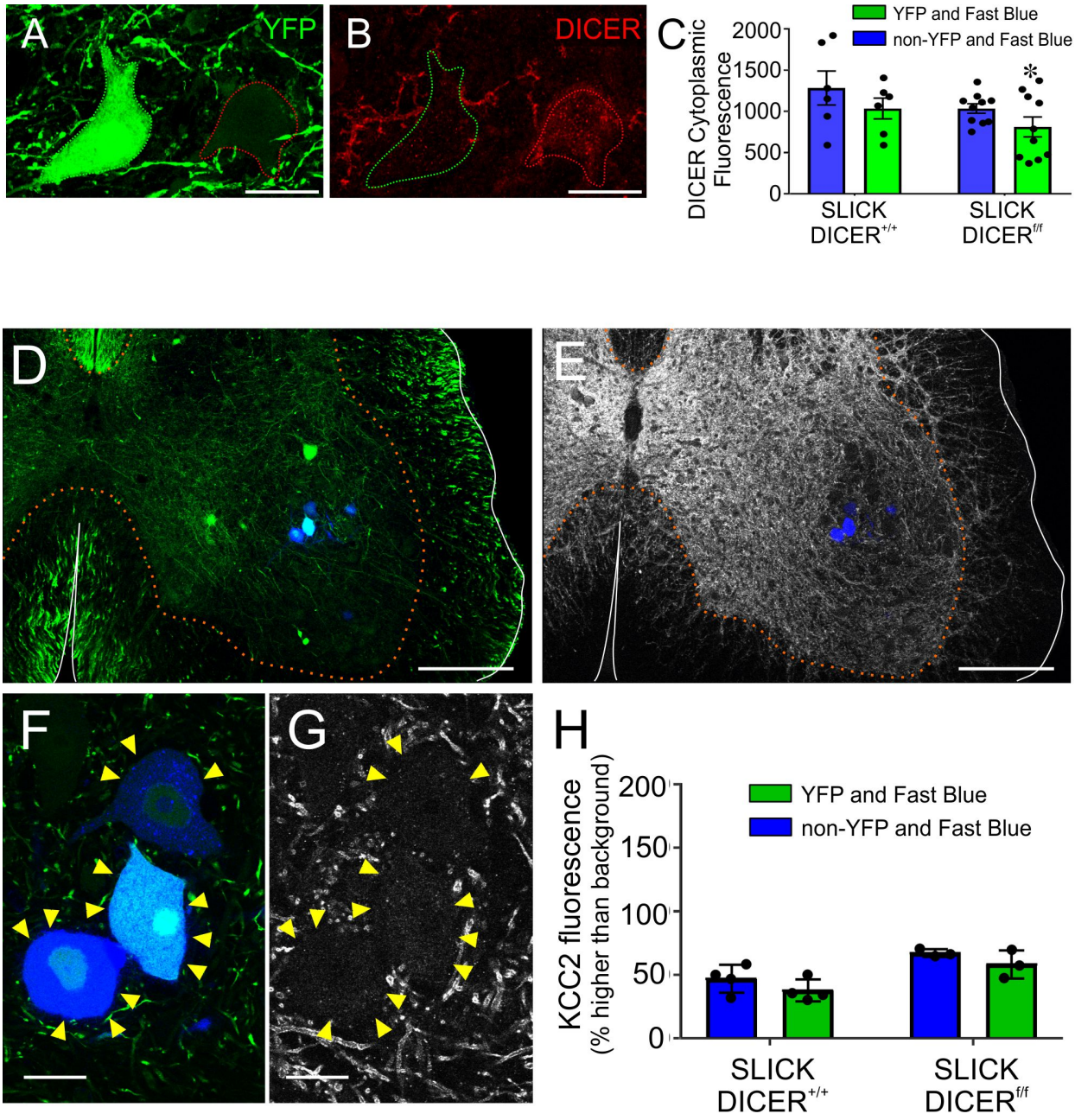

Figure A.1 DICER KO does not prevent KCC2 loss. A) YFP+ motoneuron (green) compared to non-YFP motoneuron (red outline) in thoracic spinal cord. **B**) DICER immunofluorescence in motoneurons of (A). **C**) Quantification of cytoplasmic DICER-IR illustrating that YFP+ motoneurons (individual points) in DICER$^{f/f}$ animals have reduced DICER-IR compared to non-KO motoneurons (Statistical Table A.1A). **D-G**) Representative images of spinal sections from SLICK:: DICER$^{f/f}$ mice containing FB+ motoneurons. Green:

YFP+ (KO) cells; Blue: Fast blue retrogradely labeled motoneurons; White: KCC2-IR. **D,E**) 10x images illustrating KCC2 disappearance around axotomized motoneurons 14 days after sciatic cut/ligation. Scale bars = 200 μm. **F,G**) 60x images containing YFP+ (KO) cells and non-YFP (control) cells of a from a SLICK:: DICER^{ff} animal. Regardless of DICER expression, KCC2 is similarly depleted. Scale bars = 20 μm. **H**) Quantification of KCC2-IR revealed no differences in membrane KCC2 of axotomized motoneurons regardless of YFP expression or genotype (Statistical Table A.1B). Individual points represent average KCC2-IR within animals.

A.7 References

Bail S, Swerdel M, Liu H, Jiao X, Goff LA, Hart RP, Kiledjian M (2010) Differential regulation of microRNA stability. RNA (New York, NY) 16:1032-1039.

Barbato C, Ruberti F, Pieri M, Vilardo E, Costanzo M, Ciotti MT, Zona C, Cogoni C (2010) MicroRNA-92 modulates K(+) Cl(-) co-transporter KCC2 expression in cerebellar granule neurons. J Neurochem 113:591-600.

Chen JA, Wichterle H (2012) Apoptosis of limb innervating motor neurons and erosion of motor pool identity upon lineage specific dicer inactivation. Front Neurosci 6:69.

Fedeli M, Riba M, Garcia Manteiga JM, Tian L, Vigano V, Rossetti G, Pagani M, Xiao C, Liston A, Stupka E, Cittaro D, Abrignani S, Provero P, Dellabona P, Casorati G (2016) miR-17 approximately 92 family clusters control iNKT cell ontogenesis via modulation of TGF-beta signaling. Proc Natl Acad Sci USA 113:E8286-e8295.

Hancock ML, Preitner N, Quan J, Flanagan JG (2014) MicroRNA-132 is enriched in developing axons, locally regulates Rasa1 mRNA, and promotes axon extension. J Neurosci 34:66-78.

Haramati S, Chapnik E, Sztainberg Y, Eilam R, Zwang R, Gershoni N, McGlinn E, Heiser PW, Wills AM, Wirguin I, Rubin LL, Misawa H, Tabin CJ, Brown R, Jr., Chen A, Hornstein E (2010) miRNA malfunction causes spinal motor neuron disease. Proc Natl Acad Sci USA 107:13111-13116.

Harfe BD, McManus MT, Mansfield JH, Hornstein E, Tabin CJ (2005) The RNaseIII enzyme Dicer is required for morphogenesis but not patterning of the vertebrate limb. Proc Natl Acad Sci USA 102:10898-10903.

Lopez-Gonzalez MJ, Landry M, Favereaux A (2017) MicroRNA and chronic pain: From mechanisms to therapeutic potential. Pharmacol Therapeut 180:1-15.

Nagata K, Hama I, Kiryu-Seo S, Kiyama H (2014) microRNA-124 is down regulated in nerve-injured motor neurons and it potentially targets mRNAs for KLF6 and STAT3. Neuroscience 256:426-432.

Pan YB, Sun ZL, Feng DF (2017) The Role of MicroRNA in Traumatic Brain Injury. Neuroscience 367:189-199.

Ruberti F, Barbato C, Cogoni C (2012) Targeting microRNAs in neurons: tools and perspectives. Exp Neurol 235:419-426.

Sohn EJ, Park HT (2018) MicroRNA Mediated Regulation of Schwann Cell Migration and Proliferation in Peripheral Nerve Injury. Biomed res Int 2018:8198365.

Sun X, Zhou Z, Fink DJ, Mata M (2013) HspB1 silences translation of PDZ-RhoGEF by enhancing miR-20a and miR-128 expression to promote neurite extension. Mol Cell Neurosci 57:111-119.

Vetere G, Barbato C, Pezzola S, Frisone P, Aceti M, Ciotti M, Cogoni C, Ammassari-Teule M, Ruberti F (2014) Selective inhibition of miR-92 in hippocampal neurons alters contextual fear memory. Hippocampus 24:1458-1465.

Wu D, Raafat A, Pak E, Clemens S, Murashov AK (2012) Dicer-microRNA pathway is critical for peripheral nerve regeneration and functional recovery in vivo and regenerative axonogenesis in vitro. Exp Neurol 233:555-565.

Yeo M, Berglund K, Augustine G, Liedtke W (2009) Novel Repression of Kcc2 Transcription by REST-RE-1 Controls Developmental Switch in Neuronal Chloride. J Neurosci 29:14652-14662.

Zhang J, Yu J, Kannampalli P, Nie L, Meng H, Medda BK, Shaker R, Sengupta JN, Banerjee B (2017) MicroRNA-mediated downregulation of potassium chloride-cotransporter and vesicular gamma-aminobutyric acid transporter expression in spinal cord contributes to neonatal cystitis-induced visceral pain in rats. Pain 158:2461-2474.